Impact of exercise on glucose homeostasis in different mouse models for impaired insulin sensitivity

Inaugural-Dissertation

zur Erlangung des Doktorgrades
der Mathematisch-Naturwissenschaftlichen Fakultät
der Heinrich-Heine-Universität Düsseldorf

vorgelegt von

Christian Springer
aus Duisburg

Düsseldorf, Dezember 2018

aus dem Institut für Klinische Biochemie und Pathobiochemie
des Deutschen Diabetes-Zentrums (DDZ)
Leibniz-Zentrum für Diabetes-Forschung
an der Heinrich-Heine-Universität Düsseldorf

Gedruckt mit der Genehmigung der
Mathematisch-Naturwissenschaftlichen Fakultät der
Heinrich-Heine-Universität Düsseldorf

Berichterstatter:

1. Prof. Dr. Hadi Al-Hasani
2. Prof. Dr. Michael Feldbrügge

Tag der mündlichen Prüfung: 08.04.2019

Summary

Exercise interventions represent a useful strategy for the prevention and treatment of type 2 diabetes mellitus (T2DM). Performing regular exercise has been shown to improve peripheral and whole-body insulin sensitivity, to reduce excessive fat accumulation and to enhance the physical fitness in T2DM patients. However, a large inter-individual variety in the response to exercise exists, implicating that the genetic predisposition determines the ability to improve glycaemia after exercise training. Although family-based linkage and genome-wide association studies have confirmed the polygenic nature of T2DM, rare cases represent a monogenic form of the disease, meaning that single gene variants confer insulin resistance or beta cell failure.

In the present study, the ability of a chronic exercise intervention to improve glycaemia was investigated in two specific mouse models for impaired insulin sensitivity. Mice deficient for the RabGTPase-activating protein TBC1D4 (D4KO) present a monogenic form of insulin resistance, consisting of postprandial hyperglycaemia and impaired skeletal muscle and adipose tissue insulin sensitivity. Four weeks of moderate exercise training on treadmills substantially improved glucose and insulin tolerance in D4KO mice and reduced hepatic lipid accumulation. Moreover, regular exercise led to a restored glucose uptake in the adipose tissue and to increased mitochondrial activity in D4KO mice. Thus, these findings indicate a novel TBC1D4-independent mechanism that targets the adipose tissue to compensate for the impaired skeletal muscle glycaemia in response to exercise.

Secondly, New Zealand Obese (NZO) mice, a polygenic model that closely reflects the human metabolic syndrome and T2DM, were subjected to a regular exercise intervention on treadmills. These mice were previously described as a physically inactive strain. Six weeks of chronic interval training did not prevent hyperglycaemia and only mildly improved exercise capacity and insulin tolerance in a subgroup of NZO mice that had not yet developed severe hyperglycaemia. More importantly, chronic exercise further enhanced skeletal muscle and adipose tissue insulin resistance and led to a significantly elevated hepatic fat content. Thus, the data suggests that NZO mice, presumably due to their genetic predisposition, are not responding to the regular physical activity by improving their glycaemia. Future studies will focus on identifying the possible pathways that confer the response or non-response to exercise interventions.

Zusammenfassung

Körperliche Aktivität und Bewegung zählen zu den wichtigsten Maßnahmen zur Prävention und Behandlung des Typ-2-Diabetes mellitus (T2DM). Regelmäßiges Training verbessert die Insulinsensitivität peripherer Gewebe, baut übermäßiges Körperfett ab und führt zu einer gesteigerten Fitness bei T2DM Patienten. Die Fähigkeit, mittels Bewegung die Glykämie zu verbessern, ist allerdings interindividuell unterschiedlich und wird vermutlich von der genetischen Prädisposition determiniert. Obwohl durch familienbasierte Kopplungsanalysen und genomweite Assoziationsstudien als Erkrankung polygenen Ursprungs beschrieben, lassen sich seltene Formen des T2DM auf einzelne Genvarianten zurückführen (monogener Diabetes).

Die Fähigkeit, durch regelmäßiges Training die Glykämie zu verbessern, sollte in der vorliegenden Arbeit in zwei Mausmodellen für verminderte Insulinsensitivität untersucht werden. Mäuse mit einer Defizienz für das Rab-GTPase-aktivierende Protein TBC1D4 (D4KO) zeigen eine monogene Ausprägung der Insulinresistenz, gekennzeichnet durch postprandiale Hyperglykämie und beeinträchtigter Glukoseaufnahme im Skelettmuskel und Fettgewebe. Vier Wochen moderates Laufbandtraining führten zu einer beachtlichen Steigerung der Glukose- und Insulintoleranz, sowie zu einer Reduktion des Leberfetts in D4KO-Mäusen. Des Weiteren konnte in trainierten D4KO-Mäusen die Glukoseaufnahme im Fettgewebe wiederhergestellt und die mitochondriale Aktivität erhöht werden. Zusammengefasst deuten diese Ergebnisse auf einen neuartigen TBC1D4-unabhängigen Mechanismus des Fettgewebes hin, welcher in Abhängigkeit von Bewegung die verminderte Glykämie des Skelettmuskels kompensiert.

Als zweites Mausmodell wurde die New Zealand Obese (NZO)-Maus einem Trainingsprogramm unterzogen. Die NZO-Maus verkörpert eine polygene Form des humanen metabolischen Syndroms und T2DM und wurde zuvor als körperlich inaktiv beschrieben. Sechs Wochen chronisches Intervalltraining konnten einer Hyperglykämie allerdings nicht vorbeugen und führten nur zu einer gering verbesserten Fitness und Insulintoleranz in einer nicht-diabetischen Untergruppe. Stattdessen erhöhte das regelmäßige Training die Insulinresistenz in Skelettmuskel und Fettgewebe und führte zu einer signifikanten Steigerung des Leberfetts. Daraus lässt sich ableiten, dass NZO-Mäuse nicht in der Lage sind, ihre Glykämie durch Bewegung zu verbessern, vermutlich bedingt durch genetische Faktoren. Weiterführende Untersuchungen werden sich auf die Frage konzentrieren, welche Mechanismen die positive oder negative Reaktion auf Training bestimmen.

Table of contents

Summary ... **3**

Zusammenfassung ... **4**

1. Introduction ... **9**

1.1 Diabetes and obesity ... 9

1.2 Environmental factors and genetic predisposition in the pathophysiology of T2DM ... 10

1.3 Regulation of glucose and lipid metabolism in insulin-responsive peripheral tissues ... 11

1.3.1 Glucose uptake in skeletal muscle, adipose tissue and liver ... 11

1.3.2 Glucose metabolism in skeletal muscle, adipose tissue and liver ... 13

1.3.3 Lipid metabolism in skeletal muscle, adipose tissue and liver ... 14

1.3.4 Disturbed glucose and lipid metabolism in T2DM ... 15

1.4 Chronic exercise ... 16

1.4.1 Role of chronic exercise in the prevention and treatment of T2DM ... 16

1.4.2 Modes of exercise ... 17

1.4.3 Whole-body adaptations to chronic exercise ... 18

1.4.4 Effects of chronic exercise on glucose and lipid metabolism in skeletal muscle, adipose tissue and liver ... 19

1.4.4.1 Exercise action in skeletal muscle ... 19

1.4.4.2 Exercise action in adipose tissue ... 20

1.4.4.3 Exercise action in the liver ... 21

1.5 Mouse models in T2DM research ... 22

1.5.1 Structure and function of the RabGAP protein TBC1D4 ... 23

1.5.2 Metabolic features of *Tbc1d4*-deficient (D4KO) mice ... 25

1.5.3 The NZO mice as a polygenic model for human T2DM ... 26

1.6 Aim of the study ... 27

2. Materials and methods ... **28**

2.1 Materials ... 28

2.1.1 Mouse strains ... 28

2.1.2 Mouse diets ... 28

2.1.3 Primers ... 29

2.1.4 Antibodies ... 29

2.1.5 Reaction Kits ... 30

2.1.6 Enzymes and molecular weight size markers ... 30

2.1.7 Chemicals 31
2.1.8 Buffers and solutions 33
2.2 Methods 34
2.2.1 Study design 34
2.2.2 Animal experiments 35
2.2.2.1 General animal housing 35
2.2.2.2 Treadmill training 35
2.2.2.3 Physical capacity test 36
2.2.2.4 Indirect calorimetry 37
2.2.2.5 Body composition 37
2.2.2.6 Determination of blood glucose 37
2.2.2.7 Blood lactate measurement 38
2.2.2.8 Intraperitoneal glucose tolerance test (i.p. GTT) 38
2.2.2.9 Intraperitoneal insulin tolerance test (i.p. ITT) 38
2.2.2.10 *Ex vivo* glucose uptake in isolated skeletal muscles 38
2.2.2.11 *Ex vivo* glucose uptake in isolated adipocytes 39
2.2.2.12 Dissection of animal tissues 40
2.2.3 Biochemical methods 41
2.2.3.1 Determination of plasma insulin concentration 41
2.2.3.2 Measurement of plasma triglycerides and free fatty acids (NEFA) 41
2.2.3.3 Analysis of hepatic and skeletal muscle glycogen content 41
2.2.3.4 Analysis of hepatic and skeletal muscle triglyceride content 42
2.2.3.5 Preparation of protein lysates from mouse tissue 42
2.2.3.6 Determination of protein concentration 43
2.2.3.7 Western Blot analysis 43
2.2.3.7.1 SDS-PAGE 43
2.2.3.7.2 Transfer and immunochemical detection of separated proteins 43
2.2.3.7.3 Separation and transfer of proteins using stain-free gels 44
2.2.4 Molecular biological methods 45
2.2.4.1 RNA isolation from mouse tissue 45
2.2.4.2 cDNA synthesis 45
2.2.4.3 Quantitative Real-Time PCR (qPCR) 46
2.2.5 Statistical analysis 46

3. Results 48

3.1 Impact of chronic exercise on glucose homeostasis in *Tbc1d4*-deficient (D4KO) mice 48
3.1.1 Physical capacity of D4KO mice 48
3.1.2 Body composition and plasma parameters of D4KO mice 49
3.1.3 Glucose tolerance and insulin tolerance of D4KO mice.....50
3.1.4 Analysis of glucose uptake in skeletal muscle of D4KO mice.....51
3.1.5 Hepatic and skeletal muscle glycogen content of D4KO mice.....54
3.1.6 Abundance of GCK and PCK in the liver of D4KO mice.....54
3.1.7 Determination of hepatic triglyceride content of D4KO mice.....55
3.1.8 Analysis of glucose uptake in white adipose tissue of D4KO mice 56
3.1.9 Abundance of glucose transporters in brown adipose tissue of D4KO mice.....58
3.1.10 Expression of browning markers in scWAT of D4KO mice 59

3.2 Impact of chronic exercise on glucose homeostasis in NZO mice.....62
3.2.1 Establishment of a new chronic exercise protocol in B6 mice 62
3.2.1.1 Physical capacity and glucose tolerance of B6 mice 62
3.2.1.2 Body composition and hepatic triglyceride content of B6 mice 63
3.2.1.3 Whole-body energy expenditure of B6 mice.....64
3.2.1.4 Abundance of PGC-1α and AMPK in skeletal muscle of B6 mice.....65
3.2.2 Physical capacity and glucose tolerance of trained NZO mice fed a SD.....67
3.2.3 Establishment of the HFD-induced T2DM development in NZO mice 68
3.2.4 Blood glucose of NZO mice fed a HFD before and after chronic interval training .69
3.2.5 Physical capacity of NZO mice fed a HFD 70
3.2.6 Whole-body energy expenditure of NZO mice fed a HFD 71
3.2.7 Body composition and plasma parameters of NZO mice fed a HFD.....72
3.2.8 Hepatic and skeletal muscle glycogen content in NZO mice fed a HFD 72
3.2.9 Glucose tolerance and insulin tolerance of NZO mice fed a HFD.....73
3.2.10 Analysis of glucose uptake in skeletal muscle of NZO mice fed a HFD.....74
3.2.11 Analysis of glucose uptake in white adipose tissue of NZO mice fed a HFD 76
3.2.12 Abundance of GCK and PCK in the liver of NZO mice fed a HFD.....77
3.2.13 Hepatic triglyceride and FASN protein content in NZO mice fed a HFD 78

4. Discussion 81
4.1 The role of TBC1D4 in exercise-mediated metabolism 81
4.1.1 Lack of TBC1D4 impairs exercise capacity, probably due to impaired skeletal muscle glucose uptake 81

4.1.2 Chronic exercise improves exercise capacity and whole-body insulin sensitivity in D4KO mice, independent of skeletal muscle glucose uptake 83
4.1.3 Increased adipose tissue glucose uptake accounts for the improved insulin sensitivity in D4KO mice 85
4.1.4 Increased browning contributes to adipose tissue insulin sensitivity in D4KO mice 87
4.1.5 Reduced whole-body and hepatic fat content contribute to the improved insulin sensitivity in trained D4KO mice 88

4.2 The impact of exercise on glycaemia of NZO mice 90
4.2.1 HFD-feeding leads to hyperglycaemia and clustering of blood glucose, which is not prevented by chronic exercise 90
4.2.2 Exercise capacity is only improved in the non-diabetic NZO subgroup, independent of skeletal muscle glucose uptake 91
4.2.3 Increased rates of whole-body FAO compensate for the impaired glycaemia in diabetic NZO mice 92
4.2.4 Chronic exercise further aggravates adipose tissue and hepatic insulin resistance in NZO mice....93
4.2.5 NZO mice are rather non-responders to exercise 95
4.3 Reduced hepatic triglyceride content determines the response to exercise 97
4.4 Conclusion and future perspectives 98

5. Literature....100
5.1 Scientific publications 100
5.2 Additional references 116

6. Supplement....117
6.1 Contribution to manuscripts 117
6.2 Abbreviations....119
6.3 Supplemental Tables 124
6.4 Supplemental Figures 128
6.5 List of Figures 132
6.6 List of Tables 134

Acknowledgments....135

Erklärung 137

1. Introduction

1.1 Diabetes and obesity

Diabetes is a chronic disorder caused by pancreatic beta cell dysfunction and/ or insulin resistance. Global health organisations estimate that 400 million people are living with diabetes worldwide, with 7.5 million people being affected in Germany, thus emphasising the global health burden of diabetes (WHO 2016, IDF 2017). Besides gestational diabetes and other specific forms, diabetes can be mainly classified into two types. Type 1 diabetes mellitus (T1DM) is caused by an autoimmune destruction of the insulin-secreting pancreatic beta cells, finally leading to deficient insulin secretion. Type 2 diabetes mellitus (T2DM) represents the most commonly occurring form and is caused by a progressive development of insulin resistance (ADA 2010). The term “insulin resistance” can be described as the impaired ability of peripheral tissues such as skeletal muscle, liver and adipose tissue to respond to physiological levels of insulin (Gastaldelli 2011). As a consequence of insulin resistance, impaired insulin-stimulated glucose uptake in skeletal muscle and adipose tissue, disturbed hepatic glucose production and disrupted regulation of lipid metabolism (dyslipidaemia) contribute to elevated blood glucose levels, i.e. hyperglycaemia. Hyperglycaemia further impairs the pancreatic secretory capacity, since the beta cells are insufficient to compensate for the increased demand of insulin, finally leading to failure and death of the beta cells (Muoio & Newgard 2008). The failure of pancreatic beta cells drives the development from insulin resistance to a manifested T2DM, which is associated with additional long-term complications such as cardiovascular disease, neuropathy, retinopathy and nephropathy (ADA 2010).

Besides various factors including the genetic predisposition, inflammatory factors or endoplasmic reticulum (ER) stress in insulin-responsive tissues, the development of insulin resistance and T2DM is closely associated with obesity (Muoio & Newgard 2008, Gastaldelli 2011). Obesity is defined as the excessive accumulation of mainly visceral fat, resulting in a body mass index (BMI) of ≥ 30 kg/m² in adult people. According to the WHO, more than 650 million adults were considered obese in 2016 (WHO 2018). Comparing the estimated numbers for diabetic and obese people, it becomes obvious that obesity not necessarily leads to hyperglycaemia and T2DM. This is due to the ability of the beta cells to secrete sufficient amounts of insulin to maintain normoglycaemia, although insulin resistance has already developed (Al-Goblan et al. 2014). Nevertheless, obesity represents a major risk factor for T2DM, since the ectopic accumulation of visceral fat reduces peripheral insulin sensitivity, induces inflammation and leads to hepatic and skeletal muscle lipotoxicity due to the excess

release of free fatty acids (Hardy et al. 2012). The combination of obesity, hyperglycaemia and insulin resistance together with dyslipidaemia, hypertension and hypercholesterolemia is referred to as the so-called “metabolic syndrome” (Mbata et al. 2017). Evidence from prospective studies suggest that the metabolic syndrome precedes the onset of T2DM (Ford et al. 2008, Sattar et al. 2008), emphasising the importance of all of these impairments to increase the risk of developing T2DM.

1.2 Environmental factors and genetic predisposition in the pathophysiology of T2DM

The increasing global prevalence of T2DM is mainly caused by environmental factors due to the nowadays western and urban lifestyle, including excessive energy intake of a high-caloric diet and physical inactivity. In addition, clear evidence exists for the impact of a genetic predisposition causing obesity and T2DM (Prasad & Groop 2015). The most obvious evidence for a genetic impact has arisen from family studies, showing that the risk of developing T2DM is strongly inherited in first degree relatives of T2DM patients (Meigs et al. 2000, Köbberling & Tillil 1982). Although the identification of the exact genetic factors contributing to T2DM remains challenging, various approaches such as family-based linkage analyses or genome-wide association studies (GWAs) have confirmed the polygenic nature of T2DM, meaning that a large variety of genes are contributing to the onset of T2DM (Bonnefond & Froguel 2015, Prasad & Groop 2015). Using these approaches, several gene variants have been identified to be associated with increased T2DM prevalence, e.g. variants in genes encoding for the peroxisome proliferator-activated receptor-δ (PPAR-δ), the fat mass and obesity-associated protein (FTO) or the insulin receptor substrate IRS-1 (Deeb et al. 1998, Frayling et al. 2007, Rung et al. 2009). Besides polygenic T2DM, a small portion of T2DM cases represents a monogenic form of diabetes, e.g. maturity-onset diabetes of the young (MODY). Here, variants in one single gene confer insulin resistance, as it has been discovered for a mutation in the gene encoding for the glucokinase (GCK; Froguel et al. 1992). However, these rare mutations only affect less than 5 % of T2DM patients (Bonnefond & Froguel 2015).

While most of the GWAs are usually performed in large populations, historical isolated populations have gained interest to identify new T2DM-associated gene variants, such as the East Asian or Pima Indian populations (Cho et al. 2011, Hanson et al. 2014). In a Greenlandic Inuit population, association mapping in combination with array-based genotyping recently identified a nonsense variant (p.Arg684Ter) in the gene encoding for TBC1D4, a protein involved in the regulation of insulin-mediated glucose uptake in peripheral tissues. Homozygous carriers of this variant were characterized by postprandial hyperglycaemia and

increased T2DM prevalence (Moltke et al. 2014). The increased T2DM prevalence in the Inuit can presumably be explained by the admixture of the population with Europeans during recent decades, consequentially leading to the transition from a physically active to a sedentary lifestyle (Grarup et al. 2015). Therefore, the incidence of gene variants causing T2DM in isolated populations highlights the complex interaction of the genetic predisposition with environmental factors. Moreover, therapies such as diet or chronic exercise interventions that may overcome the genetic predisposition to prevent hyperglycaemia and T2DM are of particular importance.

1.3 Regulation of glucose and lipid metabolism in insulin-responsive peripheral tissues

The insulin-stimulated regulation of glucose and lipid metabolism is crucial to maintain whole-body energy homeostasis (Leney & Tavare 2009). In response to postprandial elevations of blood glucose, insulin is synthesized and secreted by the pancreatic beta cells. Once secreted, insulin stimulates the uptake of glucose into skeletal muscle and adipose tissue and suppresses hepatic glucose production in order to reduce the blood glucose levels. In addition, insulin promotes the synthesis and storage of lipids as triglycerides in the liver and adipose tissue and inhibits the hydrolysis of triglycerides and release as free fatty acids (lipolysis) from adipocytes (Gastaldelli 2011, Zhang & Liu 2014). Thus, an efficient inter-organ crosstalk between skeletal muscle, adipose tissue and liver is important to maintain normoglycaemia and energy homeostasis.

1.3.1 Glucose uptake in skeletal muscle, adipose tissue and liver

Skeletal muscle and adipose tissue represent the main tissues for glucose disposal during insulin-stimulated conditions. With approximately 80 %, skeletal muscle is the predominant site for glucose uptake, while adipose tissue accounts for about 10 % of whole-body glucose uptake (DeFronzo et al. 1981, Smith & Kahn 2016). Upon elevated blood glucose levels, insulin mediates the uptake of glucose into muscle and adipose cells by an intracellular signalling cascade that increases the translocation of glucose transporter proteins to the plasma membrane (Figure 1). In skeletal muscle and adipose tissue, the facilitated glucose transporter member 4 (GLUT4; gene name *SLC2A4*) represents the major insulin-regulated glucose transporter (Watson & Pessin 2001), while the ubiquitously expressed GLUT1 (gene name *SLC2A1*) isoform accounts for basal glucose uptake across the membrane (Gorovits & Charron 2003). Insulin initiates the signalling cascade by binding to the insulin receptor (IR), resulting in a conformational change, i.e. auto-phosphorylation of the transmembrane β subunits via tyrosine kinase activity. This in turn induces the tyrosine phosphorylation of

several intracellular substrate proteins, e.g. insulin receptor substrate proteins (IRS) that are recruited to the IR (Wilcox 2005). The recruitment of IRS to the IR leads to the activation of the phosphatidylinositol-3-kinase (PI3K) pathway, involving the phosphorylation of serine/ threonine kinases such as protein kinase B (PBK, known as AKT). Subsequently, the activated AKT phosphorylates further downstream proteins including TBC1D1 and TBC1D4. Phosphorylation of these RabGTPase-activating proteins finally leads to the translocation of intracellular GLUT4 vesicles to the plasma membrane, where the GLUT4 vesicles fuse with the membrane and release GLUT4 to finally mediate glucose uptake into the cell (Sakamoto & Holman 2008, Zhang & Liu 2014).

In skeletal muscle, a second pathway mediates GLUT4 translocation and glucose uptake by an insulin-independent pathway in response to muscle contraction during physical activity (Figure 1). This pathway involves the 5'-AMP-activated protein kinase (AMPK) that is activated by at least two cellular events. A muscle stimulus leads to a rise in intracellular calcium (Ca^{2+}) concentrations that trigger the interaction of the myofibrillar actin-myosin complex, thereby causing the adenosine triphosphate (ATP)-dependent muscle contraction. The increasing energy demand for ATP in contracting muscle fibres increases the ratio of adenosine monophosphate (AMP)/ ATP. Both the increased AMP/ ATP ratio as well as the elevated Ca^{2+} levels activate the AMPK. Similar to AKT, AMPK in turn phosphorylates TBC1D1 and TBC1D4 and thereby enhances GLUT4 translocation and glucose uptake (Sakamoto & Holman 2008, O'Neill 2013). The activation of AMPK was also found to be involved in the regulation of glucose uptake in adipose tissue, but whether AMPK directly regulates GLUT4 translocation in adipocytes remained unclear (Daval et al. 2006, Ceddia 2013).

In contrast to skeletal muscle and adipose tissue, glucose uptake into liver cells (hepatocytes) is insulin-independent and mainly mediated by the GLUT2 (gene name *SLC2A2*) transporter (Sharabi et al. 2015). In the postprandial state, elevated insulin concentrations induce AKT-dependent insulin signalling in the liver that suppresses hepatic glucose production (gluconeogenesis) and promotes the uptake and storage of glucose as glycogen. In contrast, fasting and exercise increase hepatic gluconeogenesis and glycogen breakdown (glycogenolysis) in order to release glucose into the circulation for skeletal muscle and adipose tissue substrate utilization (Rui 2014, Honka et al. 2018).

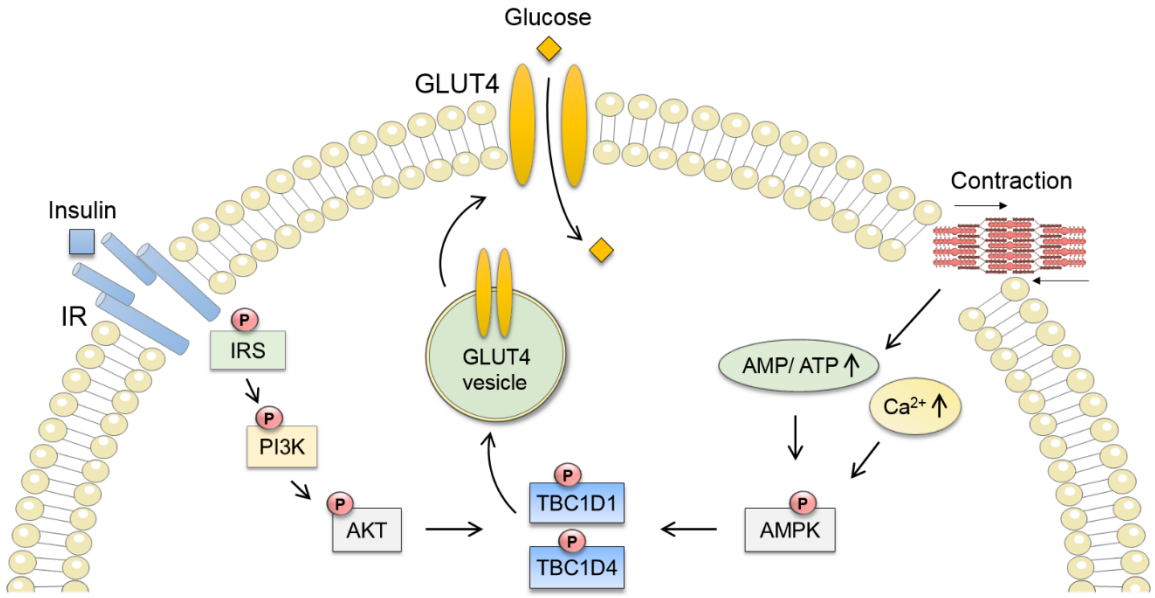

Figure 1: Insulin- and contraction-mediated glucose uptake in skeletal muscle. Glucose uptake is mediated by GLUT4 translocation either via the insulin-dependent pathway involving PI3K and AKT, or via the insulin-independent AMPK-pathway during muscle contraction. Translocation of GLUT4 to the plasma membrane is regulated by the two RabGTPase-activating proteins TBC1D1 and TBC1D4 that are directly phosphorylated by either AKT or AMPK. P, phosphorylation (modified from Sakamoto & Holman 2008).

1.3.2 Glucose metabolism in skeletal muscle, adipose tissue and liver

Following glucose uptake, the glucose serves as an important energy source for substrate utilization in skeletal muscle, adipose tissue and liver. Once incorporated into the cytoplasm, glucose is immediately phosphorylated to glucose-6-phosphate (G6P), catalysed by tissue-specific hexokinases (HK). The HK-II represents the predominant isoform in skeletal muscle and adipose tissue, while HK-IV (known as GCK) catalyses the formation of G6P in hepatocytes (Heikkinen et al. 2000, Roberts & Miyamoto 2015). G6P is then further metabolized to pyruvate during glycolysis in order to produce energy via generation of ATP molecules. Under aerobic conditions, pyruvate enters the mitochondria and is converted to acetyl coenzyme A (acetyl-CoA), which is further oxidized in the citric acid cycle and oxidative phosphorylation pathway to provide additional energy in the form of NADH and ATP. Under anaerobic conditions, e.g. during physical activity, pyruvate is converted to lactate in skeletal muscle and adipose tissue and released into circulation. The secreted lactate is taken up by hepatocytes, where it is further utilized for either gluconeogenesis or re-oxidized to pyruvate and acetyl-CoA for energy supply (Rui 2014, Guo et al. 2012). In addition to entering the glycolytic pathway, glucose is stored as glycogen mainly in skeletal muscle and liver upon insulin-stimulated glucose uptake. After phosphorylation of glucose, G6P is first converted to glucose-1-phosphate (G1P) and subsequently metabolized to UDP-glucose. The final

synthesis of glycogen from UDP-glucose molecules is catalysed by the enzyme glycogen synthase (GS). In the postprandial state, insulin promotes the storage of glucose via activation of AKT, while during fasting the glycogenolysis is increased in order to regenerate glucose molecules (Dimitriadis et al. 2011, Zhang & Liu 2014). Moreover, skeletal muscle and hepatic glycogenolysis contribute to whole-body energy supply during exercise (Trefts et al. 2015).

Although glycogenolysis ensures a constant glucose supply during short-term fasting, glycogen is depleted during long-term fasting. Hepatic gluconeogenesis is an alternative pathway to provide the required glucose supply during prolonged fasting (Gimenez-Cassina et al. 2014). Skeletal muscle or adipose tissue-deriving non-carbohydrate metabolites such as lactate, glycerol or amino acids are transported to the liver and serve as precursors for the gluconeogenic pathway. For the conversion of lactate to glucose, lactate is oxidized to pyruvate, which is further metabolized to oxaloacetate (OAA) in the mitochondria. There, OAA is reduced to malate and transported into the cytosol, where it is re-oxidized to OAA. The rate-limiting step of gluconeogenesis involves the conversion of OAA to phosphoenolpyruvate, catalysed by the phosphoenolpyruvate carboxylase (PCK). Two isoforms of PCK are found in cells, the cytosolic (PCK-1) and the mitochondrial (PCK-2) form, whereas PCK-1 is believed to be the main contributor to hepatic gluconeogenesis (Stark & Kibbey 2014). After several reaction steps that mostly reflect the reversed glycolytic pathway, phosphoenolpyruvate is metabolized to G6P, which is finally dephosphorylated to glucose. Therefore, hepatic gluconeogenesis contributes to skeletal muscle and adipose tissue energy supply during fasting or exercise, while insulin suppresses hepatic glucose production in order to maintain normoglycaemia (He et al. 2009, Trefts et al. 2015).

1.3.3 Lipid metabolism in skeletal muscle, adipose tissue and liver

Upon dietary intake, not only glucose but also fatty acids serve as an important energy source for peripheral tissues. Skeletal muscle, adipose tissue and the liver are the main organs storing lipids as triacylglycerols (triglycerides) that are hydrolysed for internal energy consumption or released into circulation for further substrate utilization (Frayn et al. 2006). In the postprandial state, insulin stimulates the uptake of dietary fatty acids from the plasma (plasma triglycerides) into adipose tissue and promotes the storage of lipids as triglycerides. During conditions of high energy demands, e.g. during fasting or exercise, increased adipose tissue lipolysis leads to elevated release of lipids as non-esterified free fatty acids (NEFA) into circulation. Skeletal muscle takes up NEFA as an additional fuel after depletion of glycogen stores by the activity of distinct fatty acids transporters such as fatty acid translocase (also known as FAT/CD36) or fatty acid transport proteins (FATP1 and FATP4). After transport into the muscle cell, fatty

acids are further stored as triglycerides or directly converted to acetyl-CoA in the mitochondrial β-oxidation to fuel the citric acid cycle and the oxidative phosphorylation pathway (Watt & Hoy 2012). Similar to skeletal muscle, the liver takes up NEFA via diverse transport proteins (FAT/CD36, FATP2 and FATP5), where they either fuel the mitochondrial β-oxidation or serve as substrate for triglyceride synthesis (Frayn et al. 2006). Upon intake of excess carbohydrate-containing diets, adipose tissue and mainly the liver are able to synthesise fatty acids from these excess carbohydrates including glucose. This so-called *de novo* lipogenesis (DNL) pathway involves the conversion of the glycolysis-derived pyruvate to acetyl-CoA that enters the mitochondrial citric acid cycle. The resultant citrate enters the cytosol and is converted to acetyl-CoA again, catalysed by the ATP-citrate lyase (ACLY). Subsequently, acetyl-CoA is converted to malonyl-CoA, which serves as the substrate for the generation of saturated palmitate by the enzyme fatty acid synthase (FASN), representing the rate-limiting step of DNL. The generated palmitate is further elongated to complex long-chain fatty acids that are stored as triglycerides, which in turn provide energy via β-oxidation (Frayn et al. 2006, Ameer et al. 2014). While insulin-signalling increases DNL to clear excess glucose from the blood, fasting and exercise supresses hepatic DNL (Ameer et al. 2014, Brouwers et al. 2016).

1.3.4 Disturbed glucose and lipid metabolism in T2DM

In insulin-resistant states, this highly regulated glucose and lipid metabolism is disturbed, further contributing to the progress of T2DM and its comorbidities (Figure 2). In skeletal muscle and adipose tissue, impaired translocation of GLUT4 leads to reduced glucose uptake, thereby contributing to hyperglycaemia and insulin resistance (Garvey et al. 1998, Miura et al. 2001). Although the exact pathways leading to the impaired GLUT4 translocation remain to be elucidated, several studies hint towards multiple defects in the intracellular insulin signalling cascade, such as dysregulated phosphorylation of the IR (Dunaif et al. 1995), IRS-1 (Aguirre et al. 2000), AKT (Cozzone et al. 2008) or TBC1D1 and TBC1D4 (Middelbeek et al. 2013). As a consequence of peripheral insulin resistance, the insulin-stimulated glycogen synthesis in skeletal muscle and hepatocytes declines, probably due to a reduced GS activity (Damsbo et al. 1991). Moreover, hepatic insulin resistance leads to increased rates of gluconeogenesis, causing fasting hyperglycaemia in T2DM patients (Magnusson et al. 1992).

The impaired insulin signalling in adipose tissue contributes to increased lipolysis, resulting in elevated plasma NEFA levels. Consequently, excess rates of NEFA are transported into skeletal muscle and the liver and contribute to ectopic fat accumulation (Gastaldelli 2011). Accumulation of triglycerides as intramyocellular lipids (IMCL) in skeletal muscle and elevated intrahepatic triglyceride content have been shown to further impair insulin sensitivity (Boden et

al. 2001, Gastaldelli et al. 2007). Furthermore, hepatic DNL is increased in the insulin-resistant state through the upregulation of lipogenic transcription factors, thereby promoting the accumulation of hepatic triglycerides. This in turn drives the release of fatty acids from the liver, contributing to elevated plasma triglyceride concentrations and overall dyslipidaemia (Adams et al. 2005, Mooradian 2009). Taken together, these findings emphasize the importance of an intact insulin-signalling for the regulation of glucose and lipid metabolism, since once disturbed, the impaired peripheral glucose uptake further contributes to hyperglycaemia and dyslipidaemia.

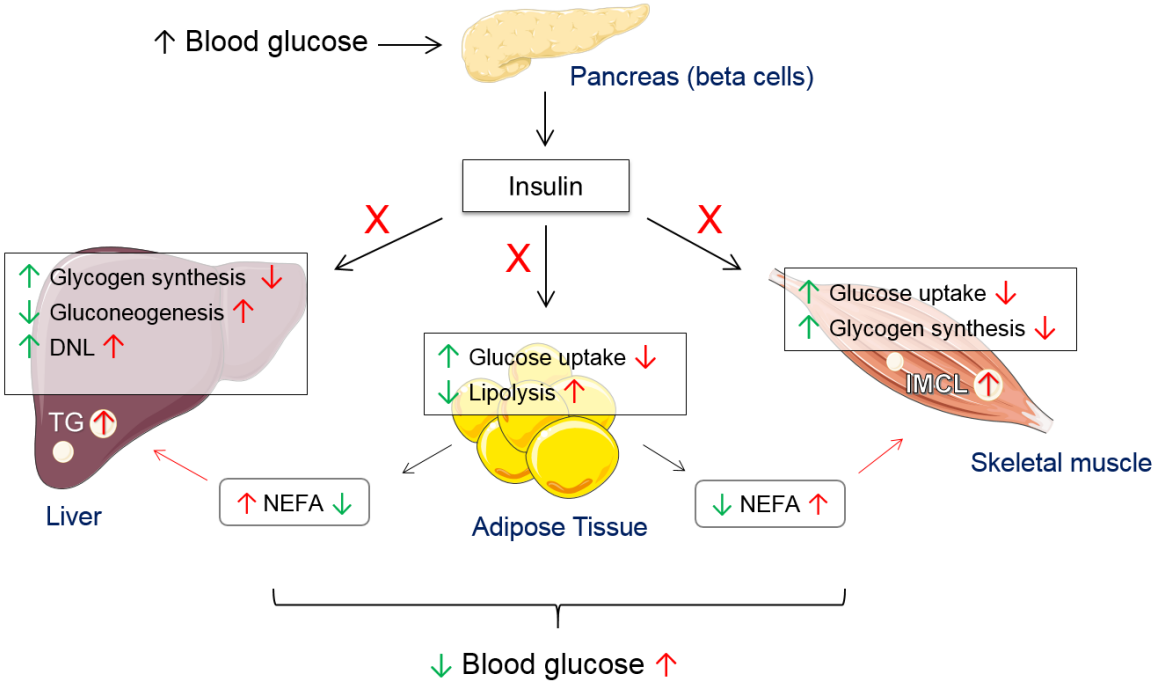

Figure 2: Disturbed glucose and lipid metabolism in T2DM. At healthy postprandial states (green arrows), insulin increases skeletal muscle and adipose tissue glucose uptake and promotes skeletal muscle and hepatic glycogen synthesis, leading to reduced blood glucose levels. Insulin suppresses lipolysis in adipocytes, thereby reducing plasma NEFA concentrations. At T2DM states (red arrows), peripheral insulin resistance (marked as "X") leads to reduced peripheral glucose uptake and reduced hepatic and muscle glycogen synthesis, resulting in hyperglycaemia. Increased lipolysis leads to elevated plasma NEFA concentrations, which accumulate in the liver and skeletal muscle. Exacerbated hepatic DNL contributes to increased dyslipidaemia. TG, triglycerides; IMCL, intramyocellular lipids (modified from Samuel & Shulman 2012).

1.4 Chronic exercise

1.4.1 Role of chronic exercise in the prevention and treatment of T2DM

Chronic exercise interventions represent a useful strategy to improve glycaemia and prevent the onset of T2DM due to peripheral insulin resistance, since the exercise-induced glucose uptake in skeletal muscle is insulin-independent (see Figure 1). Indeed, regular exercise training has been shown to improve glycaemia and whole-body insulin sensitivity (van Dijk et

al. 2012, Madsen et al. 2015), to reduce visceral fat mass and plasma triglycerides (Kasumov et al. 2015, Maillard et al. 2016) and to reduce hepatic fat content in T2DM patients (Cheng et al. 2017). More importantly, combining exercise with dietary interventions sufficiently prevented the onset of T2DM in obese subjects and thereby represents an alternative strategy to pharmacological treatments (Tuomilehto et al. 2001, Knowler et al. 2002). In addition, regular physical activity has been shown to lower the risk of developing T2DM at later ages of life, clearly emphasizing the importance of using exercise as a preventive tool to reduce the global health burden of T2DM (Lao et al. 2018). However, studies revealed the existence of a large diversity in the ability to respond to exercise, with a substantial percentage of T2DM patients not improving their glycaemia and insulin sensitivity despite performing intensive exercise regimens (Stephens & Sparks 2015). Due to the incidence of these so-called “non-responders”, understanding the cellular signalling pathways and identifying possible new targets that drive the exercise-induced improvements of glycaemia is crucial for the treatment of each T2DM individual.

1.4.2 Modes of exercise

Research studies largely vary in the mode of exercise used. In general, resistance and endurance exercise represent the two main types of training. While resistance (or strength) exercise involves the contraction of defined muscle groups at low frequency, e.g. during weight lifting, endurance (or aerobic) exercise consists of the contraction of diverse muscle groups at high frequency, e.g. during running. Resistance training primarily aims at increasing muscle hypertrophy, strength and power, whereas the primary outcome of endurance training is an elevated skeletal muscle oxidative function and endurance capacity (Roden 2012, Methenitis 2018). Since both modes are in general sufficient to improve insulin sensitivity, a combination of endurance and resistant exercise is recommended for the treatment of T2DM nowadays (Colberg et al. 2016, Pesta et al. 2017). Besides the mode, exercise studies greatly vary in the duration, intensity and frequency of training sessions. Regular training programs used to improve glycaemia usually involve a five-day exercise program lasting for several weeks, including daily exercise sessions of approximately 60 minutes of running at moderate intensity (Nishida et al. 2004). However, those types of exercise interventions require a high time commitment of the participants. Thus, High-intensity training (HIT) programs have recently emerged as a time-efficient alternative to moderate exercise (Jung et al. 2014). HIT consists of short high-intensity intervals of physical activity, interspersed by periods of low-intensity intervals or recovery. Weekly training sessions of HIT programs are usually reduced to three days a week (Madsen et al. 2015). Although inducing similar metabolic adaptations, HIT has

been shown to be more effective to increase aerobic capacity and to reduce T2DM-associated risk factors (Hafstad et al. 2013).

1.4.3 Whole-body adaptations to chronic exercise

Chronic exercise induces a variety of improvements in whole-body metabolism, such as reducing whole-body fat content, increasing insulin sensitivity and reducing inflammation processes. Furthermore, endurance training induces cardiovascular improvements by increasing blood circulation and cardiac stroke volume, while simultaneously reducing blood pressure (Egan & Zierath 2013). Thus, regular exercise training improves overall physical fitness. An important parameter to assess physical or aerobic fitness is the maximal oxygen consumption (VO_{2max}). During exercise, a sufficient supply of oxygen is required for the working skeletal muscles in order to provide energy via the mitochondrial oxidative phosphorylation pathway. VO_{2max} represents the maximum amount of oxygen that can be taken up and utilized by the muscles. With increasing workload during prolonged exercise, the oxygen consumption (VO_2) will concomitantly increase until it reaches a plateau, representing the upper limit of the cardiorespiratory system to supply the muscles with oxygen. Thus, higher VO_{2max} values are associated with increased endurance capacity (Bassett & Howley 2000, MacInnis et al. 2015). Healthy individuals exhibit a 10 - 20 % increase of VO_{2max} after performing chronic exercise, depending on the intensity of the exercise protocol (Gormley et al. 2008, Nybo et al. 2010). Although physical fitness is usually impaired in patients with metabolic syndrome or T2DM and thereby contributes to the pathophysiological course of the diseases (Reusch et al. 2013), chronic interval training has been shown to substantially increase VO_{2max} in these patients (Mora-Rodriguez et al. 2014, Stoa et al. 2017). In addition to VO_{2max}, the length of time running (time to exhaustion) is accepted as an adequate readout for endurance capacity (Booth et al. 2012).

During aerobic endurance exercise, the working skeletal muscles convert glucose or lipids to CO_2 and H_2O in order to provide energy via ATP generation. Depending on the duration and intensity of the training, the metabolism switches between either lipids or glucose as preferred substrate for energy provision. At moderate intensities, skeletal muscle is supplied by both, glucose and lipids derived from hepatic glycogenolysis or adipocyte lipolysis, respectively. During prolonged exercise, lipid oxidation represents the main contributor to energy supply. At high exercise intensities, the skeletal muscle substrate utilization changes from lipid oxidation towards increased use of carbohydrates, mainly derived from increased muscle glycogen breakdown (Egan & Zierath 2013). Thus, the amount of consumed O_2 and produced CO_2 changes in response to altered substrate utilization, depicted in the respiratory exchange ratio

(RER). The RER is the ratio of exhaled CO_2 and consumed O_2 (VCO_2/ VO_2) and can be used as a surrogate parameter for the determination of the preferred substrate used for energy metabolism. RER values around 1.0 indicate primary carbohydrate oxidation (CHO), since the amount of O_2 needed for the oxidation of glucose is equal to the amount of produced CO_2. In contrast, low RER values (< 0.7) indicate increased oxidation of fatty acids (FAO), since the oxidation of lipids requires more O_2 molecules (Manore et al. 2009). Therefore, the RER is considered to be elevated at high-intensities, whereas prolonged moderate exercise leads to a reduced RER (Egan & Zierath 2013).

Another important metabolic adaptation to exercise is the synthesis of lactate as an additional fuel source. With increasing exercise intensity, the higher rates of glycolysis exceed the mitochondria's capacity to metabolise the generated pyruvate. Therefore, the metabolism switches towards anaerobic substrate utilization and converts pyruvate to lactate, which is released into circulation to fuel extra-muscular tissues such as the liver (Nalbandian & Takeda 2016). However, when high-intensity exercise continues, the blood lactate concentration rises, since the rate of lactate production exceeds the rate of removal from the blood. The threshold of reaching a certain blood lactate concentration represents an accurate marker for aerobic endurance capacity, i.e. to maintain the exercise performance without reaching excessive blood lactate accumulation (Ferreira et al. 2007, Goodwin et al. 2007).

1.4.4 Effects of chronic exercise on glucose and lipid metabolism in skeletal muscle, adipose tissue and liver

1.4.4.1 Exercise action in skeletal muscle

During physical activity, the skeletal muscle significantly contributes to whole-body glucose disposal by increased glucose uptake via contraction-mediated GLUT4 translocation. Human studies have shown that already acute bouts of exercise are able to increase plasma membrane GLUT4 content in both healthy and T2DM patients (Kennedy et al. 1999). Likewise, chronic exercise substantially increases GLUT4 abundance in skeletal muscle (Stuart et al. 2010). The translocation of muscular GLUT4 to the plasma membrane during exercise is mainly regulated by the AMPK (see Figure 1), which is activated via phosphorylation at Threonine residue Thr^{172}. Depending on the intensity of the exercise protocol, acute bouts of exercise induce AMPK phosphorylation, which promotes glucose uptake and G6P synthesis (Egan et al. 2010). Furthermore, AMPK regulates glycogenolysis to ensure skeletal muscle fuel supply during high intensities, by inhibiting glycogen synthesis and promoting glycogen breakdown. Since glycogenolysis represents an important fuel source for the working skeletal muscle, glycogen availability determines the endurance capacity. Regular training has been

described to increase skeletal muscle glycogen content and thereby counteracts the rapid depletion during exercise performance (Manabe et al. 2013). Furthermore, AMPK regulates lipid metabolism by increasing fatty acid uptake and subsequent oxidation, while simultaneously inhibiting fatty acid synthesis (Jeon 2016). In addition, chronic exercise has been shown to increase total AMPK protein abundance, indicating increased basal activity (Frosig et al. 2004). Chronic activation of AMPK in turn alters the gene expression of important exercise-responsive transcription factors, such as the peroxisome proliferator-activated receptor γ coactivator-1α (PGC-1α; gene name *PPARGC1A*). PGC-1α is considered as a key transcription factor in mediating metabolic changes in skeletal muscle upon exercise. Endurance exercise substantially upregulates PGC-1α expression, which in turn activates various other transcription factors that promote mitochondrial biogenesis, FAO and increased skeletal muscle oxidative capacity (Baar et al. 2002, Arany 2008).

1.4.4.2 Exercise action in adipose tissue

The main function of the white adipose tissue (WAT) during exercise is to supply the skeletal muscle with lipids by increased lipolysis and release of NEFA into circulation (see 1.3.3). Thus, plasma NEFA concentrations are elevated during exercise, but often remain unchanged due to the immediate removal by skeletal muscle (Karpe et al. 2011). In contrast, chronic endurance exercise reduces fasting plasma NEFA concentrations, presumably due to decreased adipose tissue lipolysis (Phielix et al. 2012). Thus, chronic exercise may prevent elevated plasma NEFA concentrations in T2DM conditions (see 1.3.4). Another function of the WAT is the contribution to whole-body glucose disposal via GLUT4-mediated glucose uptake. Chronic exercise has been shown to significantly increase basal, as well as insulin-stimulated glucose uptake in WAT, probably due to increased abundance of GLUT4 (Stephenson et al. 2013, Trevellin et al. 2014, Marcinko et al. 2015). These findings mainly derive from rodent studies, however, a small number of human studies have reported similar effects of endurance training on glucose uptake and GLUT4 protein content in WAT (Hussey et al. 2011, Motiani et al. 2017).

The brown adipose tissue (BAT) represents the second major fat site. Compared to WAT, the BAT is a mitochondrial-rich tissue that mainly functions in energy expenditure by performing thermogenesis, i.e. producing heat in order to protect the metabolism from environmental cold exposure. The process of thermogenesis is mediated by the BAT-specific mitochondrial uncoupling protein 1 (UCP-1), which uncouples the proton entry from ATP synthesis in the mitochondrial oxidative phosphorylation pathway and thereby releases energy as heat (Lowell & Spiegelman 2000). Although the BAT has long been considered to be only functional in

rodents and human newborns, its appearance and function for energy metabolism in adult humans was confirmed in later years (Nedergaard et al. 2007, Cypess et al. 2009). In addition to thermogenesis, brown fat has been shown to utilize high amounts of glucose by GLUT1- and GLUT4-dependent glucose uptake and thus substantially contributes to glucose homeostasis (Stanford et al. 2013, Olsen et al. 2014). In subcutaneous white adipose tissue (scWAT), regular exercise has been shown to induce adipocytes that share characteristics of brown adipose cells. This so-called “browning” or “beiging” process involves the upregulation of UCP-1 expression and various other brown adipocyte-specific marker genes, resulting in increased mitochondrial activtiy and biogenesis of the scWAT (Trevellin et al. 2014, Stanford, Middelbeek, & Goodyear 2015). Since brown adipocytes utilize fatty acids for thermogenesis, the exercise-induced browning of scWAT is considered as a possilbe mechanism to reduce overall obesity in T2DM patients (Ishibashi & Seale 2010). Furthermore, exercise-trained scWAT was associated with improved glucose tolerance in mice, suggesting a possible impact of browning on improved insulin sensitivity (Stanford, Middelbeek, Townsend, et al. 2015).

1.4.4.3 Exercise action in the liver

The release of hepatic glucose via glycogenolysis contributes to skeletal muscle and adipose tissue energy supply during moderate-intensity exercise. Thus, hepatic glycogen stores are depleted during prolonged exercise, but subsequently restored during postprandial periods (Casey et al. 2000, Gonzalez et al. 2015). With increasing duration of exercise, increased rates of gluconeogenesis contribute to total hepatic glucose output in order to supply extrahepatic tissues with glucose. This is mainly due to increased availability of gluconeogenic substrates, e.g. skeletal muscle-deriving lactate and amino acids, as well as upregulation of gluconeogenic enzymes such as the PCK (Knudsen et al. 2015, Shephard & Johnson 2015). Chronic endurance training has been reported to increase hepatic glycogen stores at rest, while rates of glycogenolysis and gluconeogenesis are reduced during exercise (Coggan et al. 1995, Murakami et al. 1997). This ensures an increased endurance capacity before reaching exhaustion due to depletion of skeletal muscle and hepatic glycogen stores during exercise. More importantly, reducing hepatic gluconeogenesis after chronic exercise contributes to improved glycaemia at insulin-resistant states, as evident from rodent studies (Chang et al. 2006). Besides its effects on glycogenolysis and gluconeogenesis, chronic exercise reduces hepatic triglyceride content. After performing regular exercise, T2DM patients exhibited a marked reduction of hepatic triglycerides, associated with improved insulin sensitivity (Bacchi et al. 2013, Lee et al. 2013). The reduction of hepatic triglyceride content can presumably be attributed to reduced plasma NEFA uptake, increased mitochondrial oxidative phosphorylation, reduced fatty acid synthesis, as well as reduced DNL (Brouwers et al. 2016).

Taken together, chronic exercise increases skeletal muscle and adipose tissue glucose uptake, reduces adipose tissue lipolysis and reduces hepatic triglyceride content (Figure 3). Thereby, chronic exercise counteracts the disturbed glucose and lipid homeostasis in T2DM conditions (cp. Figure 2).

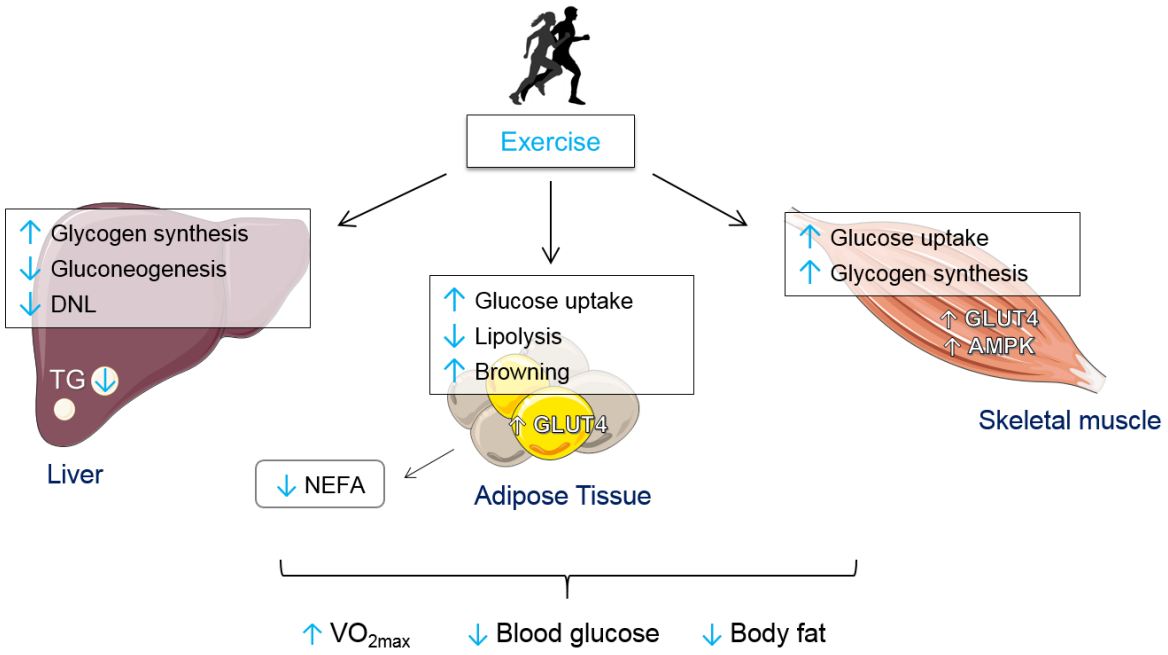

Figure 3: Improved glucose and lipid metabolism after chronic exercise. Chronic exercise increases AMPK- and GLUT4-mediated skeletal muscle glucose uptake. Both, increased skeletal muscle and hepatic glycogen synthesis contribute to improved endurance capacity during exercise. Gluconeogenesis, DNL and hepatic triglycerides are reduced, resulting in improved insulin sensitivity. Effects of chronic exercise on adipose tissue include increased glucose uptake, reduced lipolysis and increased browning of scWAT. Consequently, chronic exercise improves physical fitness, reduces whole-body fat content and improves glycaemic control. TG, triglycerides.

1.5 Mouse models in T2DM research

The generation of mouse models represents a useful tool to investigate the pathophysiology of human T2DM. Although human GWAs contributed to the discovery of gene variants associated with T2DM prevalence, the function of a high proportion of these genes remains unknown. Thus, using transgenic or knockout (KO) techniques, mouse models are helpful to elucidate the role and function of specific gene variants in T2DM (Joost et al. 2012). Importantly, the human and murine genome share an almost 96 % identity, allowing the transfer of murine findings to the human phenotype of the disease (Waterston et al. 2002). Since human T2DM is closely linked to obesity, mouse models for T2DM usually consist of an obesity-associated hyperglycaemic or beta cell failure-phenotype. Apart from naturally occurring mutations and genetic manipulations using transgenic or KO-lines, feeding a high-fat diet (HFD) is a common intervention to induce obesity-linked insulin resistance in mice.

Although mainly representing a polygenic disease, rare forms of T2DM are of monogenic origin (see 1.2). Concomitantly, monogenic mouse models are used to elucidate the role of single gene variants in the pathophysiology of T2DM. Most prominently, mice deficient in leptin signalling were discovered as a monogenic form of obesity (King 2012). Leptin is a hormone secreted by the adipose tissue that regulates satiety. Both, the lack of leptin in $Lep^{ob/ob}$ mice or the lack of the leptin receptor in $Lepr^{db/db}$ mice causes obesity, hyperinsulinemia and hyperglycaemia, a phenotype similar to reported mutations in the orthologous human genes (Kobayashi et al. 2000, Lindstrom 2007, Joost & Schürmann 2014). However, single gene variants are rare and therefore may not explain the polygenic pathophysiology of T2DM in the general population. Thus, polygenic mouse models such as the diabetic KK mice are useful to discover new T2DM-associated genes, since they exhibit similar characteristics of the human disease including obesity, hyperinsulinemia and peripheral insulin resistance (King 2012).

In the present thesis, the impact of exercise on improving glycaemia should be investigated in both, a monogenic and polygenic mouse model for insulin resistance and T2DM. Whole-body *Tbc1d4*-KO mice were used as a monogenic mouse model, since the deletion of this protein has been shown to impair whole-body glycaemia and insulin sensitivity (Wang et al. 2013, Chadt et al. 2015, Xie et al. 2016). A similar impaired phenotype has previously been described for humans carrying a nonsense mutation in the *TBC1D4* gene (Moltke et al. 2014). Secondly, the New Zealand Obese (NZO) mice was selected as a polygenic mouse model, since it virtually resembles the phenotype of the human metabolic syndrome and T2DM (Ortlepp et al. 2000, Jürgens et al. 2007). Metabolic features of the two mouse models are presented in the following sections.

1.5.1 Structure and function of the RabGAP protein TBC1D4

The protein TBC1D4 (also known as AS160, AKT substrate of 160 kDa) belongs to the family of RabGTPase-activating proteins (RabGAPs) that regulate intracellular vesicular trafficking. A regulated vesicular transport of proteins between distinct membrane-bound organelles is essential for eukaryotic cell homeostasis. Once synthesized in the ER, proteins are packed into vesicles and transported through the Golgi complex and further delivered to their required destination. This complex pathway is regulated by Rab proteins, small GTPases that are involved in various points of vesicular trafficking, such as vesicle formation, transport and docking and fusion with the target membrane to release the proteins (Stenmark 2009, Fukuda 2011). Rab proteins change their confirmation from the inactive guanosine-diphosphate (GDP)-bound state to the active guanosine triphosphate (GTP)-bound state, which enables the regulation of vesicular processes by interaction with effector proteins. Whereas guanine

nucleotide exchange factor (GEF) proteins catalyse the conversion from GDP to GTP, GAP proteins mediate the reversed reaction and thereby inactivate the respective RabGTPase (Fukuda 2011). The RabGAP TBC1D4 is a protein of 1298 amino acids and consists of two N-terminal phosphotyrosine-binding (PTB) domains, a central calmodulin-binding (CBD) domain and the C-terminal GAP domain. Along with its close homologue TBC1D1, TBC1D4 regulates GLUT4 translocation via its GAP-activity (Sakamoto & Holman 2008). At basal states, the active GAP domain renders the GLUT4-associated RabGTPases in their inactive GDP-bound form. After insulin-stimulation or skeletal muscle contraction, TBC1D1 and TBC1D4 are phosphorylated, which inactivates the GAP domain and thereby promotes the active Rab-dependent GLUT4 translocation to the plasma membrane (Figure 4).

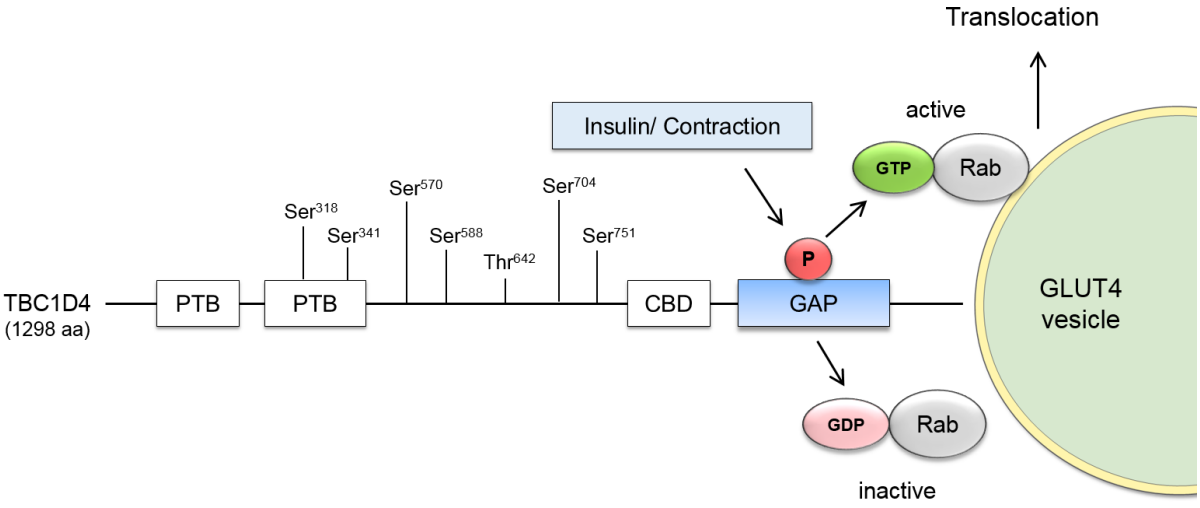

Figure 4: Structure and function of the RabGAP TBC1D4. TBC1D4 consists of two PTB domains, one CBD domain and the functional GAP domain, which renders Rab proteins in their inactive GDP-bound state at basal conditions. At stimulated conditions (insulin or skeletal muscle contraction), TBC1D4 is phosphorylated at distinct Ser and Thr residues. This inactivates the GAP domain and thereby activates the Rab protein to its GTP-bound state, resulting in enhanced GLUT4 translocation. aa; amino acids; P, phosphorylation (modified from Mafakheri et al. 2018).

The identification of several AKT and AMPK phosphorylation sites at Serine (Ser) and Threonine (Thr) residues has verified the regulation of TBC1D4 in insulin- and contraction-mediated glucose uptake, respectively (Figure 4). AKT was shown to phosphorylate TBC1D4 at Ser^{318} and Ser^{570}, whereas AMPK phosphorylates TBC1D4 at Ser^{588} and Ser^{751}. Moreover, Ser^{341}, Thr^{642} and Ser^{704} were found to be phosphorylated by both, AKT and AMPK activity (Mafakheri et al. 2018). Various studies further confirmed the role of TBC1D4 as a key regulator of insulin- and contraction-mediated glucose uptake in skeletal muscle and adipose tissue. Overexpression of TBC1D4 with mutated phosphorylation sites abrogated the insulin-stimulated GLUT4 translocation in both, skeletal muscle cells and adipocytes (Sano et al. 2003, Thong et al. 2007). Moreover, *in vivo* electroporation of mutant TBC1D4 in murine

skeletal muscles inhibited the insulin- and contraction-mediated glucose uptake, whereas disruption of its RabGAP activity prevented this inhibition (Kramer et al. 2006). Thus, these findings highlight the importance of TBC1D4 and its GAP domain in regulating insulin- and contraction-mediated GLUT4-dependent glucose uptake in skeletal muscle and adipose tissue.

1.5.2 Metabolic features of *Tbc1d4*-deficient (D4KO) mice

Further insight into the function of TBC1D4 on glucose and lipid metabolism was gained from studies using whole-body *Tbc1d4*-KO mice, in the following referred to as D4KO. Similar to the above-mentioned mutant studies, D4KO mice exhibited an impaired insulin- and contraction-mediated glucose uptake with a concomitant decrease in GLUT4 protein abundance in the oxidative *Soleus* muscle and adipose tissue. Interestingly, glucose uptake in glycolytic muscles such as *Extensor digitorum longus* (EDL) or *Gastrocnemius* remained unaffected by *Tbc1d4*-deficiency. These observations probably reflect the tissue-specific expression pattern of TBC1D4, which is highly expressed in the oxidative *Soleus* muscle and adipose tissue, with only minor expression in glycolytic muscle types (Wang et al. 2013, Chadt et al. 2015). Apart from its main impact on glucose uptake, lack of TBC1D4 substantially affects whole-body metabolism, as it has been shown to induce postprandial hyperglycaemia, hyperinsulinemia and to impair insulin tolerance after intraperitoneal injection of insulin (Lansey et al. 2012, Xie et al. 2016). Furthermore, deficiency of TBC1D4 confers hepatic insulin resistance, as indicated by impaired suppression of insulin-dependent hepatic glucose production and enhanced abundance of gluconeogenesis-regulating proteins in mice (Wang et al. 2013). When raised on a regular standard diet (SD), D4KO mice exhibited lower body weight due to reduced fat mass and a reduced RER, associated with elevated whole-body and skeletal muscle FAO. This indicated an increased use of lipids for substrate utilization in D4KO mice (Chadt et al. 2015). Taken together, these findings point towards a crucial role for TBC1D4 in regulating peripheral insulin- and contraction-mediated glucose uptake, as well as regulating glucose and lipid preference for substrate utilization.

However, no studies investigating the impact of regular exercise on whole-body metabolism of D4KO mice have been conducted so far. A previous study showed that endurance performance and exercise-mediated glucose uptake in glycolytic muscle fibres was impaired in TBC1D1-KO mice, implicating a role for TBC1D1 in regulating exercise metabolism (Stöckli et al. 2015). Whether D4KO mice may display a similarly compromised endurance performance and, more importantly, whether regular exercise may restore insulin sensitivity and glycaemia in these mice, remains to be determined.

1.5.3 The NZO mice as a polygenic model for human T2DM

The NZO mouse was discovered as a model for obesity after outbreeding experiments in the late 1940s, in which mice carrying early-onset adiposity were selected for further cross-breeding. The development of adiposity in the resulting inbred strain was shown to be associated with impaired glucose tolerance and reduced insulin sensitivity (Bielschowsky & Bielschowsky 1956, Joost et al. 2012). In addition to obesity, NZO mice display essential characteristics of the human metabolic syndrome and T2DM, including hyperglycaemia, insulin resistance, hypercholesterolemia and dyslipidaemia (Ortlepp et al. 2000). Moreover, NZO mice are characterized by a marked elevation of serum and adipose tissue leptin concentrations (hyperleptinaemia), further contributing to the obese phenotype (Igel et al. 1997). The development of insulin resistance induces hypertrophy and hyperplasia of the pancreatic beta cells already at early weeks of life, resulting in progressive beta cell loss with increasing age. However, the beta cell destruction exclusively affects the male mice, while female mice are protected from T2DM-induced beta cell loss (Junger et al. 2002). This T2DM-protective effect was at least partly attributed to the function of the hormone estrogen, since ovariectomized female NZO mice exhibited a similar impaired phenotype compared to male mice, including hyperglycaemia, insulin resistance and beta cell loss (Vogel et al. 2013). Furthermore, elevated serum insulin levels may compensate for the peripheral insulin resistance in female mice (Ortlepp et al. 2000). Thus, only male NZO mice mimic the phenotype of human T2DM.

The development of obesity and T2DM in NZO mice is caused by a complex interaction between the polygenetic predisposition and environmental factors such as excessive energy intake (Vogel et al. 2018). Exposure to a HFD has been shown to strongly accelerate the onset of obesity and hyperglycaemia in NZO mice, associated with increased T2DM prevalence. In contrast, caloric restriction or feeding a SD with reduced amount of fat prevented the early-onset of hyperglycaemia in NZO mice (Jürgens et al. 2007, Kluth et al. 2011, Baumeier et al. 2015). Interestingly, not only the fat, but also the carbohydrate content drives the development of T2DM in NZO mice. While a carbohydrate-free diet prevented the onset of hyperglycaemia in NZO mice, subsequent carbohydrate refeeding caused severe insulin resistance (Kluth et al. 2011). More importantly, the onset of obesity and T2DM in NZO mice was associated with impaired physical activity, as NZO mice exhibited reduced running wheel activity and overall reduced energy expenditure compared to the related lean New Zealand Black (NZB) and C57BL/6J (B6) mouse strains (Jürgens et al. 2006). Thus, the NZO mice can be considered as a naturally inactive strain. This raises the question, whether a regular forced exercise intervention may prevent or delay the onset of T2DM in NZO mice. However, no studies addressing this question have been reported to date.

1.6 Aim of the study

Chronic exercise represents a useful intervention for the prevention and treatment of T2DM. Regular physical activity has been shown to improve peripheral and whole-body insulin sensitivity and to reduce the excessive lipid accumulation, thereby lowering the T2DM prevalence. However, the exact cellular pathways that confer the exercise-mediated improvements in glycaemic control still remain unclear. More importantly, whether all individuals will benefit from a certain exercise intervention strongly depends on genetic and environmental factors, resulting in a heterogeneous response to exercise. The aim of this study was to investigate the impact of chronic exercise on glucose homeostasis in (1) a monogenic and (2) a polygenic mouse model for impaired insulin sensitivity, with the following research question: **Can regular exercise improve glycaemia in two mouse models for impaired insulin sensitivity?**

To investigate the impact of exercise on glycaemic control, the exercise capacity, glucose and insulin tolerance, as well as whole-body substrate utilization of the mice were measured. Moreover, skeletal muscle, adipose tissue and hepatic glucose metabolism was assessed, as these three organs represent the main tissues regulating whole-body glucose homeostasis. Dependent on the respective mouse model, specific research questions were additionally addressed in this study.

(1) *Tbc1d4*-KO (D4KO) mice as a monogenic mouse model for insulin resistance

Deficiency of TBC1D4 in mice leads to postprandial hyperglycaemia, impaired skeletal muscle and adipose tissue glucose uptake and whole-body insulin resistance (Lansey et al. 2012, Wang et al. 2013, Chadt et al. 2015, Xie et al. 2016). Thus, it should be investigated at first, whether lack of TBC1D4 affects the exercise capacity and secondly, whether regular exercise would restore glycaemia and overcome the peripheral insulin resistance in D4KO mice.

(2) New Zealand Obese (NZO) mice as a polygenic mouse model for T2DM

NZO mice are characterized by development of severe hyperglycaemia and insulin resistance, finally leading to beta cell loss and T2DM. Moreover, NZO mice are associated with impaired physical activity (Ortlepp et al. 2000, Jürgens et al. 2006). Therefore, it had to be elucidated whether regular exercise would improve physical capacity and prevent or delay the onset of T2DM in NZO mice.

2. Materials and methods

2.1 Materials

2.1.1 Mouse strains

The mouse strains used for the exercise studies are listed in Table 1. To generate *Tbc1d4*-deficient mice, an intercross of the heterozygous recombinant congenic line RCS.B6.SJL-*Nob1.10*$^{B6/SJL}$-*Tbc1d4*$^{+/-}$ mice was performed, leading to the generation of wildtype (WT, RCS.B6.SJL-*Nob1.10*$^{B6/B6}$-*Tbc1d4*$^{+/+}$) and *Tbc1d4*-deficient (D4KO, RCS.B6.SJL-*Nob1.10*$^{B6/B6}$-*Tbc1d4*$^{-/-}$) mice.

Table 1: Mouse strains

Strain	Supplier
RCS.B6.SJL-*Nob1.10*$^{B6/SJL}$-*Tbc1d4*$^{+/-}$	DDZ, Düsseldorf, Germany
C57BL/6J	DDZ, Düsseldorf, Germany
New Zealand obese (NZO/HI)	DDZ, Düsseldorf, Germany

2.1.2 Mouse diets

The standard diet (SD) was purchased from ssniff (Soest, Germany) and all the high-fat diets (HFD) were purchased from Research Diets Inc. (New Brunswick, NJ, USA). Composition of the diets is summarized in Table 2.

Table 2: Composition of mouse diets

Diet (Cat.-No.)	Fat (cal %)	Protein (cal %)	Carbohydrate (cal %)	Sucrose (cal %)	Total calorie content (kcal/g)
SD (V1126)	11	36	53	*n.s.*	3,3
60 % HFD (D12492)	60	20	20	6,8	5,2
45 % HFD (D12451)	45	20	35	17,0	4,7
30 % HFD (99041301)	30	20	50	24,5	4,3
30 % HFD-RS (D09152701)	30	20	50	17,5	4,3
20 % HFD-RS (D09152702)	20	20	60	17,5	4,1

n.s., not specified.

2.1.3 Primers

Hexanucleotide primers for cDNA synthesis were purchased from Roche (Mannheim, Germany). For quantitative Real-Time PCR experiments, SYBR Green primers were purchased from Eurogentec (Liège, Belgium, Table 3).

Table 3: SYBR Green primers

Gene symbol	Gene name	Sequence 5'-3'
Cidea	Cell death-inducing DFFA-like effector A	Fwd: CATACATGCTCCGAGTACTGG Rev: CATCCCACAGCCTATAACAGAG
Cox8b	Cytochrome c oxidase subunit 8B	Fwd: AGCCAAAACTCCCACTTCC Rev: TCTCAGGGATGTGCAACTTC
Hprt	Hypoxanthine guanine phosphoribosyl transferase	Fwd: AAGCTTGCTGGTGAAAAGGA Rev: TTGCGCTCATCTTAGGCTTT
P2rx5	Purinergic receptor P2X, ligand-gated ion channel 5	Fwd: TGATAGTTAATGGCAAGGCGG Rev: TTGTCTCGGTAAAACTCGCTC
Ppargc1a	Peroxisome proliferator-activated receptor gamma coactivator-1 alpha	Fwd: GAGTCTGAAAGGGCCAAACA Rev: TGCATTCCTCAATTTCACCA
Slc2a4	Solute carrier family 2 (facilitated glucose transporter), member 4	Fwd: CAGCGAGTGACTGGAACACT Rev: CAATCACCTTCTGTGGGGCA
Ucp-1	Uncoupling protein 1	Fwd: GCATTCAGAGGCAAATCAGC Rev: GCCACACCTCCAGTCATTAAG

2.1.4 Antibodies

Table 4: Antibodies

Antibody, Cat.-No.	Supplier
Primary antibodies	
Rabbit-anti-AMPKα, #2532	Cell Signaling Technology (Danvers, MA, USA)
Rabbit-anti-AS160/TBC1D4 (Rab-GAP), #07-741	Merck (Darmstadt, Germany)
Rabbit anti-Fatty Acid Synthase (C20G5), #3180	Cell Signaling Technology (Danvers, MA, USA)
Rabbit-anti-GAPDH (14C10), #2118	Cell Signaling Technology (Danvers, MA, USA)
Rabbit-anti-GCK (H-88), #sc-7908	Santa Cruz Biotechnology (Dallas, TX, USA)
Rabbit-anti-GLUT1, custom-made	Prof. Schürmann (DIfE, Potsdam, Germany)
Rabbit-anti-GLUT4, custom-made	Prof. Al-Hasani (DDZ, Düsseldorf, Germany)
Rabbit-anti HK-II, #2867	Cell Signaling Technology (Danvers, MA, USA)
Rabbit-anti-PCK1, #ab87340	Abcam (Cambridge, UK)

Rabbit-anti-PCK2, #6924	Cell Signaling Technology (Danvers, MA, USA)
Rabbit-anti-PGC1 alpha+beta, #ab72230	Abcam (Cambridge, UK)
Rabbit-anti-phospho-AMPKα (Thr^{172}), #2531	Cell Signaling Technology (Danvers, MA, USA)
Rabbit-anti-UCP-1, #ab10983	Abcam (Cambridge, UK)
Secondary antibodies	
Goat-anti-rabbit IgG, #111-035-003	Dianova (Hamburg, Germany)

2.1.5 Reaction Kits

Table 5: Reaction Kits

Reaction Kit	Supplier
BCA Protein Assay Kit	Pierce (Rockford, IL, USA)
Glucose Liquicolor Kit	Human (Wiesbaden, Germany)
GoScript Reverse Transcription System	Promega (Madison, WI, USA)
GoTaq qPCR Master Mix	Promega (Madison, WI, USA)
Insulin (Mouse) Ultrasensitive ELISA	DRG Instruments (Marburg, Germany)
miRNeasy Mini Kit	Qiagen (Hilden, Germany)
NEFA-HR (2) Assay Kit	Wako Chemicals (Neuss, Germany)
RNase-free DNase Set (50)	Qiagen (Hilden, Germany)
Triglycerides Assay Kit	Randox (Crumlin, UK)
Western Lightning ECL Enhanced Chemiluminescence Substrate	PerkinElmer (Waltham, MA, USA)

2.1.6 Enzymes and molecular weight size markers

Table 6: Enzymes and molecular weight size markers

Enzyme and molecular weight size marker	Supplier
Amyloglucosidase from *Aspergillus niger*	Sigma-Aldrich (St. Louis, MO, USA)
Dual Color Precision Plus Protein Standard	Bio-Rad (Hercules, CA, USA)
Precision Plus Protein All Blue Prestained Protein Standard (stain-free)	Bio-Rad (Hercules, CA, USA)
Precision Plus Protein Unstained Standard (stain-free)	Bio-Rad (Hercules, CA, USA)

2.1.7 Chemicals

Table 7: Chemicals

Chemical	Supplier
[^{3}H]-2-deoxyglucose	Hartmann Analytic (Braunschweig, Germany)
[^{14}C]-D-glucose	Hartmann Analytic (Braunschweig, Germany)
[^{14}C]-mannitol	PerkinElmer (Waltham, MA, USA)
2-deoxyglucose	Sigma-Aldrich (St. Louis, MO, USA)
2-propanol	Applichem (Darmstadt, Germany)
Acetic acid (100 %)	Carl Roth (Karlsruhe, Germany)
Acrylamid 4K Solution (37.5:1; 30 %)	Applichem (Darmstadt, Germany)
Actrapid Penfill Insulin human	Novo Nordisk (Bagsværd, Denmark)
Adenosine	Sigma-Aldrich (St. Louis, MO, USA)
Albumin Fraction V (BSA)	Merck (Darmstadt, Germany)
Ammonium persulfate (APS)	Serva (Heidelberg, Germany)
Avertin (2,2,2-Tribromoethanol)	Sigma-Aldrich (St. Louis, MO, USA)
Bromophenol blue	Applichem (Darmstadt, Germany)
Calcium chloride dihydrate ($CaCl_2 \cdot 2\ H_2O$)	Merck (Darmstadt, Germany)
Chloroform	Applichem (Darmstadt, Germany)
Collagenase Type 1	Worthington Biochemical (Lakewood, NJ, USA)
D-(+)-Glucose	Sigma-Aldrich (St. Louis, MO, USA)
Deoxynucleoside Triphosphate Set (dNTPs)	Roche (Mannheim, Germany)
Dinonyl Phthalate	PHYWE (Göttingen, Germany)
Dithiothreitol (DTT)	Carl Roth (Karlsruhe, Germany)
Ethanol, absolute (EtOH)	Merck (Darmstadt, Germany)
Ethylenediaminetetraacetic acid (EDTA)	Carl Roth (Karlsruhe, Germany)
Ethylene glycol bis(2-aminoethylether)-N, N, N', N'-tetra acetic acid (EGTA)	Carl Roth (Karlsruhe, Germany)
Glucose (20 %)	B Braun (Melsungen, Germany)
Glycerol	MP Biomedicals (Santa Ana, CA, USA)
Glycine	Applichem (Darmstadt, Germany)
HEPES (4-(2-hydroxyethyl)-1-piperazineethanesulfonic acid)	Sigma-Aldrich (St. Louis, MO, USA)

Heptane (Isomers)	Carl Roth (Karlsruhe, Germany)
Hydrochloric acid (HCl)	Carl Roth (Karlsruhe, Germany)
Isoflurane	Piramal Healthcare (Morpeth, UK)
Magnesium sulfate heptahydrate ($MgSO_4 \cdot 7\ H_2O$)	Merck (Darmstadt, Germany)
Mannitol	Applichem (Darmstadt, Germany)
Methanol	Carl Roth (Karlsruhe, Germany)
Phosphatase inhibitor tablets (PhosSTOP)	Roche (Mannheim, Germany)
Potassium chloride (KCl)	Merck (Darmstadt, Germany)
Potassium dihydrogen phosphate (KH_2PO_4)	Merck (Darmstadt, Germany)
Potassium hydroxide pellets (KOH)	Merck (Darmstadt, Germany)
Powdered milk	Carl Roth (Karlsruhe, Germany)
Protease Inhibitor Cocktail (cOmplete)	Roche (Mannheim, Germany)
QIAzol Lysis Reagent	Qiagen (Hilden, Germany)
Rotiszint eco plus	Carl Roth (Karlsruhe, Germany)
Sodium acetate	Sigma-Aldrich (St. Louis, MO, USA)
Sodium chloride (NaCl)	Carl Roth (Karlsruhe, Germany)
Sodium dodecyl sulfate (SDS)	Carl Roth (Karlsruhe, Germany)
Sodium hydrogen carbonate ($NaHCO_3$)	Merck (Darmstadt, Germany)
Sodium sulfate (Na_2SO_4)	Merck (Darmstadt, Germany)
Sulphuric acid	Carl Roth (Karlsruhe, Germany)
N, N, N', N'-Tetramethylendiamine (TEMED)	Carl Roth (Karlsruhe, Germany)
Tris	Carl Roth (Karlsruhe, Germany)
Triton X-100	Sigma-Aldrich (St. Louis, MO, USA)
Tween 20	Applichem (Darmstadt, Germany)

2.1.8 Buffers and solutions

Table 8: Buffers and solutions

Buffer and solution	Ingredients
Glucose uptake in isolated adipocytes	
Krebs-Ringer-Bicarbonate HEPES buffer (KRBH)	120 mM NaCl, 4 mM KH_2PO_4, 1 mM $MgSO_4 \cdot 7\ H_2O$, 1 mM $CaCl_2 \cdot 2\ H_2O$, 10 mM $NaHCO_3$, 30 mM HEPES, 5 % BSA, 200 nM adenosine freshly added, with/without 120 nM Insulin (pH 7.4)
Lipid extraction solution	78 Vol. % 2-propanol, 20 Vol. % heptane, 2 Vol. % sulphuric acid
Glucose uptake in isolated skeletal muscles	
Krebs-Henseleit buffer (KHB)	Stock I: 118.5 mM NaCl, 4.7 mM KCl, 1.2 mM KH_2PO_4, 25 mM $NaHCO_3$, gassing with carbogen gas for 20 min on ice; +Stock II: 2.5 mM $CaCl_2 \cdot 2\ H_2O$, 1.2 mM $MgSO_4 \cdot 7\ H_2O$, 5 mM HEPES, gassing with carbogen gas for 10 min on ice, 1 % BSA finally added
Hot incubation buffer	19 mM Mannitol, 1 mM 2-deoxyglucose with/without 120 nM Insulin, 2.5 µCi/ml [^{3}H]-2-deoxyglucose, 0.7 µCi/ml [^{14}C]-mannitol
Incubation buffer	15 mM Mannitol, 5 mM Glucose with/without 120 nM Insulin (solved in KHB)
Recovery buffer	15 mM Mannitol, 5 mM Glucose (solved in KHB)
Rinse buffer	20 mM Mannitol, with/without 120 nM Insulin (solved in KHB)
Glycogen content	
Sodium acetate buffer	0.12 M sodium acetate, 0.48 Vol. % acetic acid (pH 4.8)
Protein and Western Blot analysis	
Blocking solution	5 % powdered milk, TBS-Tween (1x)
Electrode buffer	25 mM Tris, 192 mM glycine, 0.1 % SDS
Laemmli sample buffer (4x LSB)	20 Vol. % glycerol, 8 % SDS, 10 mM EDTA, 0.25 M Tris, 6 % DTT, 0.2 % bromophenol blue (pH 6.8)
Lysis buffer	20 mM Tris-HCl, 150 mM NaCl, 1 mM EDTA, 1mM EGTA, 1 % Triton X-100 (pH 7.5) + 40 µl/ml cOmplete and 100 µl/ml PhosSTOP (freshly added)
Separating gel buffer	1.5 M Tris, 0.4 % SDS (pH 8.8)
Stacking gel buffer	0.5 M Tris, 0.4 % SDS (pH 6.8)
TBS-Tween buffer (TBS-T, 1x)	10 mM Tris, 150 mM NaCl, 0.05 Vol. % Tween 20
Transfer buffer	25 mM Tris, 192 mM glycine, 20 % methanol

2.2 Methods

2.2.1 Study design

Figure 5 shows the experimental time line for the D4KO training study. Male D4KO mice and WT littermates were fed a HFD with 60 % fat from calories at 10 weeks of life. In week 14, mice were randomly assigned to either trained mice or sedentary controls. Trained mice were subjected to a moderate four-week training program on treadmills during the light phase (2.2.2.2). To estimate the physical fitness of the mice, a physical capacity test was carried out at the beginning and end of training intervention in week 14 and 17, respectively (2.2.2.3). Body composition (2.2.2.5), indirect calorimetry (2.2.2.4), blood lactate concentrations (2.2.2.7), glucose tolerance (2.2.2.8) and insulin tolerance (2.2.2.9) were measured during the training intervention at the indicated time points. In the final week, glucose uptake was measured *ex vivo* in *Soleus* muscle (2.2.2.10) and isolated adipocytes from white adipose tissue (2.2.2.11). The remaining tissues were harvested during *ex vivo* measurements or after final heart puncture (2.2.2.12).

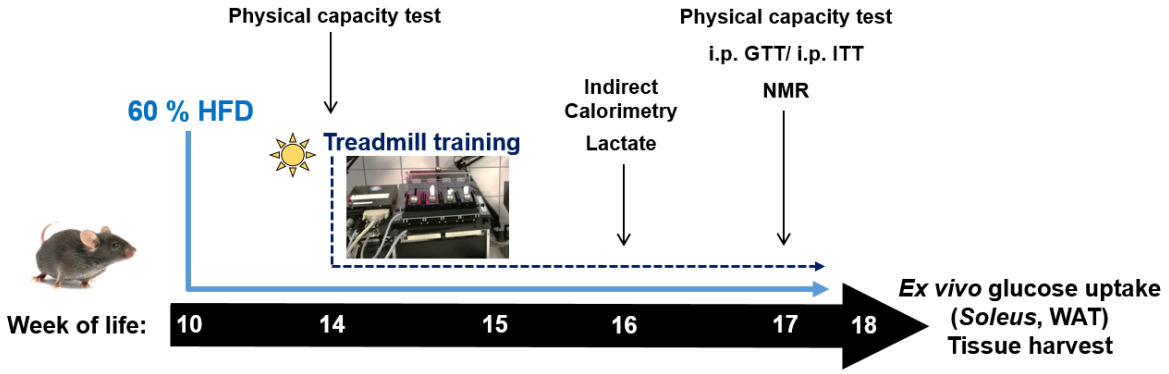

Figure 5: Study design for the four-week treadmill training with D4KO mice. From week 10 on, male D4KO or WT mice were fed a HFD with 60 % fat from calories for four weeks. At week of life 14, mice were subjected to a four-week forced treadmill training intervention during the light phase on five days a week with one exercise bout per day. Physical capacity was assessed at the beginning and end of training intervention.

For the NZO training study, the experimental design was changed towards a six-week chronic interval training, which was established in B6 mice (Figure 6). After weaning, male NZO mice were fed a HFD with 30 % fat from calories and reduced sucrose content (30 % HFD-RS). At week six of life, mice were randomly assigned to either the trained group or sedentary controls. The trained group was subjected to a six-week interval training program on treadmills during their active dark phase (2.2.2.2). Similar interventions as for the D4KO study were performed at the indicated time points. *Ex vivo* glucose uptake was measured in *EDL* muscle (2.2.2.10)

and isolated adipocytes from white adipose tissue (2.2.2.11). The remaining tissues were harvested during *ex vivo* measurements or after final heart puncture (2.2.2.12).

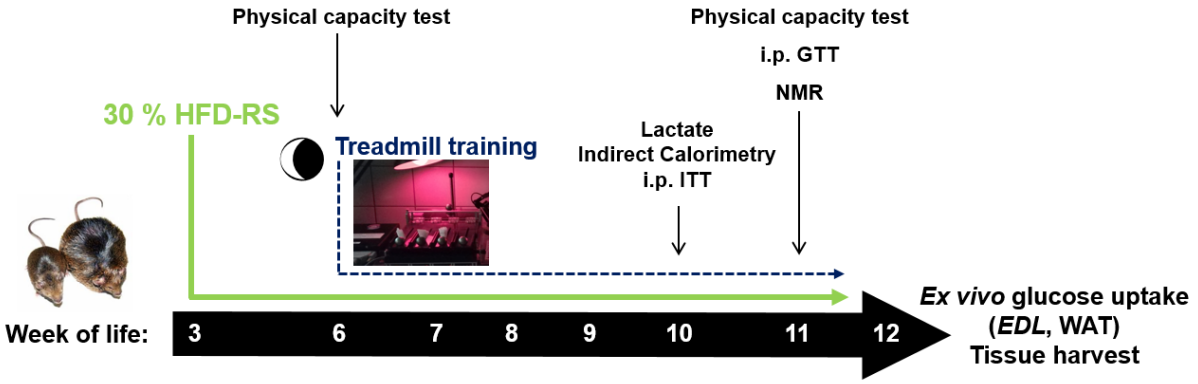

Figure 6: Study design for the six-week treadmill interval training with NZO mice. From week 3 on, male NZO mice were fed a HFD with 30 % fat from calories and reduced sucrose content (30% HFD-RS). At week of life 6, mice were subjected to a six-week forced treadmill training intervention during their active dark phase on five days a week with one exercise bout per day. Physical capacity was assessed at the beginning and end of training intervention.

2.2.2 Animal experiments

2.2.2.1 General animal housing

Animals were kept in accordance with the National Institutes of Health guidelines for the care and use of laboratory animals and all experiments were approved by the Ethics Committee of the State Agency for Nature, Environment and Consumer Protection (LANUV, North Rhine-Westphalia, Germany; reference numbers 84-02.04.2013.A010 and 84-02.04.2014.A252). Housing of mice was carried out in Makrolon type III-cages (EBECO, Castrop-Rauxel, Germany) at an environmental temperature of 22 °C and a 12 hours light-dark cycle with lights off from 6 pm to 6 am (D4KO) or 10:30 am to 10:30 pm (B6, NZO). Animals had *ad libitum* access to the respective experimental diet and tap water.

2.2.2.2 Treadmill training

A four-lane treadmill system (TSE Systems, Bad Homburg, Germany) was used for the chronic exercise training. D4KO mice and WT littermates were trained for four weeks during the light phase, with five exercise bouts per week and one training session per day. Each session consisted of a 5-minutes warm-up at 6-9 m/min running speed for acclimatization, followed by 20 to 30 minutes of running at 9-12 m/min and 5° inclination during the first week. Speed, duration and inclination were constantly increased during the next weeks. In the last week of training, total running time of each training bout was 60 minutes and speed was incrementally increased from 10 to 18 m/min at 5° to 10° inclination. This moderate exercise protocol was

modified from previously established treadmill experiments within our institute (Karpinski 2014, Master thesis). B6 and NZO mice were trained for six weeks during their active dark phase, with five exercise bouts per week and one training session per day. For the B6 mice, the protocol consisted of a 5-minutes warm-up at 6-9 m/min, followed by 20 to 35 minutes of running at 9-15 m/min in the first week. Speed and duration were increased to a maximum of 18 m/min and 38 minutes in the second week, respectively. In week 3 of training, the protocol was modified towards an interval training. This protocol consisted of alternating 5-minutes intervals with moderate to high (15 and 18 m/min) or low running intensity (10 m/min), respectively. During the last three weeks of the intervention, total running time of each training bout was 65 minutes, consisting of one 15 m/min- and five 18 m/min-intervals at constant 5° inclination. For the NZO mice, the intensity of the interval training was only slightly reduced due to the progressive development of diabetes with increasing age. Detailed protocols of the different training interventions are given in the supplement (Table S1 - S3). For all running experiments, mice were motivated to run without applying electric stimuli, but instead pushing them forward by hand of the experimenter. In order to keep similar experimental conditions for the trained and sedentary control groups, e.g. motor noise as a possible stressor, the same room was used for general animal housing and treadmill training.

2.2.2.3 Physical capacity test

To assess the physical capacity (trained vs sedentary controls or pre vs post chronic exercise), mice performed exhaustion running tests at the beginning or end of the training intervention using one-lane calorimetric treadmills (TSE PhenoMaster Treadmill Module, TSE Systems, Bad Homburg, Germany). These treadmills consist of air-tight covers and are connected to a calorimetric control unit, allowing to monitor oxygen consumption (VO_2), carbon dioxide production (VCO_2) and respiratory exchange ratio (RER; ratio VCO_2/VO_2) during the running of the mice. Calorimetry was measured at a flow-rate of 0.4 l/min and a sample flow rate of 0.25 l/min and calorimetric parameters were recorded every 5 seconds by the PhenoMaster software. The physical capacity test started with a short warm-up (2 minutes running at 9 m/min), after which the speed was constantly increased by 1.5 m/min until mice reached exhaustion. Exhaustion was defined as being unable to remain on the treadmill ribbon for at least five seconds, despite pushing them forward using sliders. The time of running until exhaustion was reached (time to exhaustion) was considered as the primary readout for endurance capacity. Inclination of the treadmill was set at constant 5°. For calculation of maximal oxygen consumption (VO_{2max}), the average of 30 seconds of the VO_2 plateau was determined. Note that total running time varies between the experiments, since the protocol was established and improved during preparation of the thesis.

2.2.2.4 Indirect calorimetry

Indirect calorimetry was measured using a calorimetric climate chamber system (TSE PhenoMaster, TSE Systems, Bad Homburg, Germany). Mice were placed in individual cages for three days at a temperature and light/dark cycle adapted to the general animal housing of the respective experiment (2.2.2.1). The calorimetric parameters VO_2, VCO_2, RER and voluntary activity were recorded every 30 minutes by the PhenoMaster software at a flow-rate of 0.4 l/min and a sample flow-rate of 0.38 l/min. Since mice were placed in the cages immediately after a treadmill exercise session, values of the first day were not taken into account for the analysis (acclimatization). The voluntary activity was given as the number of infrared light beam breaks in the x/y-axis. For energy expenditure, VO_2 was referred to the animal's body surface (ml/min/$kg^{0.75}$). All these parameters were calculated using the mean of 24 hours of measurement. Food intake was measured manually by weighting the diet pellets before and after indirect calorimetry and referring to the body weight and total energy content of the respective diet (kcal/g). For the determination of whole-body carbohydrate oxidation (CHO) and fatty acid oxidation (FAO), VO_2 and VCO_2 values were converted using the following equations: CHO = 4.585 x VCO_2 (l/min) – 3.226 x VO_2; FAO = 1.695 x VO_2 (l/min) – 1.701 x VCO_2 (l/min) (Peronnet & Massicotte 1991).

2.2.2.5 Body composition

Body weight was measured using scales (Sartorius, Goettingen, Germany). For the determination of body fat and lean mass of the mice, body composition was measured using nuclear magnetic resonance (NMR; Whole Body Composition Analyzer, Echo MRI, Houston, TX, USA). Body fat and lean mass were measured in duplicate with a 40 seconds-break between each NMR measurements. Due to possible movement of the mice in the NMR tube and due to elimination of water content during the measurements, the sum of body fat and lean mass may variate from the total body weight.

2.2.2.6 Determination of blood glucose

For the measurement of blood glucose, a small portion of the tail tip was cut and glucose concentration was determined using a glucose meter and standard glucose strips (Contour next blood glucose meter, Bayer, Leverkusen, Germany). In addition, blood was collected in microvettes (Microvette CB 300 LH, Sarstedt, Nümbrecht, Germany) by gently massaging the tail tip. Blood samples were centrifuged at 9391 x g for 5 minutes and +4 °C and blood plasma was collected and stored at -80 °C for later analysis of insulin content (2.2.3.1). Blood glucose concentration was usually measured after 6 hours of fasting (FBG) at the end of the training intervention or additionally at random fed conditions (NZO).

2.2.2.7 Blood lactate measurement

In order to assess the acute increase in blood lactate after running, blood lactate concentrations were determined before and immediately after one exercise bout in the respective training week (see 2.2.1). Therefore, the tail tip was cut and blood lactate was measured using a lactate meter and lactate test strips (StatStrip Lactate Xpress Meter, Nova biomedical, Waltham, MA, USA).

2.2.2.8 Intraperitoneal glucose tolerance test (i.p. GTT)

For the assessment of whole-body glucose clearance, intraperitoneal glucose tolerance tests (i.p. GTT) were performed during the last weeks of the training intervention, at least 24 hours after the last exercise bout. Mice were fasted for 6 hours (8 am to 2 pm) in individual cages. Body weight and basal FBG concentration were measured and blood was collected and processed for later analysis of insulin content as described before (see 2.2.2.6). Mice were injected with 2 g/kg body weight of 20 % glucose solution and blood glucose concentrations were measured 15, 30, 45, 60 and 120 minutes after injection. For the NZO study, 240 minutes was added as an additional time point for measurement, since blood glucose concentrations did not return to basal levels after 120 minutes of injection. Mice were kept without access to the diet during the test period but with *ad libitum* access to water.

2.2.2.9 Intraperitoneal insulin tolerance test (i.p. ITT)

For the determination of whole-body insulin sensitivity, intraperitoneal insulin tolerance tests (i.p. ITT) were conducted during the last weeks of the training intervention, at least 24 hours after the last exercise bout. Random fed mice were transferred to individual cages and body weight and basal blood glucose concentrations were measured. Mice were injected with 1 U/kg body weight of insulin dissolved in 0.9 % NaCl and blood glucose concentrations were measured 15, 30 and 60 minutes after injection. Mice were kept without access to the diet during the test period but with *ad libitum* access to water. Due to the high variation of basal blood glucose concentrations between the different groups, the values for glucose clearance during i.p. ITT are given as percentage of basal blood glucose.

2.2.2.10 *Ex vivo* glucose uptake in isolated skeletal muscles

Skeletal muscle glucose uptake was assessed *ex vivo* by measuring the incorporation of radioactively labelled [^{3}H]-2-deoxyglucose (2-DOG), at least 24 hours after the last exercise bout. Mice were fasted for 4 hours and subsequently anaesthetised by intraperitoneal injection of 500 mg/kg body weight Avertin. *Soleus* (D4KO) or *EDL* (NZO) muscles were carefully dissected during Avertin narcosis and immediately used for the glucose uptake assay. Mice

were sacrificed by cervical dislocation for collecting the remaining tissues (see 2.2.2.12). The dissected *Soleus* or *EDL* muscles were incubated in four different buffers (Table 8) at 30 °C in a shaking water bath under constant gassing with carbogen gas (95 % O_2, 5 % CO_2). Each incubation step was carried out in small glass vials containing 1 ml of the respective buffers, which were additionally pre-gassed. First, muscles were incubated with recovery buffer for 30 minutes. Next, muscles were transferred to new glass vials with 1 ml of incubation buffer. From here on, one muscle per animal was incubated at basal conditions, whereas the second muscle was incubated at insulin-stimulated conditions, by adding 120 nM of insulin to the respective buffer. After 30 minutes of incubation, muscles were placed into new vials containing the rinse buffer and incubated for 10 minutes at basal or insulin-stimulated conditions. Finally, muscles were incubated for 20 minutes in hot buffer that contained the radioactively labelled 2-DOG, as well as [^{14}C]-mannitol. Hot incubation was performed at basal or insulin-stimulated conditions, respectively. After incubation, the tendons of each muscle were removed and the muscles were frozen in liquid nitrogen or immediately processed for the further lysis and scintillation counting. Therefore, muscles were homogenized in 300 µl of lysis buffer (2.2.3.5) and 40 µl of the resulting protein lysate were transferred to scintillation vials and mixed with 4 ml of scintillation liquid (Table 7). Subsequently, the radioactivity of the incorporated 2-DOG and [^{14}C]-mannitol was counted in a scintillation counter (Beckman Coulter, Krefeld, Germany). The resulting counts per minutes (cpm) were normalized to the protein concentration of the muscle lysates, determined by BCA analysis (2.2.3.6). Calculation of 2-DOG uptake also takes into account the amount of extracellular bound 2-deoxyglucose, which is estimated via the detection of the extracellular space by [^{14}C]-mannitol and subtracted from the intracellular 2-deoxyglucose (Mackrell & Cartee 2012). Final values for glucose uptake are given as nmol/mg protein/20 min of hot incubation.

2.2.2.11 *Ex vivo* glucose uptake in isolated adipocytes

Adipose tissue glucose uptake was assessed *ex vivo* by measuring the incorporation of radioactively labelled [^{14}C]-D-glucose in isolated adipocytes from epididymal white adipose tissue (WAT). The assay was performed in parallel to the skeletal muscle glucose uptake assay after 4 hours of fasting and Avertin narcosis of the mice (2.2.2.10). To isolate the primary adipocyte cells, one fat pad per mice was dissected and immediately transferred to vials with 3 ml of pre-warmed (37 °C) KRBH buffer with 5 % BSA and 200 nM adenosine (Table 8). The fat pad was sheared with scissors and 16 mg of collagenase was added in each vial. Collagenase digestion was performed for 1 hour at 37 °C in a shaking water bath. The resulting cell lysate was filtered through 400 µm polyamide nylon tissue into a falcon tube and centrifuged at 50 x g for 1 minute at RT. The lower aqueous solution was carefully discharged

and the cells were washed three times with 5 ml of fresh KRBH buffer by shortly centrifuging the cells. After washing, the remaining adipocyte cells were mixed with equal volumes of KRBH buffer and further diluted to generate a 6.25 % adipocyte cell suspension using flat tips. Next, 200 µl of adipocyte suspension were incubated with 200 µl of KRBH buffer with or without 120 nM of insulin for 30 minutes at 37 °C in a shaking water bath. After incubation, 200 µl of adipocyte suspension were transferred to 2.7 ml of lipid extract solution (Table 8) and stored at +4 °C overnight for the later determination of lipid weight. For the measurement of glucose uptake, the adipocyte cell suspension was incubated for 30 minutes with 0.1 µCi/µl [^{14}C]-D-glucose at 37 °C. In order to stop the glucose uptake and to remove excess radioactivity, 280 µl of the adipocyte cell suspension were transferred to small tubes supplemented with 125 µl of dinonyl phthalate oil and centrifuged at 9391 x g for 10 minutes at RT. The tubes were cut in the middle and the upper adipocyte cells-containing piece of the tube was placed in counting vials with 3 ml of scintillation liquid. The tubes were thoroughly vortexed and the radioactivity of the incorporated [^{14}C]-D-glucose was measured in a scintillation counter (Beckman Coulter, Krefeld, Germany). The resulting counts per minutes (cpm) were normalized to the lipid weight of the samples. Therefore, 1.2 ml heptane and 800 µl ddH_2O were added to the overnight lipid extract solution. After vortexing, the samples were centrifuged at 201 x g for 5 minutes at RT and 1 ml of supernatant was transferred to tared glass tubes (Rotilabo-test tubes, Carl Roth, Karlsruhe, Germany). The lipid samples were let dried and evaporated by heating and gassing with nitrogen for 15 minutes using a Reacti-Therm and Reacti-Vap Evaporating Unit (Pierce, Rockford, IL, USA). The weight of the dried lipids was measured and used for calculating the glucose uptake as cpm/ mg lipid. Samples were measured in quintuple for basal and insulin-stimulated conditions. The glucose uptake assays in adipocytes were performed by Anette Kurowski and Heidrun Podini.

2.2.2.12 Dissection of animal tissues

Animal tissues were taken at least 24 hours after the last exercise bout. The animals that did not undergo the *ex vivo* glucose uptake assays were sacrificed by final heart puncture under isoflurane narcosis. Heart blood was collected using 0.5 M EDTA-coated syringes and centrifuged at 9391 x g for 5 minutes at +4 °C and plasma supernatant was stored at -80 °C. The hind limb muscles *EDL*, *Soleus* and *Gastrocnemius*, as well as the liver, white adipose tissue (WAT), subcutaneous white adipose tissue (scWAT) and brown adipose tissue (BAT) were dissected and directly frozen in liquid nitrogen. All tissues were stored at -80 °C until further use.

2.2.3 Biochemical methods

2.2.3.1 Determination of plasma insulin concentration

Plasma insulin concentration from 6 hours fasted (FPI) mice was measured using the Insulin (Mouse) Ultrasensitive ELISA Kit (Table 5) according to the manufacturer's instructions. Shortly, this enzyme-linked immunoassay determines insulin from plasma using an anti-insulin antibody coated to a 96-well plate and a horse radish-peroxidase (HRP)-coupled secondary antibody, which catalyses the oxidation of added 3, 3', 5, 5'-tetramethylbenzidine (TMB). The generated colour substrate was colorimetrically measured at 450 nm (iMark Microplate Absorbance Reader, Bio-Rad, Hercules, CA, USA). Samples were measured in technical duplicates or as single measurement in case of low sample volume.

2.2.3.2 Measurement of plasma triglycerides and free fatty acids (NEFA)

Plasma triglyceride content was measured using a colorimetric assay Kit (Table 5) that is based on the enzymatic hydrolysis of triglycerides by lipases and subsequent formation of a specific colour substrate by peroxidases. 1.5 µl of each plasma sample was incubated with 150 µl of enzyme reagent for 10 minutes at RT and triglyceride content was measured colorimetrically at 490 nm (iMark Microplate Absorbance Reader, Bio-Rad, Hercules, CA, USA). Plasma samples were measured in technical duplicates and values were given as mmol/l. Plasma NEFA concentration was determined with the NEFA-HR (2) Assay Kit (Table 5), which consists of the conversion of free fatty acids to Acyl-CoA and formation of a blue colour substrate by peroxidases. Plasma was diluted 1:2 with ddH_2O and incubated with two enzyme reagents for 15 minutes at RT, respectively. Absorption of duplicate samples was measured at 560 nm (iMark Microplate Absorbance Reader, Bio-Rad, Hercules, CA, USA) and values were given as mmol/l.

2.2.3.3 Analysis of hepatic and skeletal muscle glycogen content

Glycogen content from liver and *Gastrocnemius* muscle was determined using amyloglucosidase hydrolysis as previously described (Suzuki et al. 2001). Liver and muscle tissues were powdered in liquid nitrogen and 40 mg of tissue was hydrolysed with 300 µl of 30 % (wt/vol) KOH for 30 minutes at 100 °C and subsequently cooled down to RT. For precipitation of glycogen, 100 µl of 1 M Na_2SO_4 and 800 µl EtOH were added and incubated for 5 minutes at 100 °C. After centrifugation at 21130 x g for 15 minutes at +4 °C, the supernatant was discarded and the pellet was re-suspended in 200 µl ddH_2O. This precipitation was repeated twice and the final pellet was dried to let the EtOH evaporate (Centrifugal Vacuum Concentrator 5301, Eppendorf, Hamburg, Germany). The dried pellet was dissolved

in 200 µl of 0.12 M sodium acetate buffer with 0.3 mg/ml amyloglucosidase and incubated for 3 hours at 40 °C. The samples were shortly centrifuged and the supernatant was collected and transferred to new tubes. Glucose from glycogen content was measured with a colorimetric glucose assay (Glucose liquicolor, Table 5), which is based on the enzymatic oxidation of glucose by glucose oxidases. Undiluted (muscle) or 1:5 diluted (liver) samples were mixed with 200 µl of enzyme reagent and glucose content was measured colorimetrically at 490 nm after 20 minutes of incubation at RT (iMark Microplate Absorbance Reader, Bio-Rad, Hercules, CA, USA). Samples were measured in duplicate and values were normalized to the net weight of used tissue (µg/mg tissue).

2.2.3.4 Analysis of hepatic and skeletal muscle triglyceride content

For the analysis of triglyceride content, liver or skeletal muscle tissue was powdered in liquid nitrogen and 30 mg of tissue was lysed in 1.5 ml of chloroform/methanol solution (2:1 vol/vol) for 4 minutes in a TissueLyser (Qiagen, Hilden, Germany). The samples were horizontally inverted for 2 hours at RT in order to extract the lipids. After adding 200 µl of ddH_2O, the samples were centrifuged at 3381 x g for 15 minutes at RT to separate the samples into an aqueous (supernatant) and an organic phase. The supernatant was discarded and 500 µl of the lower organic phase were transferred to new tubes and subsequently centrifuged for 1 hour to let the chloroform evaporate (Centrifugal Vacuum Concentrator 5301, Eppendorf, Hamburg, Germany). The remaining lipid pellet was dissolved in 1 ml of chloroform and 3x 25 µl of the chloroform fraction were transferred to new vials and shortly centrifuged again for evaporation. Triglyceride content was measured using the Triglyceride Assay Kit with some modifications (see 2.2.3.2). Each triplicate sample was incubated with 150 µl of enzyme solution for 10 minutes at RT and mixed thoroughly in between. 130 µl of the samples and standards were transferred to a 96-well plate and triglyceride content was measured colorimetrically at 490 nm (iMark Microplate Absorbance Reader, Bio-Rad, Hercules, CA, USA). The mean of each sample triplicate was normalized to the net weight of used tissue (µg/mg tissue).

2.2.3.5 Preparation of protein lysates from mouse tissue

Frozen tissue was placed in a 2 ml safe-lock tube with 300 µl (*EDL*, *Soleus*) or 500 µl (*Gastrocnemius*, WAT, BAT and liver) of lysis buffer (Table 8), respectively. Samples were homogenized for 5 minutes (skeletal muscles) or 10 minutes (WAT, BAT) using a TissueLyser (Qiagen, Hilden, Germany) and subsequently centrifuged at 15871 x g for 10 minutes at +4 °C. For WAT and BAT tissue, the samples were centrifuged twice in order to separate the supernatant from the fat layer. The supernatant was transferred to a new tube and stored at - 80 °C or immediately used for the determination of protein concentration (see 2.2.3.6).

2.2.3.6 Determination of protein concentration

Protein concentration of protein lysates was determined using the BCA Protein Assay Kit (Table 5) according to the manufacturer's instructions. Sample dilution was increased from 1:20 to 1:50 or 1:100 for *Gastrocnemius* muscle, BAT or liver tissue, respectively. Protein concentration was measured colorimetrically at 560 nm (iMark Microplate Absorbance Reader, Bio-Rad, Hercules, CA, USA).

2.2.3.7 Western Blot analysis

2.2.3.7.1 SDS-PAGE

Protein lysates (2.2.3.5) were electrophoretically separated via denaturating SDS-PAGE. Therefore, 20 µg of protein lysates were diluted with 5 µl of 4x LSB (Table 8) and total sample volume (20 µl) was adjusted with ddH_2O. After mixing briefly, protein samples were denatured at 95 °C for 5 minutes or incubated at RT for 30 minutes (GLUT4). Samples were shortly centrifuged and subsequently loaded on 8 % (TBC1D4), 10 % (PGC-1α) or 12 % (AMPK, pAMPK, FASN, GLUT1, GLUT4, GCK, PCK-1 and PCK-2) SDS gels (Table 9). To estimate the molecular weight of the separated protein bands, a pre-stained protein standard (Table 6) was additionally loaded on the gels. Electrophoretical separation was carried out in electrode buffer (Table 8) at initial 100 V for 15 minutes and 150 V for 45 - 60 minutes using the Mini-PROTEAN Tetra Vertical Electrophoresis Cell system (Bio-Rad, Hercules, CA, USA).

Table 9: Composition of SDS gels

Separating gel	8 %	10 %	12 %	Stacking gel
Separating gel buffer	2.34 ml	2.34 ml	2.34 ml	780 µl
Acrylamide (30 %)	2.4 ml	3 ml	3.6 ml	390 µl
ddH_2O	4.26 ml	3.66 ml	3.06 ml	1.83 ml
APS	18 µl	18 µl	18 µl	6 µl
TEMED	9 µl	9 µl	9 µl	3 µl

2.2.3.7.2 Transfer and immunochemical detection of separated proteins

Separated proteins were transferred to nitrocellulose (FASN, GLUT1, GLUT4, GCK, PCK-1 and PCK-2) or PVDF (AMPK, pAMPK, PGC-1α and TBC1D4) membranes using tank blots (Tankblot Eco-Mini, Biometra, Göttingen, Germany). Prior to transfer, the PVDF membranes were equilibrated by incubation in methanol for 10 seconds, followed by a 5-minute incubation in ddH_2O and transfer buffer (Table 8), respectively. Transfer was performed in transfer buffer

at 200 mA and +4 °C for 2 hours or overnight (GLUT1, GLUT4). After transfer, the membranes were incubated in 5 % blocking solution (Table 8) for 1 hour at RT. The membranes were briefly washed two times with 1x TBS-T buffer (Table 8) and subsequently incubated with the respective primary antibody diluted in 5 % skim milk/ TBS-T at a ratio of 1:1000 or 1:5000 (GAPDH). Incubation was performed overnight or for 2 hours at RT (GLUT1, GLUT4). Subsequently, the membranes were washed three times for 10 minutes with 1x TBS-T and incubated for 1 hour at RT with the respective secondary horseradish-peroxidase (HRP)-conjugated antibodies (Table 4), which were diluted in 5 % skim milk/ TBS-T at a ratio of 1:20000. The membranes were washed again three times for 10 minutes with 1x TBS-T at RT. Immunochemical detection of the antibody-conjugated protein bands was carried out by incubating the membranes in Enhanced Chemiluminescence (ECL) Substrate (Table 5) according the manufacturer's instructions. Bands were visualized and quantified using the ChemiDoc (ChemiDoc XRS+ System, Bio-Rad, Hercules, CA, USA) and Image Lab software (Image Lab 5.2.1, Bio-Rad, Hercules, CA, USA). Each band was normalized to the abundance of the housekeeping protein GAPDH and given as percentage of the respective sedentary control group.

2.2.3.7.3 Separation and transfer of proteins using stain-free gels

If protein bands could not be normalized to a heterogeneously distributed housekeeping protein, e.g. for UCP-1 in scWAT (D4KO) and GLUT4 in WAT (NZO), protein abundance of the respective protein was normalized to the total protein content. Therefore, proteins were separated via SDS-PAGE on precast stain-free gels (Any kD Mini-PROTEAN TGX Stain-Free Protein Gels, Bio-Rad, Hercules, CA, USA). Samples were diluted with 4x LSB (2.2.3.7.1) and electrophoresis was performed for initial 20 minutes at 20 mA and additional 50 minutes at 50 mA using the Criterion Cell system (Bio-Rad, Hercules, CA, USA). Total protein content was detected by UV radiation using the ChemiDoc after successful electrophoresis. After detection, proteins were transferred to nitrocellulose membranes using a semi-dry blot system (Trans-Blot Turbo Transfer System, Bio-Rad, Hercules, CA, USA). This system allows rapid transfer of proteins in 7 minutes at 2.5 A. Subsequent antibody incubation and detection of protein bands was carried out as described previously (2.2.3.7.2). The molecular weight of the electrophoretically separated or transferred proteins was estimated by additional loading of unstained or pre-stained standards (Table 6), respectively.

2.2.4 Molecular biological methods

2.2.4.1 RNA isolation from mouse tissue

RNA from skeletal muscle or adipose tissue (WAT, scWAT) was isolated by trizol extraction using the miRNeasy-Mini Kit (Table 5). Frozen tissue was lysed in 700 µl of QIAzol lysis Reagent (Table 7) for 5 minutes using the TissueLyser. After incubating the samples for 5 minutes at RT, 700 µl of lysate were centrifuged in spin columns (QIAshredder, Qiagen, Hilden, Germany) at 18407 x g for 2 minutes at +4 °C. The flow-through was collected and the RNA was subsequently extracted by centrifugation at 12000 x g for 15 minutes at +4 °C with 140 µl of chloroform using MAXtract High Density tubes (Qiagen, Hilden, Germany). The resulting aqueous RNA solution was transferred to 1.5 ml tubes and mixed with 1.5 volume of EtOH. Subsequently, the RNA was purified using miRNeasy-Mini columns and DNase was digested using the RNase-free DNase Set (Table 5) according to the manufacturer's instructions. Concentration of the RNA eluate was measured photometrically at 260 nm using the NanoDrop (NanoDrop ND-2000, PEQLAB Biotechnology, Erlangen, Germany).

2.2.4.2 cDNA synthesis

For the synthesis of isolated RNA (2.2.4.1) into complementary DNA (cDNA), 1 µg of RNA was mixed with 1 µl of dNTPs and 2 µl of 1:10 diluted hexanucleotide primers on ice. After short centrifugation, the samples were incubated at 65 °C for 5 minutes in a thermocycler (T100 Thermal Cycler, Bio-Rad, Hercules, CA, USA) and additionally for 1 minute at +4 °C to allow for primer annealing. Subsequently, 7 µl of RNA samples were added to the reverse transcription master mix (Table 5) according to the manufacturer's instructions and cDNA synthesis was performed in a thermocycler using the following protocol (Table 10).

Table 10: cDNA synthesis protocol

Reaction	Temperature	Duration
Annealing	25 °C	5 minutes
Synthesis	42 °C	60 minutes
Reverse transcriptase inactivation	70 °C	15 minutes
Hold	+4 °C	

The resulting cDNA samples were diluted in nuclease-free H_2O at a ratio of 1:40 for the subsequent qPCR analysis (2.2.4.3).

2.2.4.3 Quantitative Real-Time PCR (qPCR)

Gene expression was quantified by quantitative Real-Time PCR (qPCR), which allows the detection of amplified DNA sequences during each cycle of the PCR reaction using specific fluorescent reporter dyes, such as SYBR Green. The amount of detected fluorescence is proportional to the amount of DNA template of each respective sample. Therefore, the amount of DNA, i.e. mRNA, can be quantified by the number of cycles needed until the fluorescence crosses the amplification threshold (Ct value). 4 µl of diluted cDNA samples were mixed with 5 µl of GoTaq qPCR Master Mix (Table 5) and 0.5 µl of 1:10 diluted forward and reverse SYBR Green primers of the desired genes (Table 3), respectively. The cDNA master mix samples were pipetted in 96 well plates and densely covered with MicroAmp adhesive films (Thermo Fisher Scientific, Waltham, MA, USA). After a short centrifuging step, the PCR plate was inserted into the StepOne Plus PCR system (Applied Biosystems, Foster City, CA, USA) and the qPCR was executed for 2 hours using the following protocol (Table 11).

Table 11: qPCR protocol

Reaction	Temperature	Duration	Cycles
Hot Start	95 °C	2 minutes	1x
Denaturation	95 °C	15 seconds	40x
Annealing/ Extension	60 °C	60 seconds	
Dissociation	60-95 °C	90 seconds	1x

The expression of each gene was normalized to the expression of the housekeeping gene *Hprt* (ΔCt). Additionally, the Ct of each sample was normalized to the mean Ct of the sedentary (WT) control ($2^{-\Delta\Delta Ct}$).

2.2.5 Statistical analysis

The data for all the experiments shown in this thesis are presented as mean ± SEM. The number of mice or samples (n) used for the respective experiment is indicated in the figure legends. Significant differences between two groups with one condition (training) were determined by unpaired or paired student's t-test. Significant differences between two groups with two conditions (training and genotype or training and diabetic state) were determined using two-way ANOVA or two-way repeated measurements (RM) ANOVA with Bonferroni's multiple comparisons test. Significant differences between more than two groups were determined by one-way ANOVA with Tukey's multiple comparisons test. Values of $p < 0.05$ were considered as statistically significant. Statistical outliers were excluded using Grubb's

test. GraphPad Prism 7 software was used for preparing the figures and performing the statistical analysis.

3. Results

3.1 Impact of chronic exercise on glucose homeostasis in *Tbc1d4*-deficient (D4KO) mice

Deletion of TBC1D4 has been shown to impair whole-body glycaemia and insulin sensitivity in mice, reflected by postprandial hyperglycaemia, insulin intolerance and reduced skeletal muscle and adipose tissue glucose uptake (Lansey et al. 2012, Wang et al. 2013, Chadt et al. 2015, Xie et al. 2016). To investigate whether regular exercise training is able to restore glycaemia, *Tbc1d4*-deficient (D4KO) mice and wildtype (WT) littermates were fed a HFD with 60 % fat from calories and subjected to a moderate four-week treadmill training (2.2.1).

3.1.1 Physical capacity of D4KO mice

In order to determine the physical capacity after chronic exercise intervention, exhaustion running tests were performed in D4KO mice and WT controls pre (sedentary) and post (trained) the four-week treadmill training (2.2.2.3). Time to exhaustion remained similar between sedentary and trained WT mice (Figure 7 A). In contrast, sedentary D4KO mice exhibited an impaired physical capacity, reflected in a reduced time to exhaustion compared to WT controls (8.2 ± 0.3 min in D4KO vs. 10.3 ± 0.5 min in WT mice, $p < 0.01$). After 4 weeks of chronic exercise, D4KO mice improved their physical capacity, represented in a significantly increased time to exhaustion (9.6 ± 0.4 min in trained vs. 8.2 ± 0.3 min in sedentary D4KO mice, $p < 0.05$). Differences in time to exhaustion were not reflected in changes of VO_{2max} or RER (Figure 7 B, C). Furthermore, blood lactate concentrations of trained mice were measured pre and post one acute exercise bout (2.2.2.7). Blood lactate concentrations remained unchanged in WT mice immediately after running, while D4KO mice showed mildly elevated basal lactate levels compared to WT controls, without additional increases after exercise (Figure 7 D).

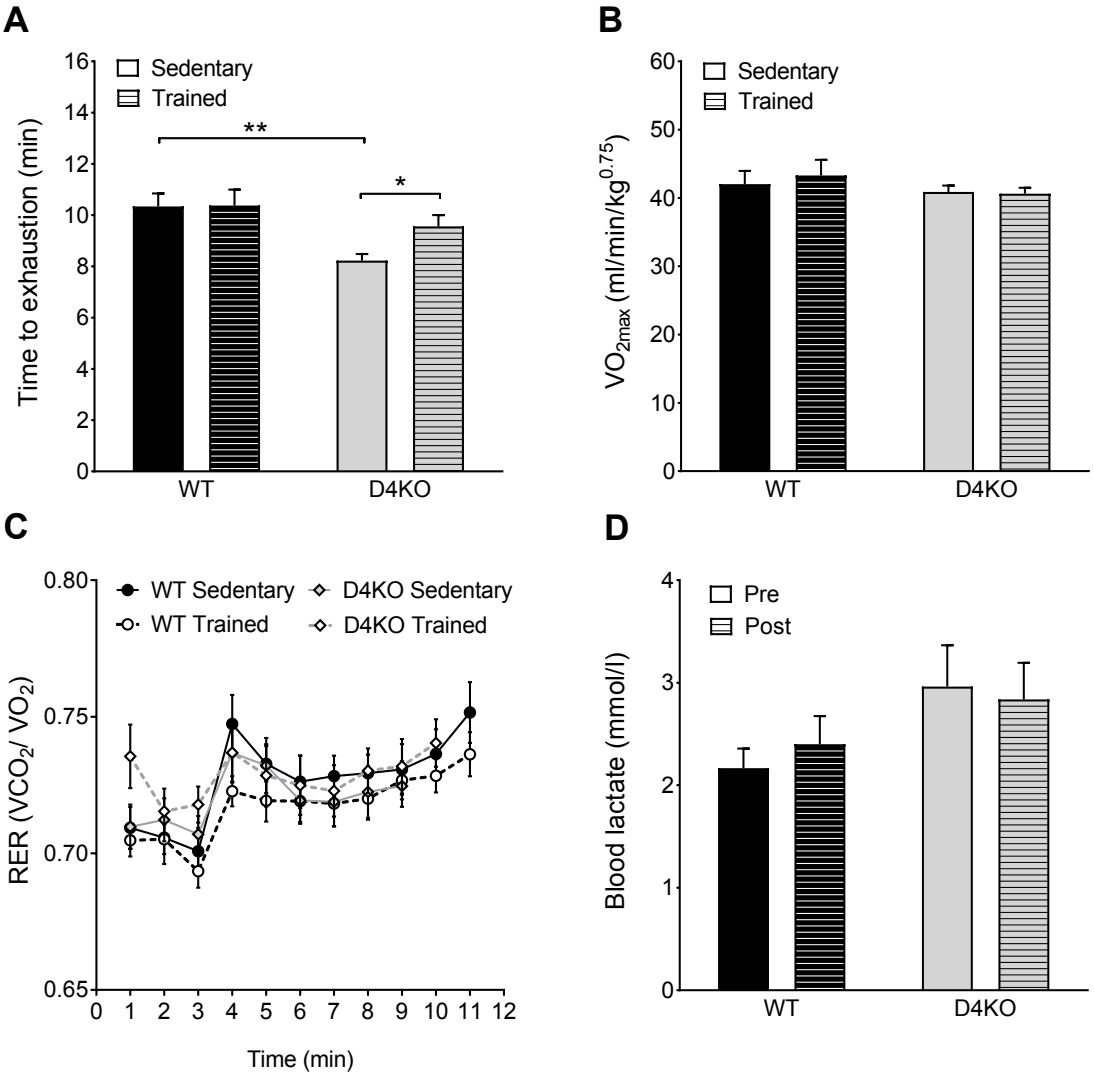

Figure 7: Physical capacity and blood lactate concentrations of WT and D4KO mice. Time to exhaustion (**A**), VO_{2max} (**B**) and RER (**C**) of WT and D4KO mice were measured pre (sedentary) and post (trained) the training intervention. Blood lactate concentrations (**D**) were analysed in trained mice pre and post a daily exercise session. Data are presented as mean ± SEM (n = 8-9). Data were analysed using two-way RM-ANOVA with Bonferroni's multiple comparisons test. *, $p < 0.05$; **, $p < 0.01$ between indicated groups.

3.1.2 Body composition and plasma parameters of D4KO mice

Table 12 summarizes the body composition (2.2.2.5) and basic plasma parameters including FBG (2.2.2.6), FPI (2.2.3.1) and plasma triglyceride and plasma NEFA content (2.2.3.2) of D4KO mice and WT littermates. Body composition as well as plasma parameters were unchanged in WT mice after chronic exercise. Sedentary D4KO mice exhibited a significantly increased body weight compared to WT controls, which tended to be reduced after exercise. The increase in body weight was due to an elevated fat mass, which was significantly reduced in trained D4KO mice. Lean mass of D4KO mice was not affected by the training intervention.

Similar to WT mice, plasma parameters were not significantly changed in D4KO mice after training, although blood glucose concentrations and plasma insulin content tended to be reduced.

Table 12: Body composition and plasma parameters of WT and D4KO mice after chronic exercise.

Parameter	WT Sedentary	WT Trained	D4KO Sedentary	D4KO Trained
Body weight (g)	32.3 ± 1.6	33.9 ± 1.0	**38.0 ± 2.1#**	33.4 ± 1.8
Fat mass (g)	5.9 ± 1.6	8.2 ± 1.3	**12.7 ± 1.7 ##**	**7.2 ± 1.4 ***
Lean mass (g)	25.9 ± 0.9	25.2 ± 0.7	24.8 ± 1.0	25.6 ± 0.7
FBG (mg/dl)	157 ± 12.3	153 ± 7.0	147 ± 6.9	127 ± 5.7
FPI (ng/ml)	1.0 ± 0.28	1.0 ± 0.19	1.6 ± 0.34	0.9 ± 0.15
Plasma TG (mmol/l)	0.49 ± 0.09	0.40 ± 0.04	0.44 ± 0.06	0.38 ± 0.07
Plasma NEFA (mmol/l)	1.0 ± 0.12	1.3 ± 0.1	1.1 ± 0.05	1.4 ± 0.1

All plasma parameters were measured after 6 hours of fasting. Data are presented as mean ± SEM (n = 7-9). Data were analysed using two-way ANOVA with Bonferroni's multiple comparisons test. #, $p < 0.05$; ##, $p < 0.01$ D4KO vs respective WT group; *, $p < 0.05$ sedentary vs. trained.

3.1.3 Glucose tolerance and insulin tolerance of D4KO mice

The improved physical capacity of D4KO mice after four weeks of exercise might be explained by improvements in whole-body glycaemia. Therefore, i.p. GTT (2.2.2.8) and i.p. ITT (2.2.2.9) experiments were performed in week 17 or week 18, respectively. While the glucose tolerance in WT mice was not changed after chronic exercise, trained D4KO mice exhibited a significantly improved glucose tolerance (AUC 33370 ± 815 in trained vs. 46422 ± 2941 in sedentary D4KO mice, $p < 0.01$; Figure 8 A, B). Similar to glucose tolerance, the insulin tolerance was not changed in WT mice, but improved in D4KO mice after chronic exercise, reflected in a significantly reduced AUC (4720 ± 255 in trained vs. 5801 ± 156 in sedentary D4KO mice, $p < 0.001$; Figure 8 C, D). Altogether, these results show that whole-body glycaemia was improved in D4KO mice after 4 weeks of exercise.

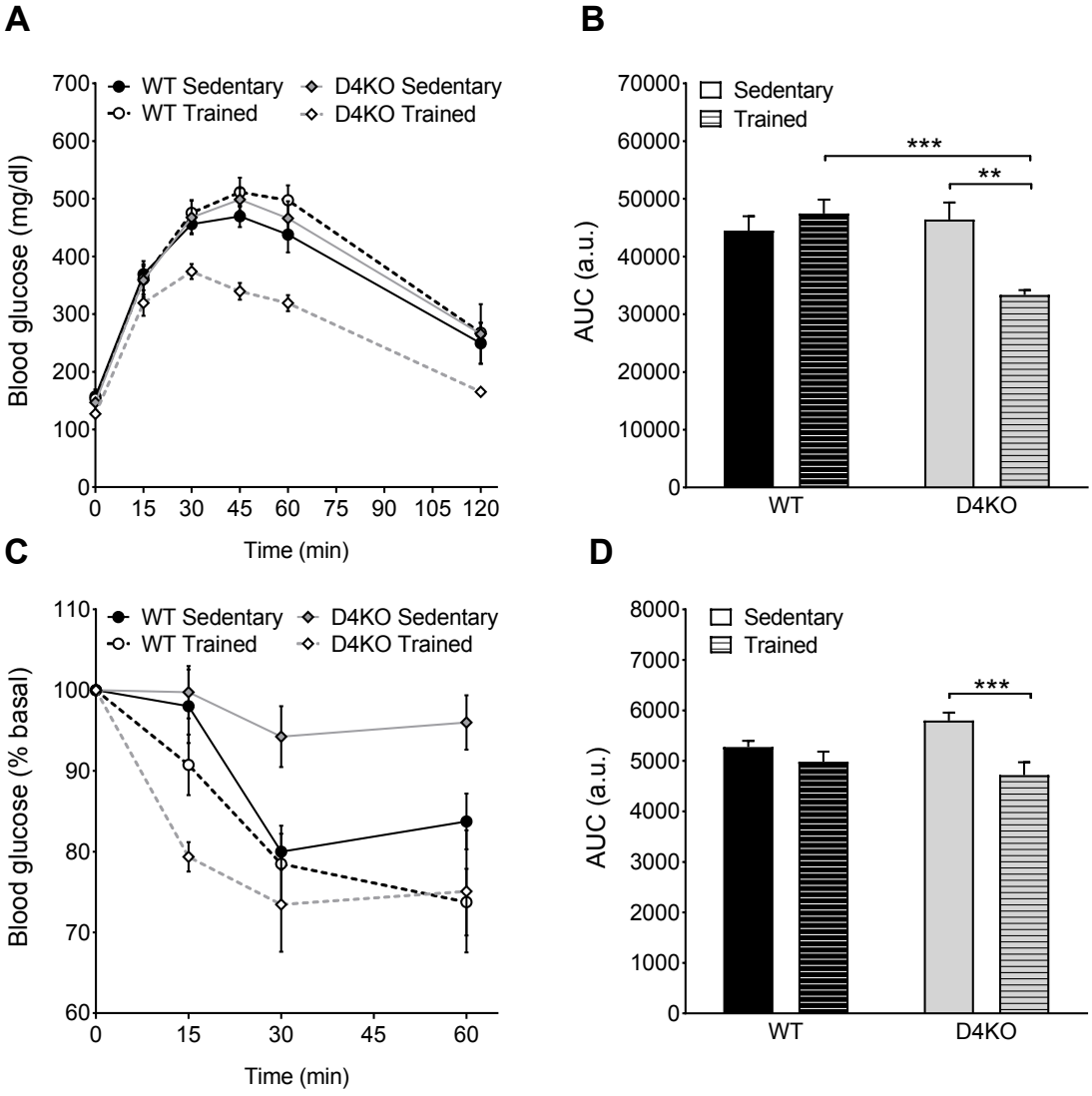

Figure 8: Glucose tolerance and insulin tolerance of WT and D4KO mice after chronic exercise. Glucose tolerance (**A**) and insulin tolerance (**C**) was measured after intraperitoneal injection of glucose or insulin, respectively. Area under curve (AUC) was determined for quantification of glucose (**B**) and insulin tolerance (**D**), respectively. Data are presented as mean ± SEM (n = 8-9). Data were analysed using two-way ANOVA with Bonferroni's multiple comparisons test. **, $p < 0.01$; ***, $p < 0.001$ between indicated groups.

3.1.4 Analysis of glucose uptake in skeletal muscle of D4KO mice

Since skeletal muscle represents the predominant organ for insulin- and exercise-regulated glucose uptake, it may contribute to the improved whole-body glycaemia in trained D4KO mice. GLUT1 and GLUT4 are the main glucose transporter proteins in skeletal muscle, regulating basal or insulin- and contraction-mediated glucose uptake, respectively (1.3.1). In order to validate the contribution of skeletal muscle to the improved whole-body glycaemia, Western Blot analysis of total GLUT1 and GLUT4 protein content was performed in *Soleus* muscle of WT and D4KO mice (2.2.3.7). Additionally, the protein abundance of TBC1D4 was measured

in order to verify the whole-body knockout. Figure 9 A shows the expected band pattern for TBC1D4 in WT and D4KO mice. GLUT1 protein content was not changed between the genotypes or after training intervention (Figure 9 A, B). In WT mice, GLUT4 protein content was only mildly increased after chronic exercise (Figure 9 A, C). Sedentary D4KO mice showed a 30 % reduction of GLUT4 protein content compared to WT controls (70.6 ± 3.5 % in D4KO vs. 100 ± 4 % in WT sedentary mice, $p < 0.01$), which was not rescued after training. To investigate whether chronic exercise might have affected the gene expression of GLUT4, qPCR analysis of the GLUT4 gene *Slc2a4* was performed in isolated RNA from *Soleus* muscle (2.2.4.3). Similar to the protein abundance, D4KO mice exhibited a reduced expression of GLUT4 compared to WT littermates, which was not increased after chronic exercise (Figure 9 D).

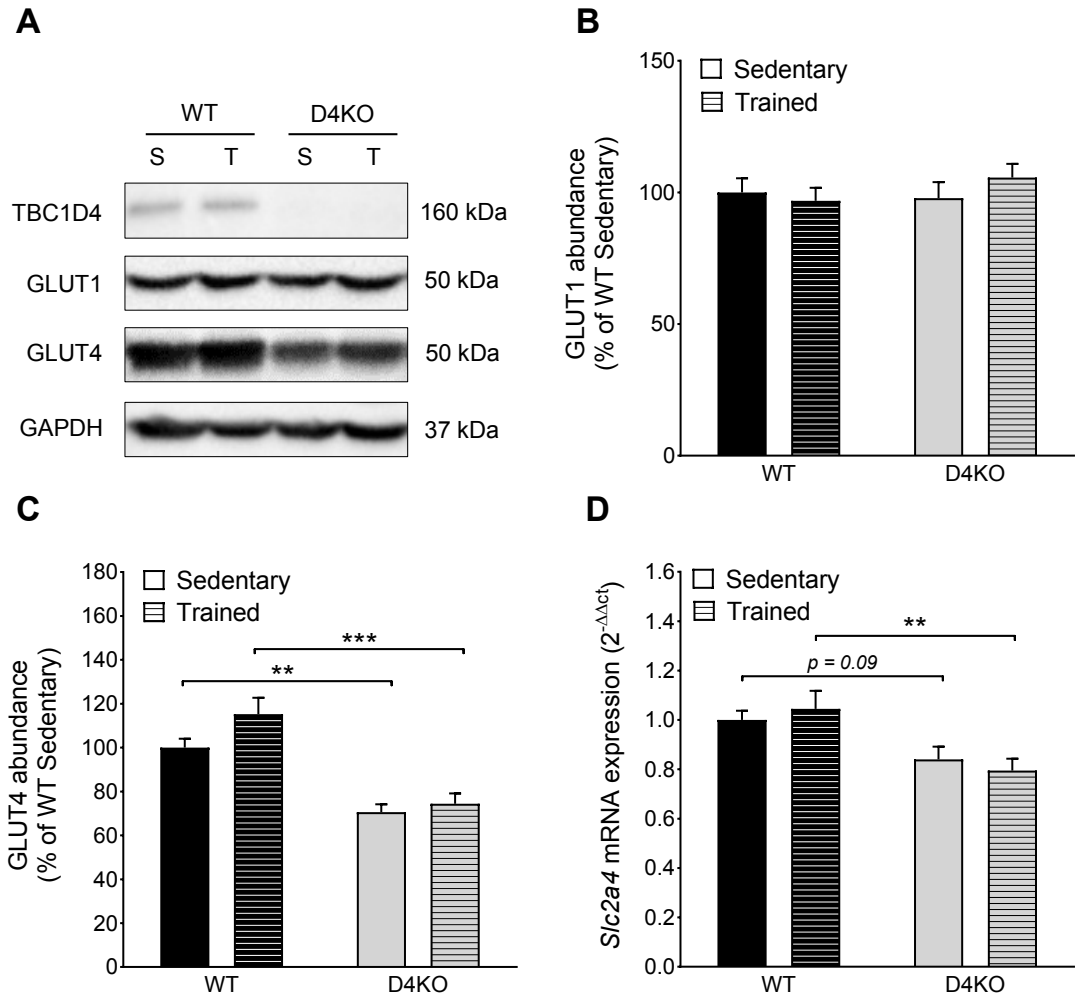

Figure 9: Protein abundance of TBC1D4, GLUT1 and GLUT4 and expression of GLUT4 (*Slc2a4)* in *Soleus* muscle of WT and D4KO mice. Representative Western Blots of TBC1D4, GLUT1 and GLUT4 (**A**) and quantification of GLUT1 (**B**) and GLUT4 (**C**) in *Soleus* muscle of WT and D4KO mice. Protein abundance was normalized to GAPDH and given as percentage of the WT sedentary group. *Slc2a4* mRNA expression (**D**) was normalized to the housekeeping gene *Hprt*. Data are presented as mean ± SEM (n = 7-9). Data were analysed using two-way ANOVA with Bonferroni's multiple comparisons test. **, $p < 0.01$; ***, $p < 0.001$ between indicated groups. S, sedentary; T, trained.

In order to further assess the impact of exercise on glucose uptake at insulin-stimulated states, *ex vivo* 2-DOG uptake was measured in isolated *Soleus* muscles of D4KO mice and WT littermates (2.2.2.10). When treated with insulin, glucose uptake was significantly increased in untrained WT mice (4.8 ± 0.3 nmol/mg/20 min at insulin vs. 3.5 ± 0.2 nmol/mg/20 min at basal conditions, $p < 0.05$; Figure 10). In contrast, the insulin-stimulated glucose uptake was significantly impaired in D4KO mice compared to WT controls (3.4 ± 0.2 nmol/mg/20 min in D4KO vs. 4.8 ± 0.3 nmol/mg/20 min in WT mice, $p < 0.001$), reflecting the previously reported impaired phenotype of D4KO mice (Wang et al. 2013, Chadt et al. 2015). After four weeks of chronic exercise, WT mice showed an additional increase in the insulin-stimulated glucose uptake. In D4KO mice, chronic exercise significantly enhanced the glucose uptake at both, basal and insulin-stimulated conditions compared to sedentary controls. However, trained D4KO mice did not show an additive increase of glucose uptake at insulin-stimulated compared to basal conditions. Thus, the insulin-stimulated glucose uptake in trained D4KO mice still remained impaired compared to the WT littermates (4.2 ± 0.3 nmol/mg/20 min in trained D4KO vs. 6.0 ± 0.5 nmol/mg/20 min in trained WT mice, $p < 0.001$). In summary, these results show that skeletal muscle GLUT4 content and glucose uptake were not restored in D4KO mice after chronic treadmill training, presumably not contributing to the improved whole-body glycaemia.

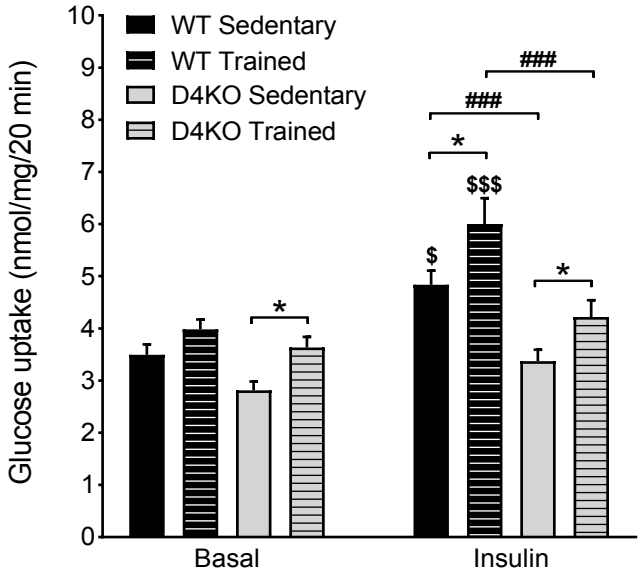

Figure 10: *Ex vivo* glucose uptake in *Soleus* muscle of WT and D4KO mice. *Ex vivo* 2-DOG uptake was measured at basal or insulin-stimulated conditions in isolated *Soleus* muscles of sedentary and trained WT and D4KO mice. Data are presented as mean ± SEM (n = 11-12). Data were analysed using two-way ANOVA with Bonferroni's multiple comparisons test. $, $p < 0.05$; $$$, $p < 0.001$ basal vs. insulin of indicated group; ###, $p < 0.001$ WT vs. D4KO; *, $p < 0.05$ sedentary vs trained of respective genotype.

3.1.5 Hepatic and skeletal muscle glycogen content of D4KO mice

Both hepatic and skeletal muscle glycogenolysis contribute to skeletal muscle energy supply at moderate or high intensities, respectively (1.4.3). In order to investigate whether hepatic or skeletal muscle glycogen content was changed after four weeks of training, total glycogen content was measured in liver and *Gastrocnemius* muscle of WT and D4KO mice (2.2.3.3). Figure 11 A shows that hepatic glycogen content was not changed between the genotypes or after chronic exercise. Skeletal muscle glycogen content was significantly elevated in trained WT mice compared to sedentary controls, whereas D4KO mice showed no changes of glycogen content (Figure 11 B).

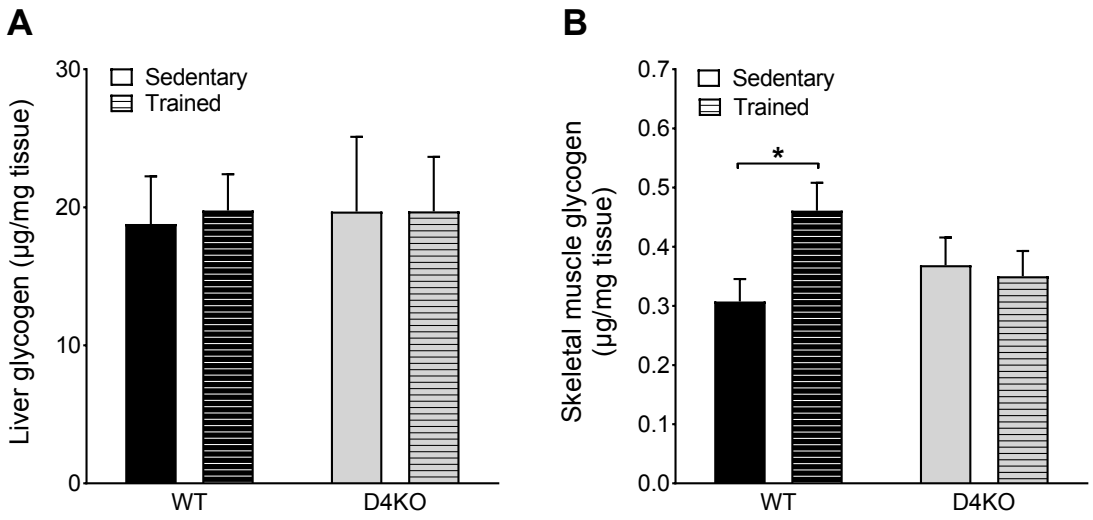

Figure 11: Hepatic and skeletal muscle glycogen content in WT and D4KO mice. Glycogen content was measured in liver (**A**) and *Gastrocnemius* muscle (**B**) of sedentary and trained WT and D4KO mice. Data are presented as mean ± SEM (n = 8-9). Data were analysed using two-way ANOVA with Bonferroni's multiple comparisons test. *, $p < 0.05$.

3.1.6 Abundance of GCK and PCK in the liver of D4KO mice

Hepatic glycolysis as well as gluconeogenesis contribute to whole-body energy supply during exercise (1.3.2). In order to estimate whether hepatic glycaemia was altered in D4KO mice, Western Blot analysis of proteins associated with glycolysis (GCK) and gluconeogenesis (PCK-1, PCK-2) was performed (2.2.3.7). Hepatic GCK abundance was not changed between the genotypes or between sedentary and trained mice (Figure 12 A, B). PCK-1 abundance tended to be increased in trained WT mice compared to sedentary controls (Figure 12 A, C). PCK-1 abundance of D4KO mice was already elevated at untrained states, but not further increased after chronic exercise. The protein abundance of PCK-2 tended to be decreased in trained WT mice, whereas no changes were detected in D4KO mice (Figure 12 A, D).

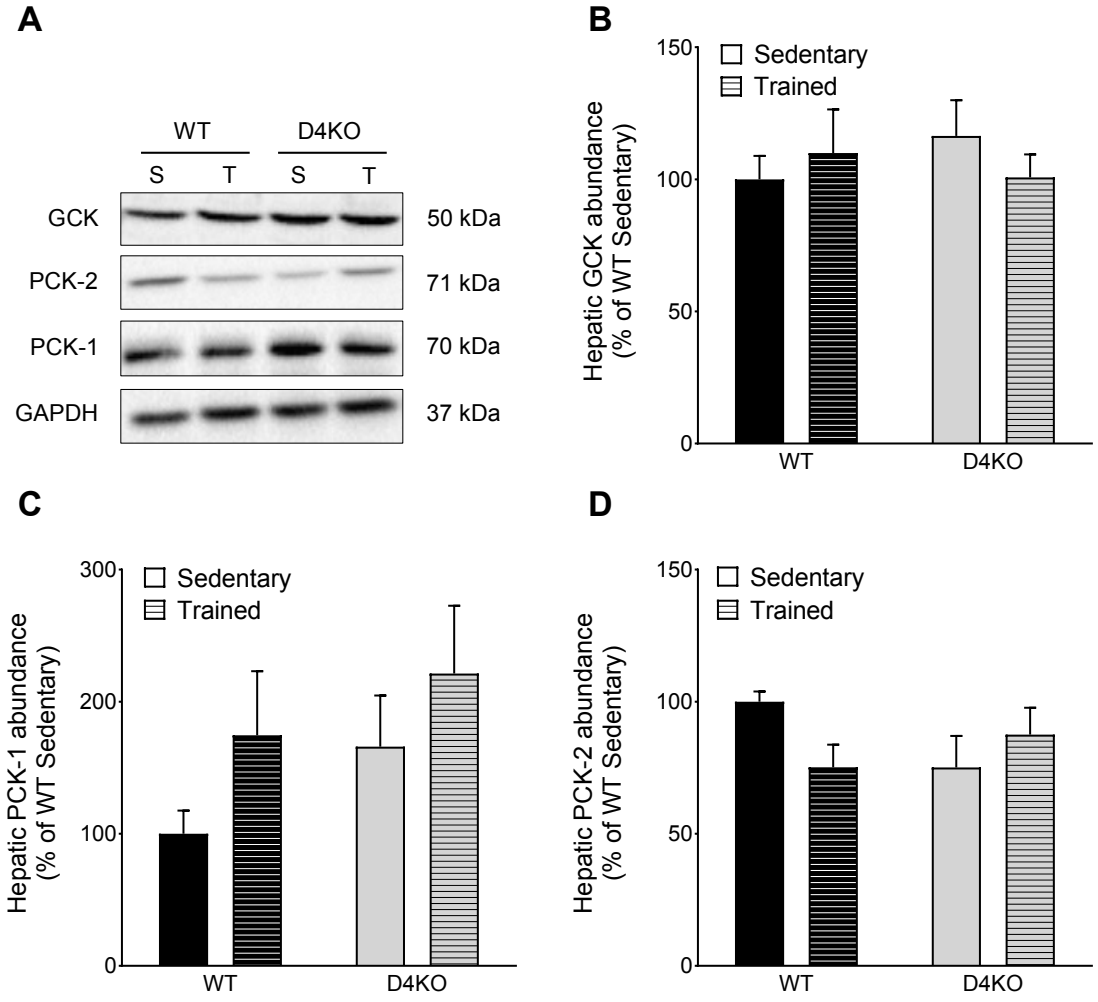

Figure 12: Protein abundance of GCK, PCK-1 and PCK-2 in liver of WT and D4KO mice. Representative Western Blots of GCK, PCK-1 and PCK-2 (**A**) and quantification of GCK (**B**), PCK-1 (**C**) and PCK-2 (**D**) in liver of WT and D4KO mice. Protein abundance was normalized to GAPDH and given as percentage of the WT sedentary group. Data are presented as mean ± SEM (n = 6-9). Data were analysed using two-way ANOVA with Bonferroni's multiple comparisons test. S, sedentary; T, trained.

3.1.7 Determination of hepatic triglyceride content of D4KO mice

Moderate exercise training has been shown to reduce hepatic triglycerides in mice (Hafstad et al. 2013, Alex et al. 2015). Since trained D4KO mice exhibited a markedly reduced fat mass (see Table 12), it should be investigated whether this was due to a reduction of hepatic fat content. Hepatic triglycerides were measured colorimetrically after chloroform/methanol extraction in the liver of WT and D4KO mice (2.2.3.4). Hepatic triglyceride content was not changed between sedentary and trained WT mice (Figure 13). In contrast, D4KO mice showed a markedly increased triglyceride content (16.8 ± 0.5 µg/mg in sedentary D4KO vs. 7.7 ± 1.4 µg/mg in sedentary WT mice, $p < 0.001$), which was reduced to WT levels after four weeks

of training (11.9 ± 1.3 µg/mg in trained vs. 16.8 ± 0.5 µg/mg in sedentary D4KO mice, p = 0.052).

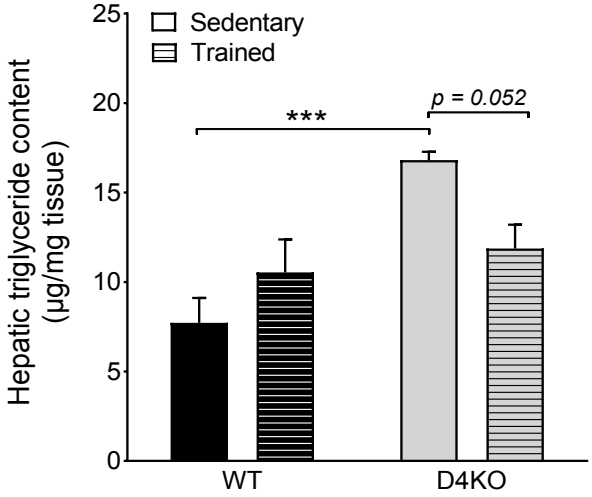

Figure 13: Hepatic triglyceride content of WT and D4KO mice. Triglyceride content was measured in liver of sedentary and trained WT and D4KO mice. Data are presented as mean ± SEM (n = 7-9). Data were analysed using two-way ANOVA with Bonferroni's multiple comparisons test. ***, p < 0.001 between indicated groups.

3.1.8 Analysis of glucose uptake in white adipose tissue of D4KO mice

Besides skeletal muscle and liver, glucose is also taken up by the white adipose tissue (WAT). This process is mediated by the translocation of the facilitative glucose transporters GLUT1 and GLUT4 at basal and insulin-stimulated conditions, respectively (1.3.1). In order to investigate whether an increased uptake of glucose into the WAT may explain the improved glycaemia in trained D4KO mice, Western Blot analysis of GLUT1 and GLUT4 protein content was performed (2.2.3.7). As expected, D4KO mice lacked the TBC1D4 protein band in the WAT (Figure 14 A). GLUT1 protein content was not affected by either genotype or training intervention (Figure 14 A, B). Similar to skeletal muscle, the lack of TBC1D4 led to a marked reduction of GLUT4 in WAT, with 40 % less protein detectable compared to WT controls (58.6 ± 6.8 % in D4KO vs. 100 ± 8 % in WT mice, p < 0.01; Figure 14 A, C). Interestingly, chronic exercise led to a significant increase of total GLUT4 in WAT of D4KO mice (91.9 ± 9.6 % in trained vs. 58.6 ± 6.8 % in sedentary D4KO mice, p < 0.05).

In order to determine whether this rise in GLUT4 protein abundance of trained D4KO mice was due to an increased gene expression, qPCR analysis of *Slc2a4* mRNA content was additionally conducted (2.2.4.3). *Slc2a4* mRNA content was significantly reduced in D4KO mice compared

to WT controls (0.48 ± 0.08 $2^{-\Delta\Delta Ct}$ in D4KO vs. 1.0 ± 0.22 $2^{-\Delta\Delta Ct}$ in WT mice, $p < 0.05$; Figure 14 D). After chronic exercise, *Slc2a4* expression in WAT of D4KO mice was mildly increased.

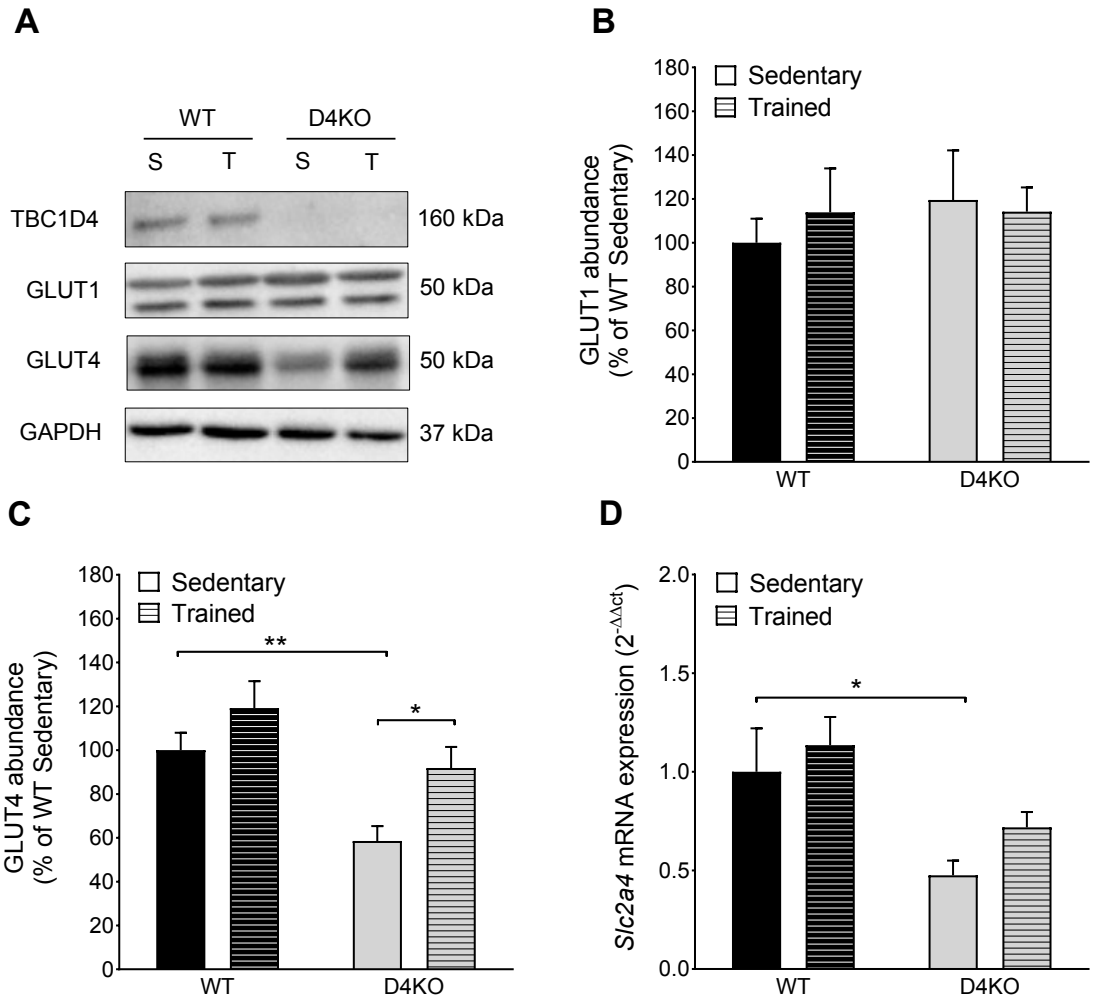

Figure 14: Protein abundance of TBC1D4, GLUT1 and GLUT4 and gene expression of GLUT4 (*Slc2a4)* in WAT of WT and D4KO mice. Representative Western Blots of TBC1D4, GLUT1 and GLUT4 (**A**) and quantification of GLUT1 (**B**) and GLUT4 (**C**) in WAT of WT and D4KO mice. Protein abundance was normalized to GAPDH and given as percentage of the WT sedentary group. Expression of *Slc2a4* (**D**) was normalized to the housekeeping gene *Hprt*. Data are presented as mean ± SEM (n = 5-15). Data were analysed using two-way ANOVA with Bonferroni's multiple comparisons test. *, $p < 0.05$; **, $p < 0.01$ between indicated groups. S, sedentary; T, trained.

To further dissect the impact of exercise on insulin-stimulated glucose uptake in WAT, *ex vivo* [^{14}C]-D-glucose uptake was measured in isolated adipocytes from epididymal white fat depots (2.2.2.11). In sedentary WT mice, glucose uptake was increased after insulin stimulation, but without reaching statistical significance (Figure 15). As expected from previous studies (Wang et al. 2013, Chadt et al. 2015), the insulin-stimulated glucose uptake was impaired in D4KO mice compared to WT controls (52.2 ± 8.1 cpm/mg in sedentary D4KO vs. 77.5 ± 10.8 cpm/mg in sedentary WT mice, $p < 0.05$). Four weeks of treadmill training led to a marked increase of

glucose uptake after insulin stimulation in WT mice (231.4 ± 45.5 cpm/mg in trained vs. 77.5 ± 10.8 cpm/mg in sedentary WT mice, $p < 0.001$). More importantly, chronic exercise was able to restore the impaired insulin-mediated glucose uptake in D4KO mice (148.7 ± 36.8 cpm/mg in trained vs. 52.2 ± 8.1 cpm/mg in sedentary D4KO mice, $p < 0.01$). Taken together, chronic exercise was able to restore both, GLUT4 protein content and glucose uptake in WAT of D4KO mice, possibly contributing to the improved whole-body insulin sensitivity.

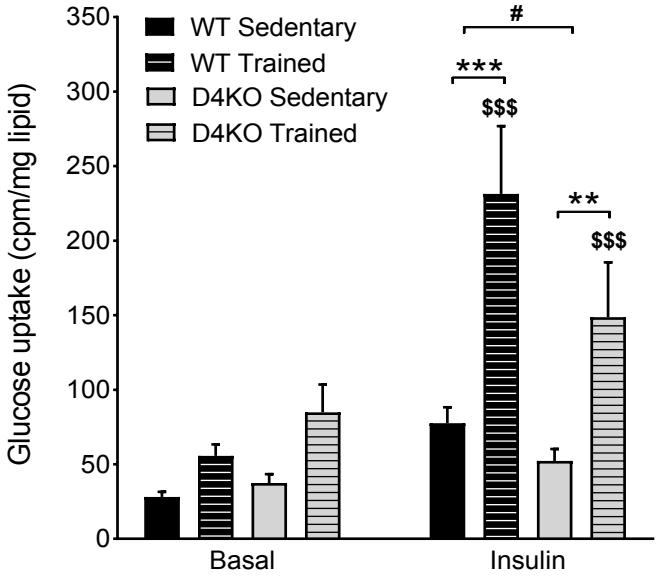

Figure 15: *Ex vivo* glucose uptake in isolated adipocytes from WAT of WT and D4KO mice. Glucose uptake was measured at basal or insulin-stimulated conditions in isolated adipocytes from WAT of sedentary and trained WT and D4KO mice. Data are presented as mean ± SEM (n = 12). Data were analysed using two-way ANOVA with Bonferroni's multiple comparisons test. $$$, $p < 0.001$ basal vs. insulin of respective group; #, $p < 0.05$ D4KO vs. WT; **, $p < 0.01$; ***, $p < 0.001$ sedentary vs trained of respective group.

3.1.9 Abundance of glucose transporters in brown adipose tissue of D4KO mice

Besides the WAT, also the brown adipose tissue (BAT) contributes to improved glucose homeostasis by GLUT1 and GLUT4-dependent glucose uptake (1.4.4.2). In order to investigate whether the abundance of glucose transporters in BAT was affected by the exercise intervention, Western Blot analysis of GLUT1 and GLUT4 protein content was performed (2.2.3.7). Figure 16 A shows the expected band pattern of TBC1D4 for both genotypes. GLUT1 protein content was not different between the genotypes or between sedentary and trained mice (Figure 16 A, B). In trained WT mice, total GLUT4 abundance was significantly elevated compared to sedentary controls (137.5 ± 5.7 % in trained vs. 100 ± 5.0 % in sedentary WT mice, $p < 0.001$, Figure 16 A, C). Similar to the findings in the WAT, GLUT4 protein content was approximately 40 % reduced in the BAT of D4KO mice. Four weeks of

moderate exercise were able to increase, but not fully restore the abundance of GLUT4 in D4KO mice (74.3 ± 5.5 % in trained vs. 57.5 ± 4.4 % in sedentary D4KO mice, $p < 0.05$).

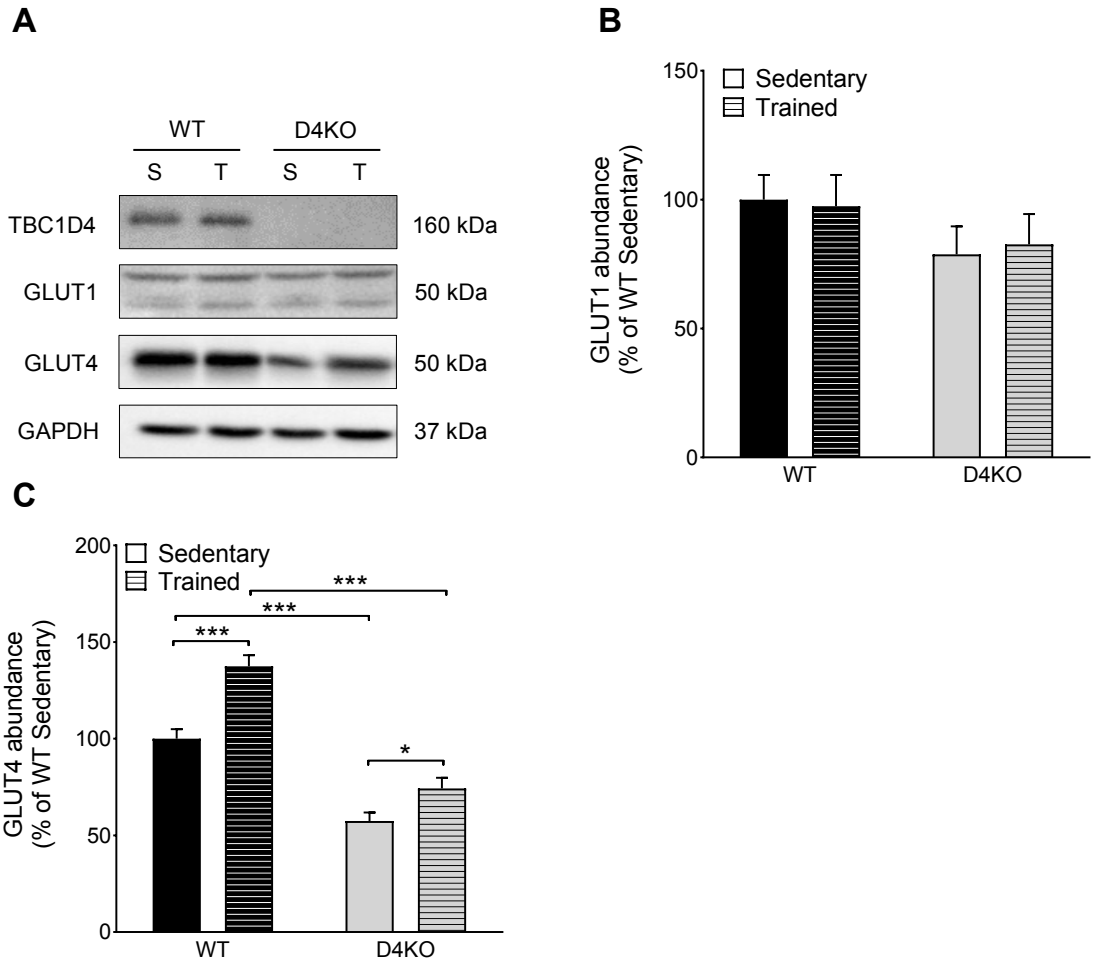

Figure 16: Protein abundance of TBC1D4, GLUT1 and GLUT4 in BAT of WT and D4KO mice. Representative Western Blots of TBC1D4, GLUT1 and GLUT4 (**A**) and quantification of GLUT1 (**B**) and GLUT4 (**C**) in BAT of WT and D4KO mice. Protein abundance was normalized to GAPDH and given as percentage of the WT sedentary group. Data are presented as mean ± SEM (n = 9-18). Data were analysed using two-way ANOVA with Bonferroni's multiple comparisons test. *, $p < 0.05$; ***, $p < 0.001$ between indicated groups. S, sedentary; T, trained.

3.1.10 Expression of browning markers in scWAT of D4KO mice

Regular exercise has been shown to increase the mitochondrial activity and biogenesis of adipocytes from subcutaneous white adipose tissue (scWAT), thus sharing characteristics of brown fat cells (1.4.4.2). This browning process involves the upregulation of several brown adipocytes-marker genes, such as *Ucp-1*, *Cidea*, *Cox8b*, *Ppargc1a* and *P2rx5* (Trevellin et al. 2014, Stanford, Middelbeek, & Goodyear 2015, Garcia et al. 2016). In a pilot study within our institute, these 5 genes have been shown to be highest upregulated in trained B6 mice fed a HFD (Crepcia-Pevzner 2017, Master thesis). In order to determine whether the improved

glycaemia in WAT of trained D4KO mice was associated with increased browning of adipose tissue, qPCR analysis of the respective genes was conducted (2.2.4.3). *Ucp-1* mRNA was not changed in WT mice, but highly induced in D4KO mice after chronic exercise (5.1 ± 2.7 $2^{-\Delta\Delta Ct}$ in trained vs. 0.2 ± 0.1 $2^{-\Delta\Delta Ct}$ in sedentary D4KO mice, $p < 0.05$; Figure 17 A). Expression levels of *Cidea*, *Cox8b* and *P2rx5* were not significantly changed in WT mice, but significantly elevated in trained D4KO mice compared to sedentary controls (Figure 17 B - D). *Ppargc1a* mRNA expression was elevated in both, WT and D4KO mice after chronic exercise (Figure 17 E).

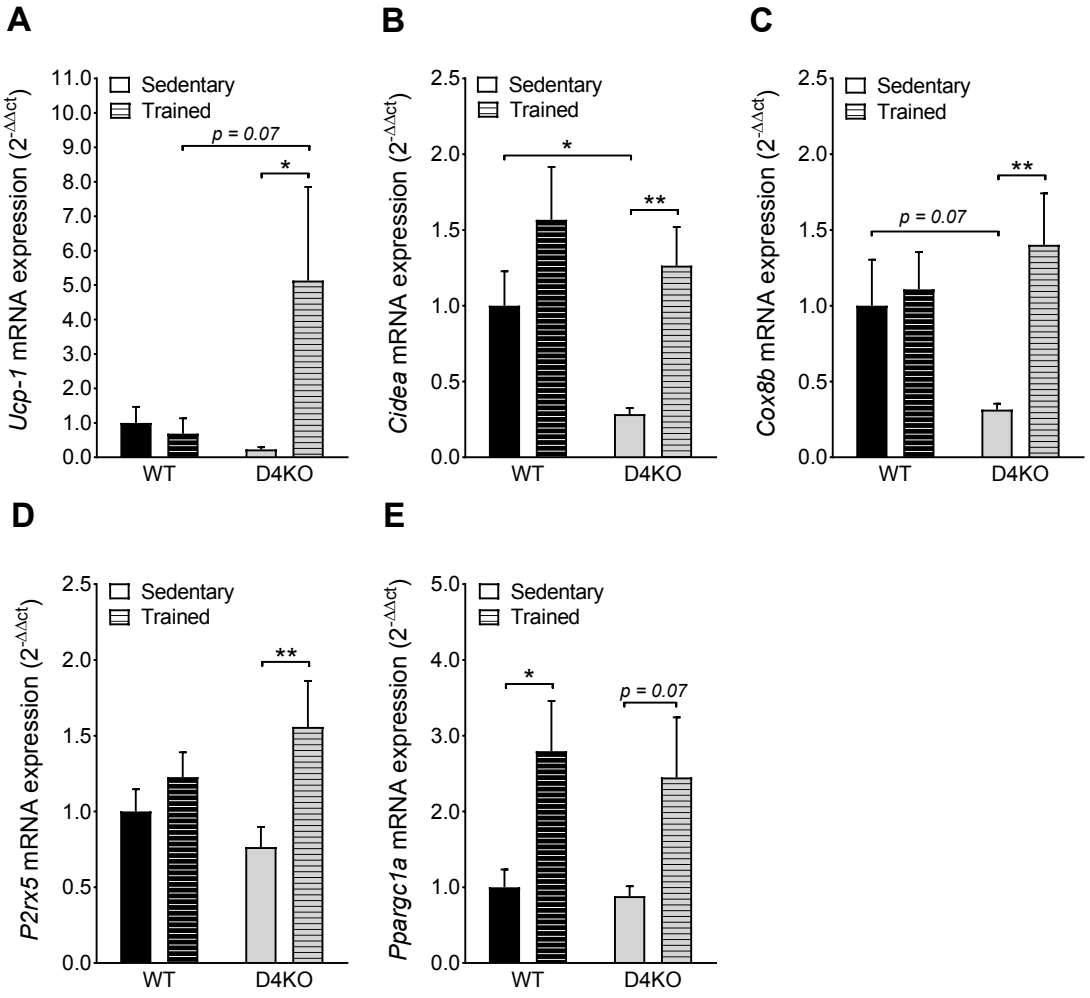

Figure 17: Expression of markers for mitochondrial biogenesis and browning in scWAT of WT and D4KO mice. qPCR analysis of the browning markers *Ucp-1* (**A**), *Cidea* (**B**), *Cox8b* (**C**), *P2rx5* (**D**) and *Ppargc1a* (**E**) in sedentary and trained WT and D4KO mice. Expression was normalized to the housekeeping gene *Hprt*. Data are presented as mean ± SEM (n = 9-16). Data were analysed using two-way ANOVA with Bonferroni's multiple comparisons test. *, $p < 0.05$; **, $p < 0.01$ between indicated groups.

The increase of UCP-1 gene expression could also be validated on protein level via Western Blot analysis using stain-free gels (2.2.3.7.3), which revealed a markedly elevated abundance of UCP-1 in scWAT of trained D4KO mice (108.0 ± 15.5 % in trained vs. 64.7 ± 9.4 % in sedentary D4KO mice, $p < 0.05$; Figure 18 A, B).

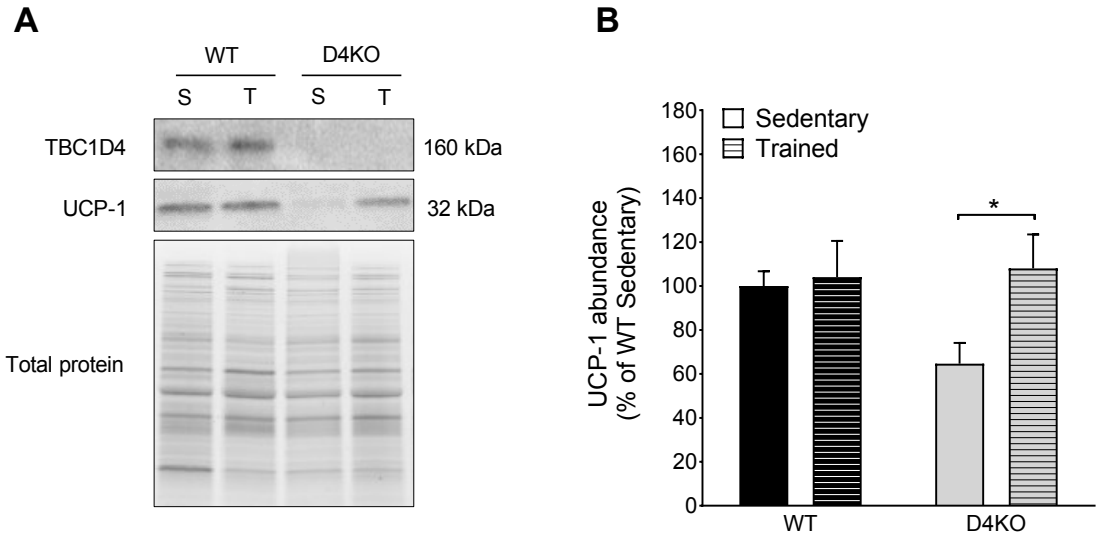

Figure 18: Protein abundance of UCP-1 in scWAT of WT and D4KO mice. Representative Western Blots of TBC1D4 and UCP-1 (**A**) and quantification of UCP-1 (**B**) in scWAT of WT and D4KO mice. Protein abundance was normalized to total protein content and given as percentage of the WT sedentary group. Data are presented as mean ± SEM (n = 10-12). Data were analysed using two-way ANOVA with Bonferroni's multiple comparisons test. *, $p < 0.05$ between indicated groups. S, sedentary; T, trained.

In conclusion, four weeks of chronic exercise improved endurance capacity and whole-body glycaemia in D4KO mice, presumably due to rescue of glucose uptake and GLUT4 protein content in adipose tissue, as well as increased browning in scWAT. In addition, reduction of hepatic triglycerides contributed to improved whole-body fat disposal in trained D4KO mice.

3.2 Impact of chronic exercise on glucose homeostasis in NZO mice

The development of obesity and T2DM in NZO mice has been shown to be associated with impaired physical activity (Jürgens et al. 2006). No studies subjecting NZO mice to a chronic and forced exercise intervention have been reported so far. Thus, the impact of regular exercise on physical capacity and T2DM development of NZO mice should be investigated in the second part of the present thesis.

However, the previous results have shown that despite the improvements in D4KO mice, the phenotype of WT controls was only mildly affected by the four-week training intervention, as endurance capacity and glucose tolerance were not improved (see Figure 7 and Figure 8). Moreover, whole-body fat mass and liver fat content of WT mice tended to be increased with exercise (see Table 12 and Figure 13), suggesting that the intensity of the exercise protocol used was not sufficient to induce exercise-mediated changes in WT control mice. Previous exercise studies in mice have shown that regular exercise training improves glucose tolerance (Ritchie et al. 2014, Samaan et al. 2014), prevents the diet-induced weight gain (E et al. 2013, Evans et al. 2014) and reduces liver fat content (Magkos 2012, Hafstad et al. 2013). Consequently, the exercise protocol needed to be modified in order to create an adequate training program that would clearly improve physical capacity and glycaemia in mice. Subsequently, this protocol should be used for the following exercise intervention study with NZO mice.

3.2.1 Establishment of a new chronic exercise protocol in B6 mice

Establishment of a new exercise protocol was carried out in a small cohort of B6 mice fed a HFD with 60 % fat from calories (Table 2). The training period was extended from four to six weeks, with five training sessions per week. More importantly, the exercise protocol was changed to a chronic interval training (2.2.2.2 and Table S2), which is considered to increase the performance and reduce physical injury of the mice (Samaan et al. 2014). In order to adjust for the circadian rhythm, the mice were housed in a reversed light-dark cycle (2.2.2.1) and subjected to the treadmill training at the beginning or during the active dark phase.

3.2.1.1 Physical capacity and glucose tolerance of B6 mice

Physical capacity of B6 mice was measured during exhaustion running tests at the end of the training intervention (2.2.2.3). Trained mice exhibited an improved physical capacity compared to sedentary controls, reflected in a significantly increased time to exhaustion (24.6 ± 0.9 min in trained vs. 17.1 ± 1.1 min in sedentary B6 mice; $p < 0.01$, Figure 19 A). In addition, blood lactate concentrations of trained mice were measured before and after one acute exercise bout

(2.2.2.7). Figure 19 B shows that blood lactate concentrations of trained mice were mildly but significantly increased after treadmill running. To investigate the impact of chronic interval training on glucose tolerance, i.p. GTTs were performed in sedentary and trained B6 mice in week 21 (2.2.2.8). Blood glucose clearance after injection of glucose was faster in trained mice, reflected in a significantly reduced AUC (42825 ± 1207 in trained vs. 49769 ± 2409 in sedentary B6 mice, $p < 0.05$, Figure 19 C, D).

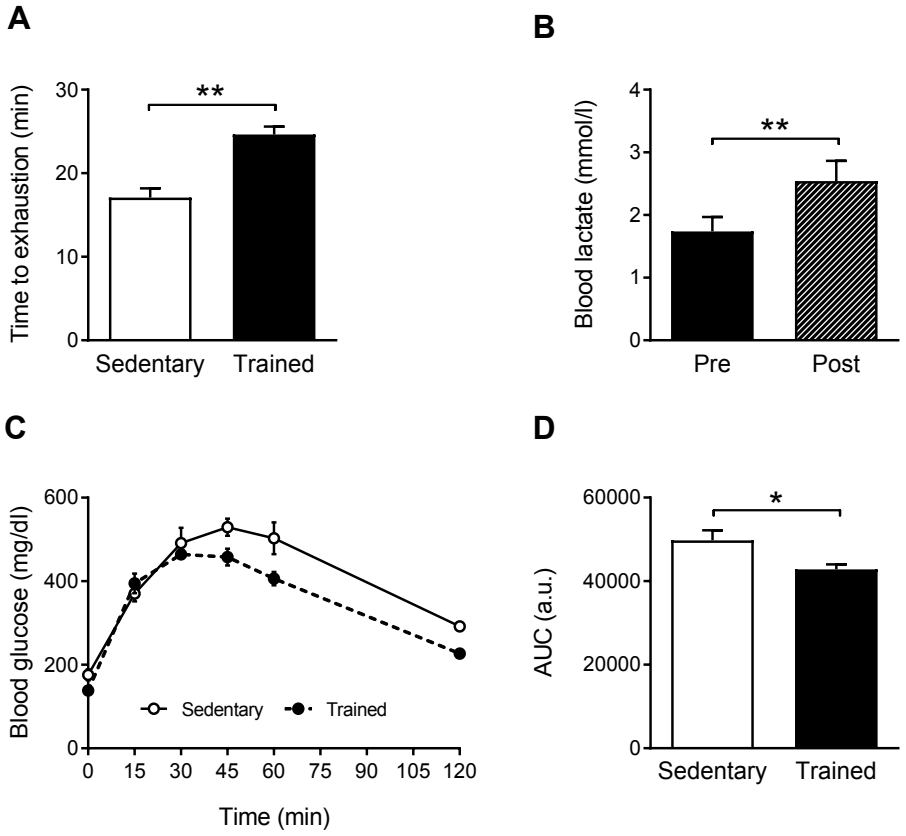

Figure 19: Physical capacity, blood lactate concentrations and glucose tolerance of B6 mice after chronic interval training. Time to exhaustion (**A**) was measured at the end of training intervention in sedentary and trained mice. Blood lactate concentrations (**B**) were measured in trained mice pre and post a daily exercise session. Glucose tolerance (**C**) was measured during intraperitoneal glucose tolerance tests. AUC was determined for quantification of glucose tolerance (**D**). Data are presented as mean ± SEM (n = 4-6). Data were analysed using unpaired (A, D) or paired (B) student's t-test. *, $p < 0.05$; **, $p < 0.01$.

3.2.1.2 Body composition and hepatic triglyceride content of B6 mice

In order to determine the effect of chronic interval training on the development of body composition, NMR analysis of sedentary and trained B6 mice was performed in week 15, 18 and 21, respectively. Feeding the HFD led to an increased body weight due to elevated fat mass in sedentary mice (Figure 20 A, B). In contrast, the increase of body weight was prevented in trained mice, due to a significantly reduced fat mass (8.8 ± 1.4 g in trained vs.

13.6 ± 1.2 g in sedentary B6 mice at week 21, $p < 0.05$; Figure 20 B). Lean mass was similar between sedentary and trained mice (Figure 20 C). In order to investigate whether the reduced body weight and fat mass in trained mice was associated with reduced liver fat, hepatic triglyceride content was measured after chloroform/ methanol extraction (2.2.3.4). Importantly, trained B6 mice showed a 50 % reduction of hepatic triglyceride content compared to sedentary controls (12.7 ± 1.6 µg/mg in trained vs. 23.9 ± 2.2 µg/mg in sedentary B6 mice, $p < 0.001$; Figure 20 D).

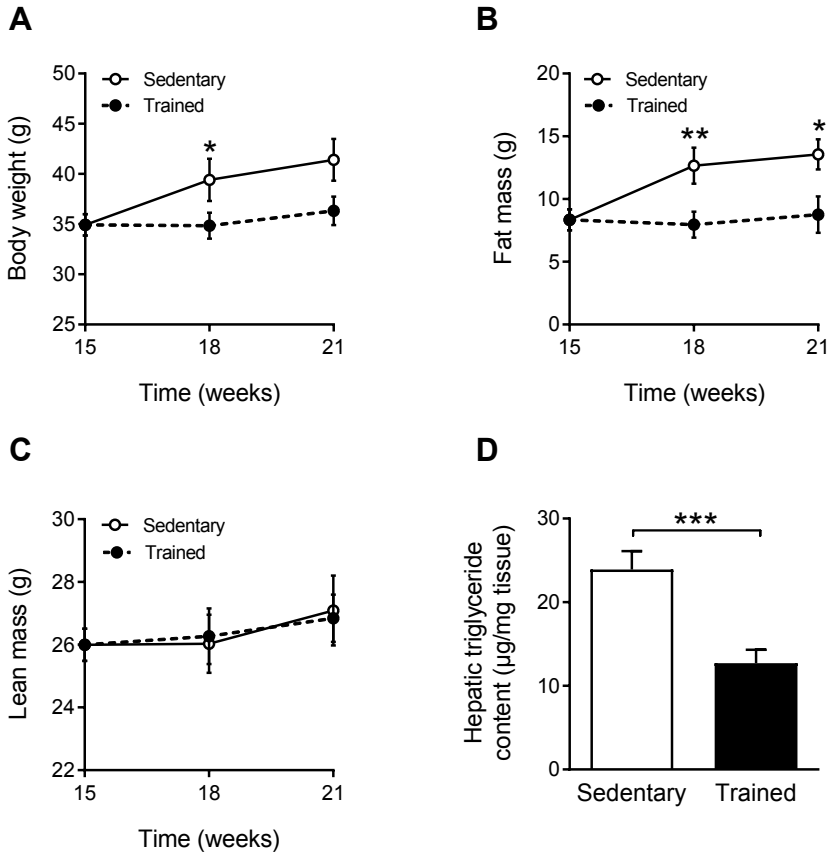

Figure 20: Body composition and hepatic triglyceride content of B6 mice after chronic interval training. Body weight (**A**), fat mass (**B**) and lean mass (**C**) of sedentary and trained B6 mice was measured by NMR analysis in week 15, 18 and 21, respectively. Triglyceride content (**D**) was measured in liver of sedentary and trained mice. Data are presented as mean ± SEM (Body composition: n = 5-6, Hepatic triglyceride content: n = 15-20). Data were analysed using unpaired student's t-test. *, $p < 0.05$; **, $p < 0.01$; ***, $p < 0.001$ sedentary vs. trained.

3.2.1.3 Whole-body energy expenditure of B6 mice

In order to assess the impact of chronic interval treadmill training on whole-body energy expenditure and substrate utilization, indirect calorimetry of sedentary and trained B6 mice was conducted in week 20 (2.2.2.4). Trained B6 mice showed a higher RER compared to sedentary controls, especially during the active dark phase (Figure 21 A, B). Concomitantly,

whole-body CHO tended to be enhanced in trained B6 mice, whereas whole-body FAO was significantly reduced (Figure S2). Thus, these results pointed towards increased use of carbohydrates for substrate utilization in trained B6 mice. In addition, food intake, oxygen consumption and voluntary activity as estimators for energy expenditure were analysed. Trained B6 mice exhibited an increased food intake (0.75 ± 0.07 kcal/g in trained vs. 0.49 ± 0.05 kcal/g in sedentary B6 mice, $p < 0.05$, Figure 21 C), as well as an increased VO_2 consumption (Figure 21 D). Voluntary activity was not different between sedentary and trained mice (Figure S2).

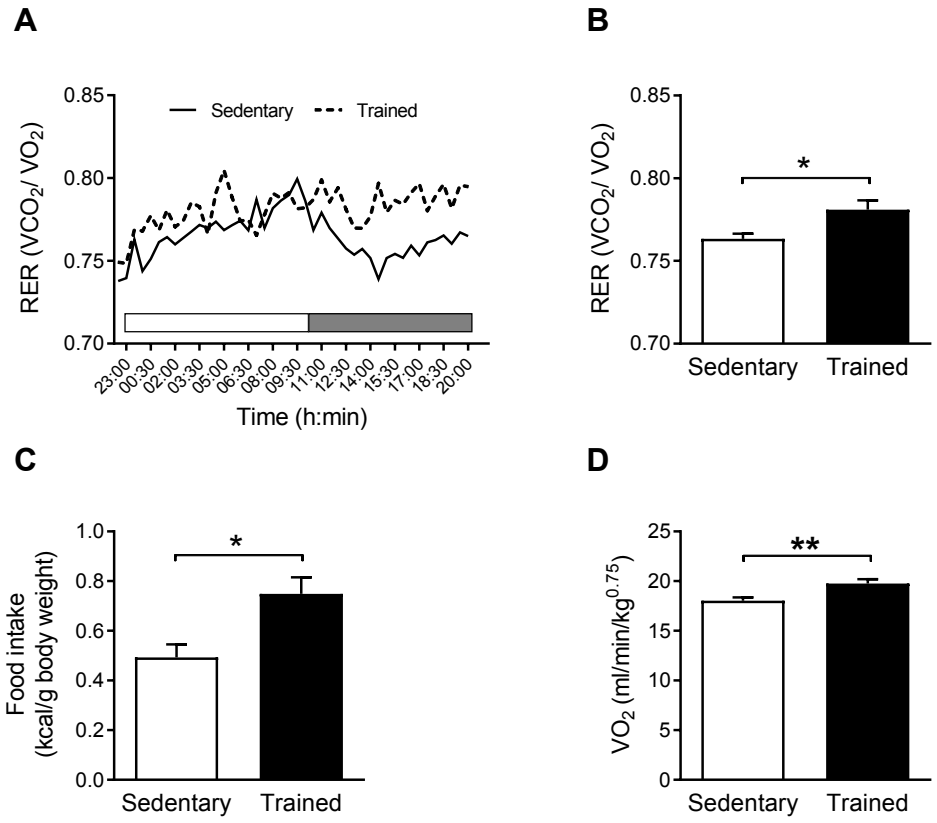

Figure 21: Whole-body energy expenditure of B6 mice after chronic interval training. RER was monitored over 24 hours during indirect calorimetry measurements (**A**). White and grey horizontal bar represents light and dark phase, respectively. **B** shows the mean average of RER measurements. Food intake (**C**) and VO_2 consumption (**D**) were measured as an estimate of energy expenditure. Data are presented as mean ± SEM (n = 6-7). Data were analysed using unpaired student's t-test *, $p < 0.05$; **, $p < 0.01$.

3.2.1.4 Abundance of PGC-1α and AMPK in skeletal muscle of B6 mice

The activation of the transcriptional coactivator PGC-1α and the contraction-dependent AMPK represents an important readout for exercise-induced improvements in skeletal muscle metabolism (1.4.4.1). In order to prove the activation of PGC-1α and AMPK after chronic interval training, Western Blot analysis of PGC-1α, AMPK and phosphorylated AMPK (pAMPK)

was performed in the oxidative *Soleus* muscle of sedentary and trained B6 mice (2.2.3.7). A non-significant trend for increased protein abundance of PGC-1α was observed in trained B6 mice (Figure 22 A, B). Moreover, the phosphorylation of the AMPK was significantly elevated in *Soleus* muscle of trained mice (Figure 22 A, C).

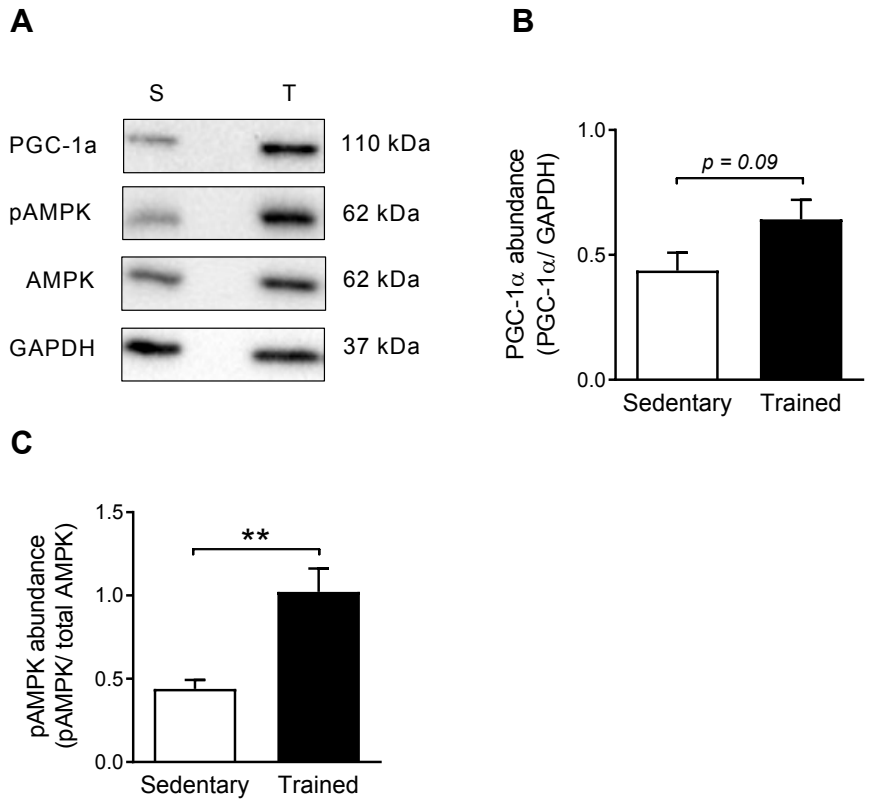

Figure 22: Protein abundance of PGC-1α, AMPK and pAMPK in *Soleus* muscle of B6 mice after chronic interval training. Representative Western Blots of PGC-1α, pAMPK and total AMPK (**A**) and quantification of PGC-1α (**B**) and pAMPK (**C**) in *Soleus* muscle of sedentary and trained B6 mice. Protein abundance was normalized to GAPDH. Abundance of pAMPK was quantified in relation to total AMPK. Data are presented as mean ± SEM (n = 5-6). Data were analysed using unpaired student's t-test. **, $p < 0.01$. S, sedentary; T, trained.

In conclusion, chronic interval training clearly improved physical capacity and glucose tolerance in B6 mice. Despite increased food intake, the HFD-induced weight gain was prevented and hepatic fat content was reduced after six weeks of interval training, indicating increased energy expenditure in trained mice. Moreover, the increased abundance of muscular PGC-1α and AMPK suggested an improved skeletal muscle metabolism in response to exercise. Therefore, this treadmill protocol served as the basis for the following exercise intervention study with NZO mice.

3.2.2 Physical capacity and glucose tolerance of trained NZO mice fed a SD

To investigate whether regular exercise would improve the physical capacity of NZO mice and, more importantly, whether they would be willing to run on motorized treadmills, mice were initially rendered normoglycaemic using a SD (Table 2). Using a SD has been shown to prevent the early-onset of hyperglycaemia in NZO mice, before diabetes develops at later stages of life (Jürgens et al. 2007). Therefore, chronic interval training was performed with six week-old mice. Although the number of high intensity (18 m/min) phases had to be slightly reduced, the NZO mice were able to pass a similar chronic interval training that was used for the B6 mice (cp. Table S2 and Table S3). Treadmill training lasted for six weeks and body composition, physical capacity and glucose tolerance were determined.

Overall body composition was not changed between sedentary and trained mice, apart from a mildly reduced lean mass in trained NZO mice (Table S5). To evaluate improvements of physical capacity, exhaustion running tests were conducted in the last week of training (2.2.2.3). Trained NZO mice significantly improved their physical capacity, reflected in an elevated time to exhaustion (15.8 ± 0.3 min in trained vs. 10.3 ± 0.5 min in sedentary NZO mice, $p < 0.001$; Figure 23 A). Furthermore, the RER during the running test was mildly reduced in trained NZO mice compared to sedentary controls (Table S5). In addition, blood lactate concentrations of trained NZO were measured pre and post one acute exercise session (2.2.2.7). Figure 23 B shows that blood lactate concentrations were significantly increased in trained NZO mice (2.2 ± 0.2 mmol/l post vs. 1.4 ± 0.2 mmol/l pre exercise, $p < 0.01$).

To verify the successful prevention of hyperglycaemia, random fed blood glucose was measured in sedentary and trained NZO mice. NZO mice that exhibited random fed blood glucose concentrations higher than 300 mg/dl were considered as hyperglycaemic, according to a commonly used threshold (Joost & Schürmann 2014, Voigt et al. 2015). Figure 23 C shows that none of the NZO mice became hyperglycaemic, since blood glucose concentrations were below the threshold. FBG and FPI concentrations of trained mice were not significantly different compared to sedentary controls (Table S5). In addition, glucose tolerance was measured during i.p. GTTs at the end of training intervention (2.2.2.8). Blood glucose clearance after injection of glucose was not different between sedentary and trained NZO mice (Figure 23 D). Taken together, normoglycaemic NZO mice fed a SD were able to perform a six-week chronic interval training on treadmills. Although trained NZO mice showed an increased physical capacity, whole-body glycaemia was not significantly improved by the chronic exercise intervention.

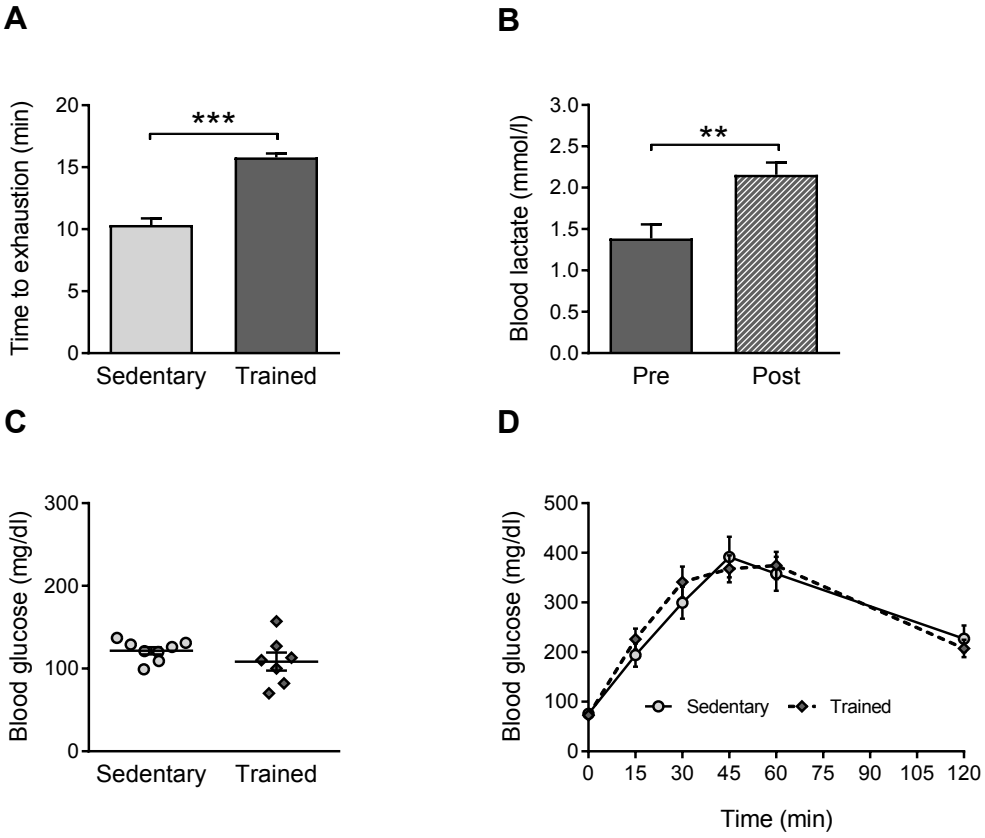

Figure 23: Physical capacity, blood lactate concentrations and glycaemia of NZO mice fed a SD after chronic interval training. Time to exhaustion (**A**) was measured during exhaustion running tests in sedentary and trained NZO mice fed a SD. Blood lactate concentrations (**B**) were measured in trained mice pre and post a daily exercise session. Random fed blood glucose (**C**) and glucose tolerance during i.p. GTTs (**D**) were determined at the end of training intervention. Data are presented as mean ± SEM (n = 5-8). Data were analysed using unpaired (A, C) or paired (B) student's t-test. **, $p < 0.01$; ***, $p < 0.001$.

3.2.3 Establishment of the HFD-induced T2DM development in NZO mice

After validating the adaptation of NZO mice to the treadmill training, the next step was to investigate the impact of chronic exercise on T2DM development. Studies have shown that the onset of hyperglycaemia and diabetes in NZO mice is rapidly induced by exposure to a HFD (1.5.3). Since the aim was to examine a possible preventive effect of exercise on T2DM development, the given HFD should induce a moderate but not severe hyperglycaemia in NZO mice. Therefore, different HFDs were tested before starting the training intervention (Table 2). Besides altering the fat content, also the amount of sucrose was varied in these diets, since high amount of sucrose has been shown to be an essential risk factor for obesity and insulin resistance (Jürgens et al. 2005, Softic et al. 2017). From the four different diets tested, the HFD with 30 % fat from calories and reduced sucrose content (30 % HFD-RS) was chosen, since this diet induced obesity and a moderate but not highly impaired hyperglycaemia in NZO

mice (Figure S3, S4). To answer the question whether chronic exercise would prevent or delay the progress of hyperglycaemia and T2DM, NZO mice fed the 30 % HFD-RS subsequently underwent a six-week chronic interval training on treadmills (2.2.1).

3.2.4 Blood glucose of NZO mice fed a HFD before and after chronic interval training

In order to assess the glycaemic state of sedentary and trained NZO mice at the beginning and end of training intervention, FBG was measured in week 6 and 11, respectively. At 6 weeks of age, all NZO mice showed average FBG concentrations at around 100 mg/dl (Figure 24). At 11 weeks of age, the mean FBG increased to approximately 300 mg/dl in NZO mice, which was not reduced after chronic exercise (307 ± 31 mg/dl in trained vs. 296 ± 27 mg/dl in sedentary NZO mice). However, in both sedentary and trained mice, the FBG concentrations had clustered into two subgroups, with approximately 50 % of mice remaining below and 50 % of mice exceeding FBG concentrations of 300 mg/dl.

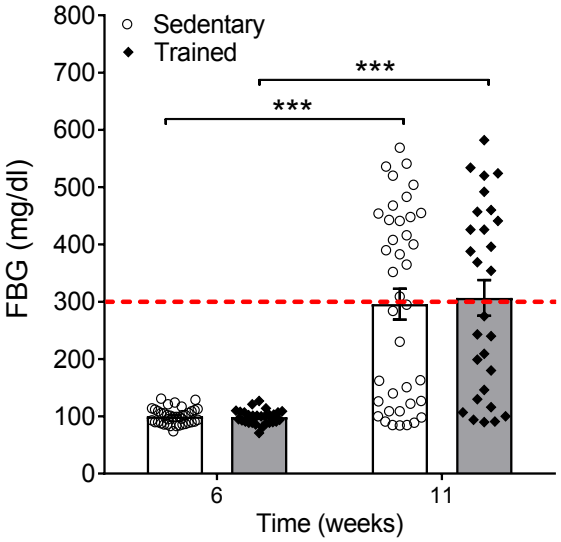

Figure 24: FBG of NZO mice fed a HFD after chronic interval training. FBG was measured before (week 6) and at the end (week 11) of training intervention in sedentary and trained NZO mice fed a HFD. Data are presented as single values (scatter plot) and mean bars ± SEM (n = 28-39). Data were analysed using two-way ANOVA with Bonferroni's multiple comparisons test. ***, $p < 0.001$ between indicated groups. Dashed line illustrates the diabetic threshold of 300 mg/dl after 6 hours of fasting.

The incidence of severely high FBG values in both the sedentary and trained group already showed that chronic exercise did not prevent the NZO mice from developing hyperglycaemia. However, to address the question whether the response to the training intervention was altered in the two subgroups, the NZO mice were divided into a non-diabetic (ND) and diabetic (T2D) group, whereas animals exhibiting FBG values greater than 300 mg/dl were considered as diabetic (King 2012, Fox et al. 2006). Therefore, all the following analyses show data for sedentary and trained, as well as ND and T2D NZO mice.

3.2.5 Physical capacity of NZO mice fed a HFD

For the determination of physical capacity, sedentary and trained NZO mice performed exhaustion running tests at the end of training intervention in week 12 (2.2.2.3). Trained ND mice showed an improved time to exhaustion compared to sedentary controls (13.9 ± 0.6 min in trained vs. 10.4 ± 0.7 min in sedentary ND mice, $p < 0.01$; Figure 25 A). Although not significantly improved, the time to exhaustion of trained T2D mice was similar to trained ND mice. VO_{2max} was not changed after training in both groups (Figure 25 B). Interestingly, the RER was not affected by chronic exercise, but overall reduced in T2D compared to ND mice (Figure 25 C). In addition to the exhaustion running tests, blood lactate concentrations of NZO mice were measured pre and post one daily exercise bout in week 10 (2.2.2.7). Blood lactate concentrations were not increased, but mildly decreased after treadmill training in both the ND and T2D group (Figure 25 D).

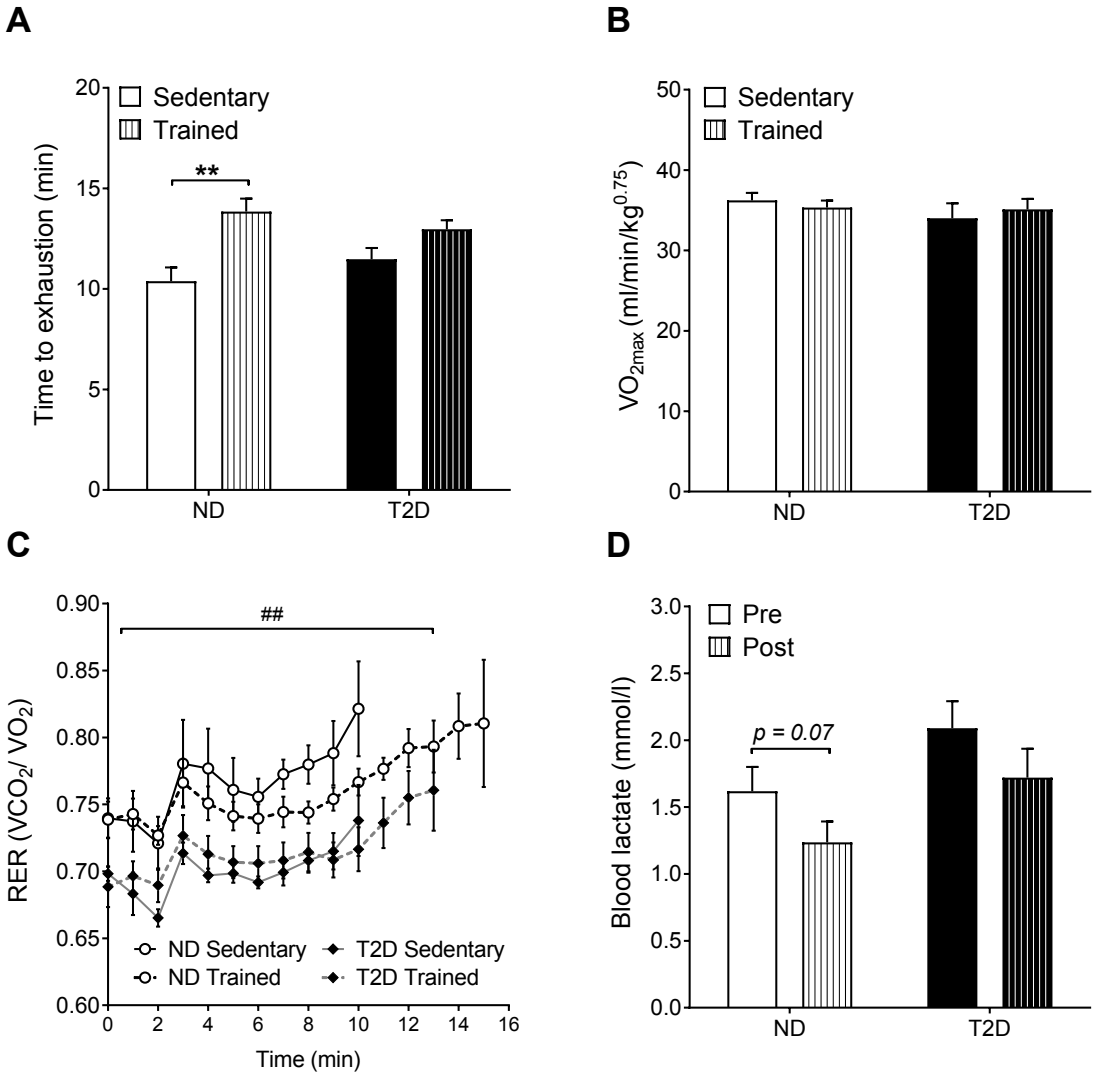

Figure 25: Physical capacity and blood lactate concentrations of ND and T2D mice after chronic interval training. Time to exhaustion (**A**), VO_{2max} (**B**) and RER (**C**) of sedentary and trained ND and

T2D NZO mice were measured during exhaustion running tests in week 12. Blood lactate concentrations (**D**) were measured in trained mice pre and post a daily exercise session. Data are presented as mean ± SEM (Sedentary: n = 4-5, Trained: n = 9-14). Data were analysed using two-way ANOVA with Bonferroni's multiple comparisons test (A, B, D) or using unpaired student's t-test (C). **, $p < 0.01$ between indicated groups; ##, $p < 0.01$ between ND and T2D mice (mean RER).

3.2.6 Whole-body energy expenditure of NZO mice fed a HFD

In addition to the calorimetric treadmill measurements, indirect calorimetry was performed with sedentary and trained NZO mice, in order to gain insight into whole-body substrate utilization (2.2.2.4). Similar to the RER during the physical capacity test, the RER was significantly reduced in both sedentary and trained T2D compared to ND mice (Figure 26 A). Transferring the VO_2 and VCO_2 data into indices for whole-body CHO and FAO led to reduced rates of CHO but increased rates of FAO in diabetic NZO mice (Figure 26 B, C). In addition, food intake was significantly elevated in trained T2D mice compared to sedentary controls (Figure 26 D), whereas voluntary activity and VO_2 consumption were not changed within the groups (Figure S5).

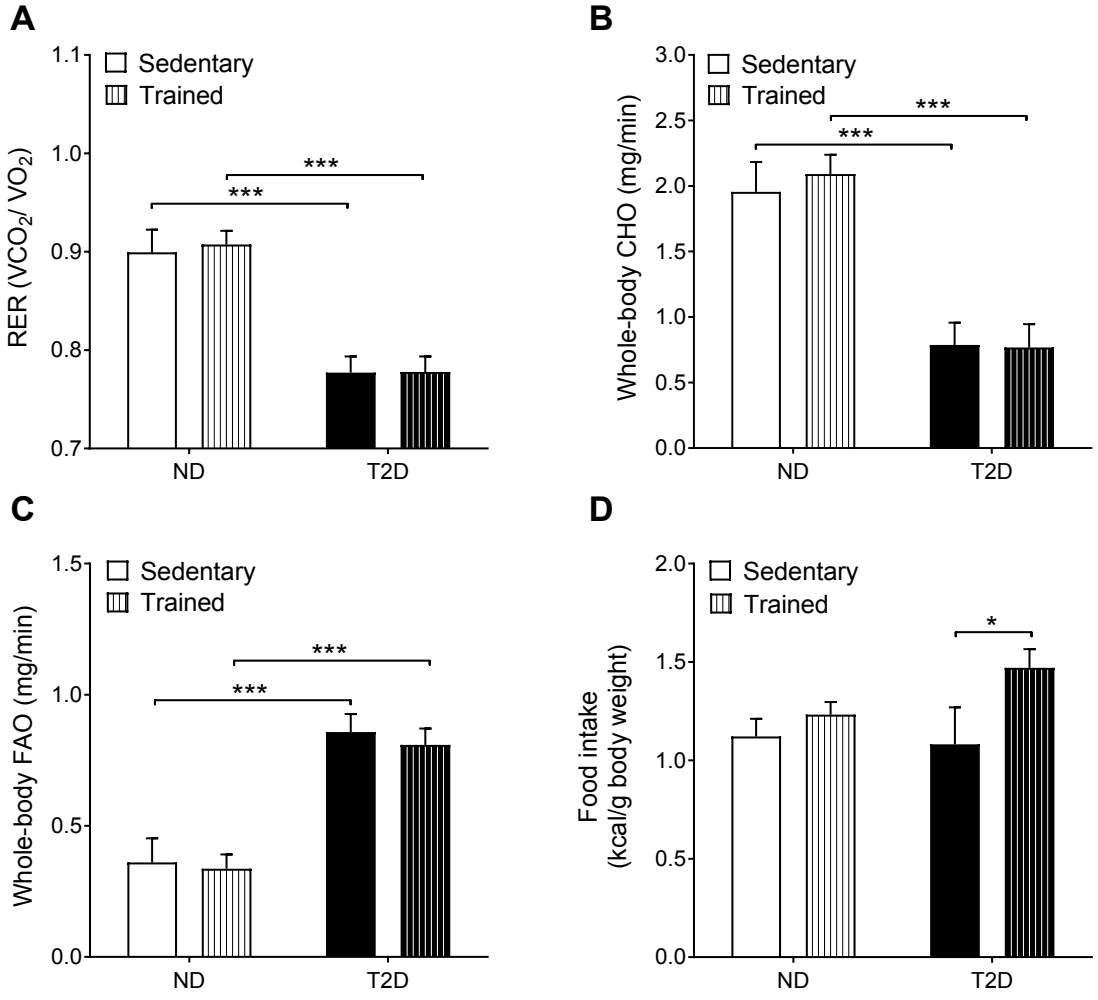

Figure 26: Whole-body energy expenditure of ND and T2D mice after chronic interval training. Mean RER (**A**), whole-body CHO (**B**), whole-body FAO (**C**) and food intake (**D**) of sedentary and trained ND and T2D NZO mice were measured during indirect calorimetry for 24 hours. Data are presented as mean ± SEM (n = 5-7). Data were analysed using two-way ANOVA with Bonferroni's multiple comparisons test. *, $p < 0.05$; ***, $p < 0.001$ between indicated groups.

3.2.7 Body composition and plasma parameters of NZO mice fed a HFD

Table 13 summarizes the body composition (2.2.2.5) and basic plasma parameters including FBG (2.2.2.6), FPI (2.2.3.1) and plasma triglyceride and plasma NEFA concentrations (2.2.3.2) of ND and T2D mice. Body composition and plasma parameters were not significantly changed between sedentary and trained ND mice. T2D mice represented an overall reduced body composition, with a significantly reduced body weight and fat mass in trained T2D compared to trained ND mice. Moreover, the hyperglycaemic T2D group exhibited a markedly reduced insulin content compared to ND mice. Plasma triglyceride and plasma NEFA content tended to be elevated in T2D conditions.

Table 13: Body composition and plasma parameters of ND and T2D NZO mice after chronic interval training.

Parameter	ND Sedentary	ND Trained	T2D Sedentary	T2D Trained
Body weight (g)	48.2 ± 0.6	47.2 ± 0.9	46.2 ± 1.0	**43.6 ± 1.1$^{\#}$**
Fat mass (g)	16.0 ± 0.5	17.0 ± 1.1	13.4 ± 1.1	**12.2 ± 1.2$^{\#\#}$**
Lean mass (g)	31.0 ± 0.6	30.0 ± 0.7	29.4 ± 0.5	28.6 ± 0.6
FBG (mg/dl)	140 ± 15	159 ± 17	**444 ± 15$^{\#\#\#}$**	**455 ± 18$^{\#\#\#}$**
FPI (ng/ml)	8.0 ± 1.0	9.1 ± 1.1	**2.7 ± 0.5$^{\#\#\#}$**	**2.7 ± 0.4$^{\#\#\#}$**
Plasma TG (mmol/l)	1.33 ± 0.21	1.21 ± 0.25	1.72 ± 0.3	2.13 ± 0.28
Plasma NEFA (mmol/l)	0.54 ± 0.06	0.59 ± 0.09	0.77 ± 0.1	0.85 ± 0.1

FBG and FPI content were measured after 6 hours of fasting, plasma TG and NEFA concentrations were measured from random fed samples. Data are presented as mean ± SEM (Body composition, FBG, FPI: n = 8-20; Plasma TG, NEFA: n = 6-10). Data were analysed using two-way ANOVA with Bonferroni's multiple comparisons test. #, $p < 0.05$; ##, $p < 0.01$; ###, $p < 0.001$ T2D vs respective ND group.

3.2.8 Hepatic and skeletal muscle glycogen content in NZO mice fed a HFD

To estimate whether chronic exercise altered hepatic or skeletal muscle glycogen stores as important contributors to skeletal muscle energy supply, glycogen content was measured in liver and *Gastrocnemius* muscle of sedentary and trained ND and T2D mice (2.2.3.3). A non-

significant trend for reduced hepatic glycogen content was observed in trained ND and trained T2D mice compared to the respective sedentary controls (Figure 27 A). Skeletal muscle glycogen content remained unchanged in ND mice, while T2D mice showed a significant reduction after chronic exercise (0.16 ± 0.02 µg/mg in trained vs. 0.29 ± 0.03 µg/mg in sedentary T2D mice, $p < 0.05$; Figure 27 B).

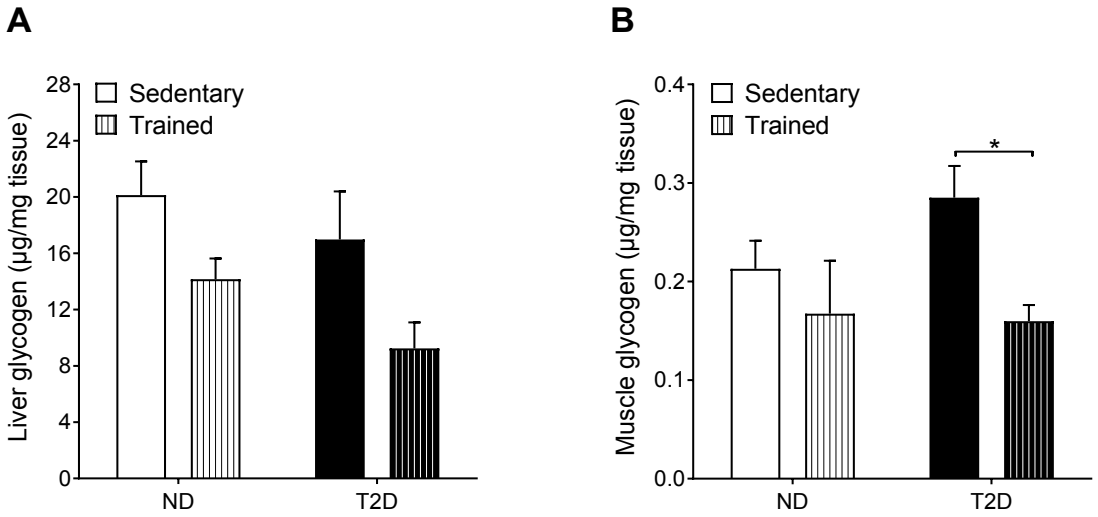

Figure 27: Hepatic and skeletal muscle glycogen content of ND and T2D mice after chronic interval training. Glycogen content was measured in liver (**A**) and *Gastrocnemius* muscle (**B**) of sedentary and trained ND and T2D NZO mice. Data are presented as mean ± SEM (n = 6-11). Data were analysed using two-way ANOVA with Bonferroni's multiple comparisons test. *, $p < 0.05$.

3.2.9 Glucose tolerance and insulin tolerance of NZO mice fed a HFD

To determine the impact of chronic exercise on whole-body insulin sensitivity of NZO mice, i.p. GTT (2.2.2.8) and i.p. ITT (2.2.2.9) experiments were performed in week 11 or week 10, respectively. ND mice tended to have an improved glucose tolerance after chronic interval training (Figure 28 A, B). This improvement only reached statistical significance, when blood glucose concentrations were normalized to basal values (Figure S6). In T2D mice, glucose tolerance was severely impaired compared to ND controls, reflected in a significantly elevated AUC (127519 ± 2465 in sedentary T2D vs. 85428 ± 3856 in sedentary ND mice, $p < 0.001$). Six weeks of chronic exercise did not improved the glucose tolerance in T2D mice. Moreover, insulin tolerance was significantly improved in ND but not in T2D mice after training (Figure 28 C, D). However, insulin tolerance was not highly impaired in diabetic NZO mice compared to non-diabetic controls.

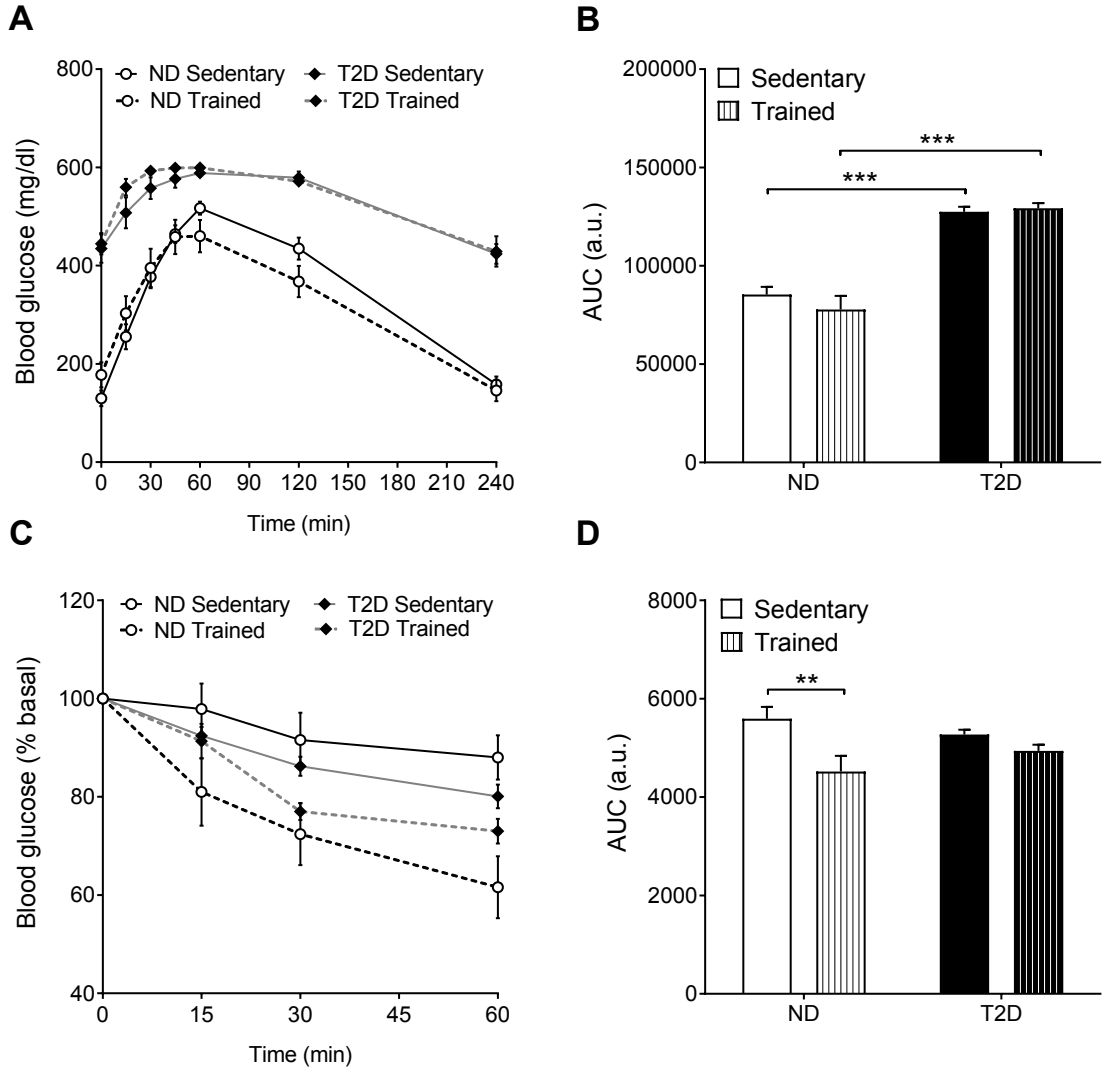

Figure 28: Glucose tolerance and insulin tolerance of ND and T2D mice after chronic interval training. Glucose tolerance (**A**) and insulin tolerance (**C**) were measured after intraperitoneal injection of glucose or insulin, respectively. AUC was determined for quantification of glucose (**B**) and insulin tolerance (**D**). Data are presented as mean ± SEM (GTT: n = 7-12, ITT: n = 3-10). Data were analysed using two-way ANOVA with Bonferroni's multiple comparisons test. **, $p < 0.01$; ***, $p < 0.001$ between indicated groups.

3.2.10 Analysis of glucose uptake in skeletal muscle of NZO mice fed a HFD

The previous results have shown that the trained non-diabetic NZO mice exhibited an improved physical capacity, accompanied by improved insulin tolerance. In order to investigate whether these improvements might be due to an enhanced skeletal muscle glucose uptake, abundance of the glucose uptake-regulating proteins AMPK, pAMPK and GLUT4 were measured in the mixed *Gastrocnemius* muscle via Western Blot analysis (2.2.3.7). Six weeks of chronic exercise did not lead to increased abundance of total or phosphorylated AMPK in skeletal muscle of ND mice (Figure 29 A, B). T2D mice exhibited an increased pAMPK protein

content already at sedentary states, without any further increases after exercise. In addition, T2D mice exhibited a 20 % reduction of GLUT4 compared to ND mice (Figure 29 A, C). However, GLUT4 protein content was not increased after exercise in both groups.

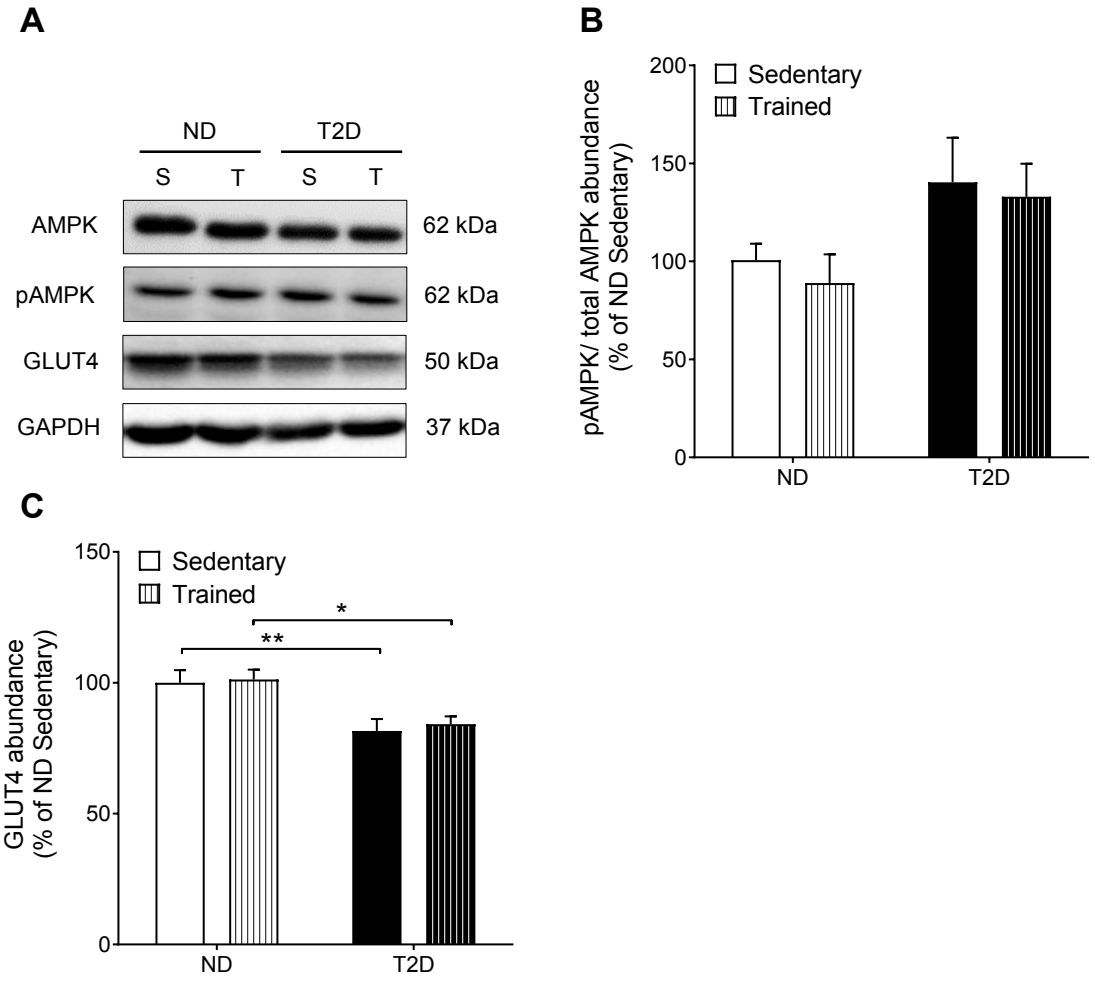

Figure 29: Protein abundance of AMPK, pAMPK and GLUT4 in *Gastrocnemius* muscle of ND and T2D mice after chronic interval training. Representative Western Blots of total AMPK, pAMPK and GLUT4 (**A**) and quantification of pAMPK (**B**) and GLUT4 (**C**) in *Gastrocnemius* muscle of sedentary and trained ND and T2D NZO mice. Protein abundance was normalized to GAPDH and given as percentage of the ND sedentary group. Abundance of pAMPK was quantified in relation to total AMPK. Data are presented as mean ± SEM (n = 8-12). Data were analysed using two-way ANOVA with Bonferroni's multiple comparisons test. *, $p < 0.05$; **, $p < 0.01$ between indicated groups. S, sedentary; T, trained.

Additionally, *ex vivo* 2-DOG uptake in isolated *EDL* muscles of ND and T2D mice was performed in the last week of the training intervention (2.2.2.10). Figure 30 shows that glucose uptake in sedentary ND mice was significantly increased after insulin stimulation. Unexpectedly, training did not further increase but decrease the insulin-stimulated glucose uptake in the ND group (5.1 ± 0.3 nmol/mg/20min in trained vs. 6.9 ± 0.4 nmol/mg/20min in sedentary ND mice, $p < 0.01$). In T2D mice, glucose uptake was increased in both, sedentary and trained mice after insulin stimulation, reaching values similar to those of the ND controls.

Taken together, skeletal muscle glucose uptake and GLUT4 protein content of NZO mice were not increased in response to exercise. Thus, skeletal muscle did not account for the improved insulin sensitivity in non-diabetic NZO mice.

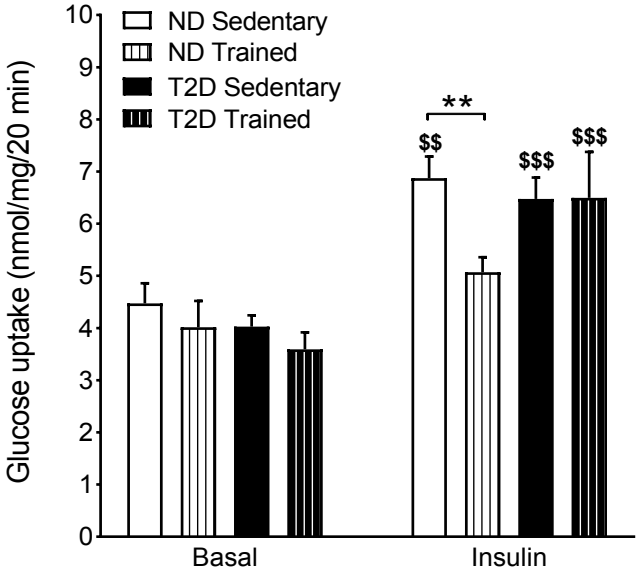

Figure 30: *Ex vivo* glucose uptake in *EDL* muscle of ND and T2D mice after chronic interval training. Glucose uptake was measured at basal or insulin-stimulated conditions in isolated *EDL* muscles of sedentary and trained ND and T2D NZO mice. Data are presented as mean ± SEM (n = 7-13). Data were analysed using two-way ANOVA with Bonferroni's multiple comparisons test. $$, $p < 0.01$; $$$, $p < 0.001$ basal vs. insulin of indicated group; **, $p < 0.01$ between indicated groups.

3.2.11 Analysis of glucose uptake in white adipose tissue of NZO mice fed a HFD

In order to investigate whether the WAT contributed to the improved insulin sensitivity in trained ND mice by increased glucose uptake, GLUT4 protein content in WAT (2.2.3.7.3) as well as *ex vivo* [^{14}C]-D-glucose uptake of isolated adipocytes from epididymal white adipose tissue (2.2.2.11) was determined in ND and T2D mice. GLUT4 protein content was not altered between ND and T2D or sedentary and trained NZO mice (Figure 31 A, B). However, chronic exercise significantly affected the insulin-stimulated glucose uptake in WAT (Figure 31 C). While ND and T2D sedentary mice exhibited an insulin-stimulated increase, the glucose uptake was abrogated in both groups after chronic interval training (36.6 ± 10.0 nmol/mg/20min in trained vs. 96.8 ± 13.2 nmol/mg/20min in sedentary ND mice, $p < 0.05$; 45.4 ± 14.7 nmol/mg/20min in trained vs. 124.8 ± 17.3 nmol/mg/20min in sedentary T2D mice, $p < 0.01$). These results show that chronic exercise did not improve but reduced the insulin-stimulated glucose uptake into WAT of NZO mice, pointing towards increased insulin resistance of the adipose tissue.

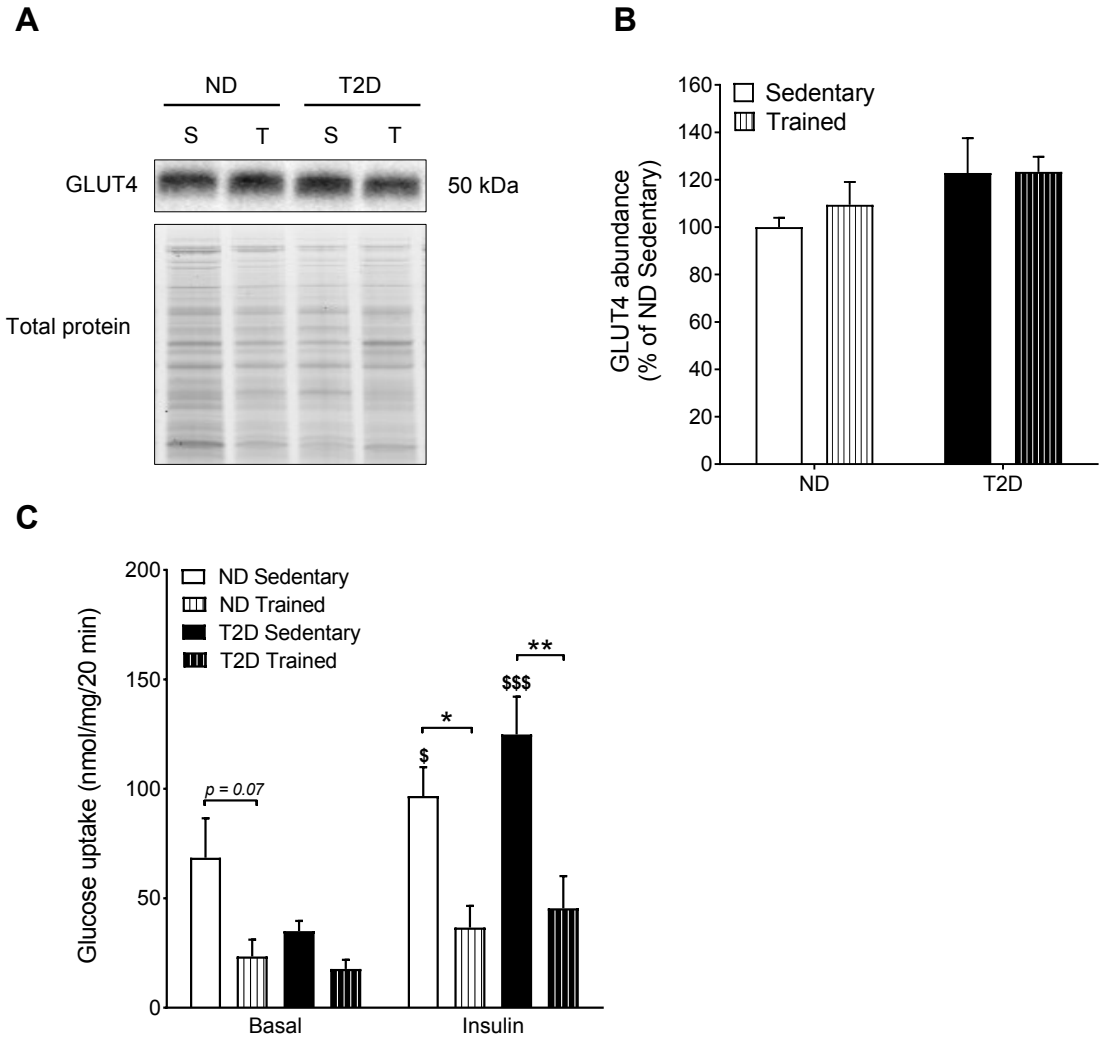

Figure 31: GLUT4 protein abundance and *ex vivo* glucose uptake in isolated adipocytes from WAT of ND and T2D mice after chronic interval training. Representative Western Blot of GLUT4 (**A**) and quantification of GLUT4 (**B**) in WAT of ND and T2D NZO mice. Protein abundance was normalized to total protein content and given as percentage of the ND sedentary group. Glucose uptake (**C**) was measured at basal or insulin-stimulated conditions in isolated adipocytes from WAT. Data are presented as mean ± SEM (n = 6-10). Data were analysed using two-way ANOVA with Bonferroni's multiple comparisons test. $, $p < 0.05$; $$$, $p < 0.001$ basal vs. insulin of indicated group; *, $p < 0.05$; **, $p < 0.01$ between indicated groups. S, sedentary; T, trained.

3.2.12 Abundance of GCK and PCK in the liver of NZO mice fed a HFD

The improvement of physical capacity and insulin sensitivity in trained ND mice could not be explained by increased glucose uptake in skeletal muscle or adipose tissue. In fact, the NZO mice appeared rather insulin-resistant in response to training. To elucidate whether this was accompanied by impaired hepatic glucose uptake and increased gluconeogenesis, protein abundance of respective proteins (GCK, PCK-1 and PCK-2) was measured by Western Blot analysis (2.2.3.7). Compared to sedentary controls, GCK protein abundance was reduced in trained ND mice (Figure 32 A, B). T2D mice exhibited a significantly reduced GCK abundance

compared to ND controls, without additional changes after exercise. While the abundance of the gluconeogenic enzyme PCK-1 was not altered in ND mice, trained T2D mice demonstrated a significantly elevated PCK-1 content (Figure 32 A, C). The abundance of PCK-2 was not changed between the groups (Figure 32 A, D). In summary, these results point towards reduced hepatic glycolysis and elevated hepatic gluconeogenesis in the exercised and diabetic state of NZO mice.

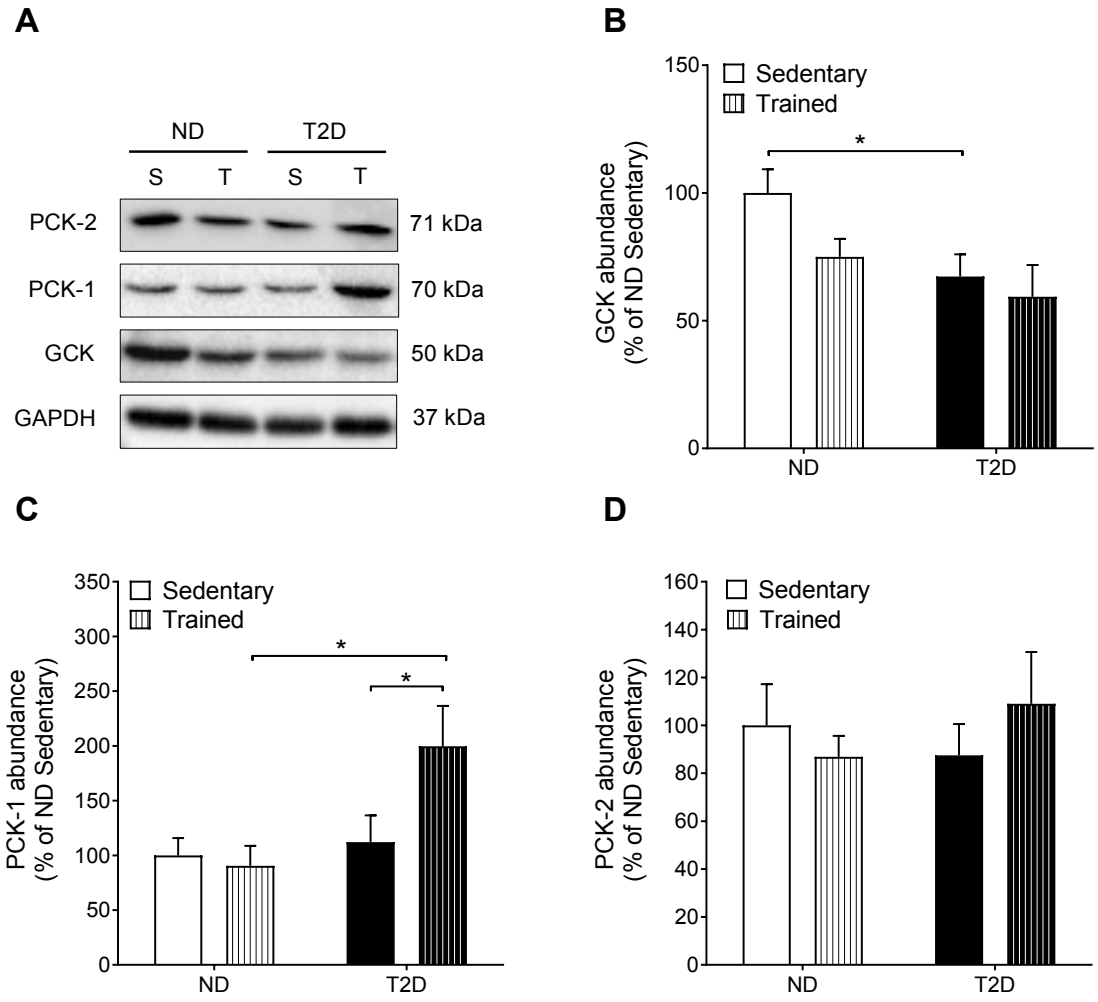

Figure 32: Protein abundance of GCK, PCK-1 and PCK-2 in liver of ND and T2D mice after chronic interval training. Representative Western Blots of GCK, PCK-1 and PCK-2 (**A**) and quantification of GCK (**B**), PCK-1 (**C**) and PCK-2 (**D**) in liver of sedentary and trained ND and T2D NZO mice. Protein abundance was normalized to GAPDH and given as percentage of the ND sedentary group. Data are presented as mean ± SEM (n = 5-8). Data were analysed using two-way ANOVA with Bonferroni's multiple comparisons test. *, $p < 0.05$ between indicated groups. S, sedentary; T, trained.

3.2.13 Hepatic triglyceride and FASN protein content in NZO mice fed a HFD

Reduced hepatic triglyceride content has been shown to be a reliable readout for the exercise-response in the previously shown mouse models (see Figure 13 and Figure 20 D). In order to elucidate whether the hepatic lipid content was reduced in trained NZO mice, triglyceride

content was measured in sedentary and trained ND and T2D mice (2.2.3.4). Surprisingly, six weeks of chronic interval training did not reduce but increased the hepatic triglyceride content in trained ND (33.5 ± 1.7 µg/mg in trained vs. 26.3 ± 1.7 µg/mg in sedentary ND mice, $p < 0.05$), as well as in trained T2D mice (37.5 ± 2.3 µg/mg in trained vs. 26.7 ± 1.7 µg/mg in sedentary T2D mice, $p < 0.01$; Figure 33 A). In order to investigate whether the increase of hepatic fat content was due to an elevated DNL, protein content of the major DNL-regulating protein FASN was measured by Western Blot analysis (2.2.3.7). Protein abundance of FASN was not changed in the ND subgroup, but markedly reduced in T2D mice (40.6 ± 10 % in sedentary T2D vs. 100 ± 23.3 % in sedentary ND mice, $p < 0.05$, Figure 33 B, C). The protein content of FASN remained reduced in trained T2D mice, indicating that the exercise-induced increase of hepatic fat content was not due to elevated rates of DNL in trained NZO mice.

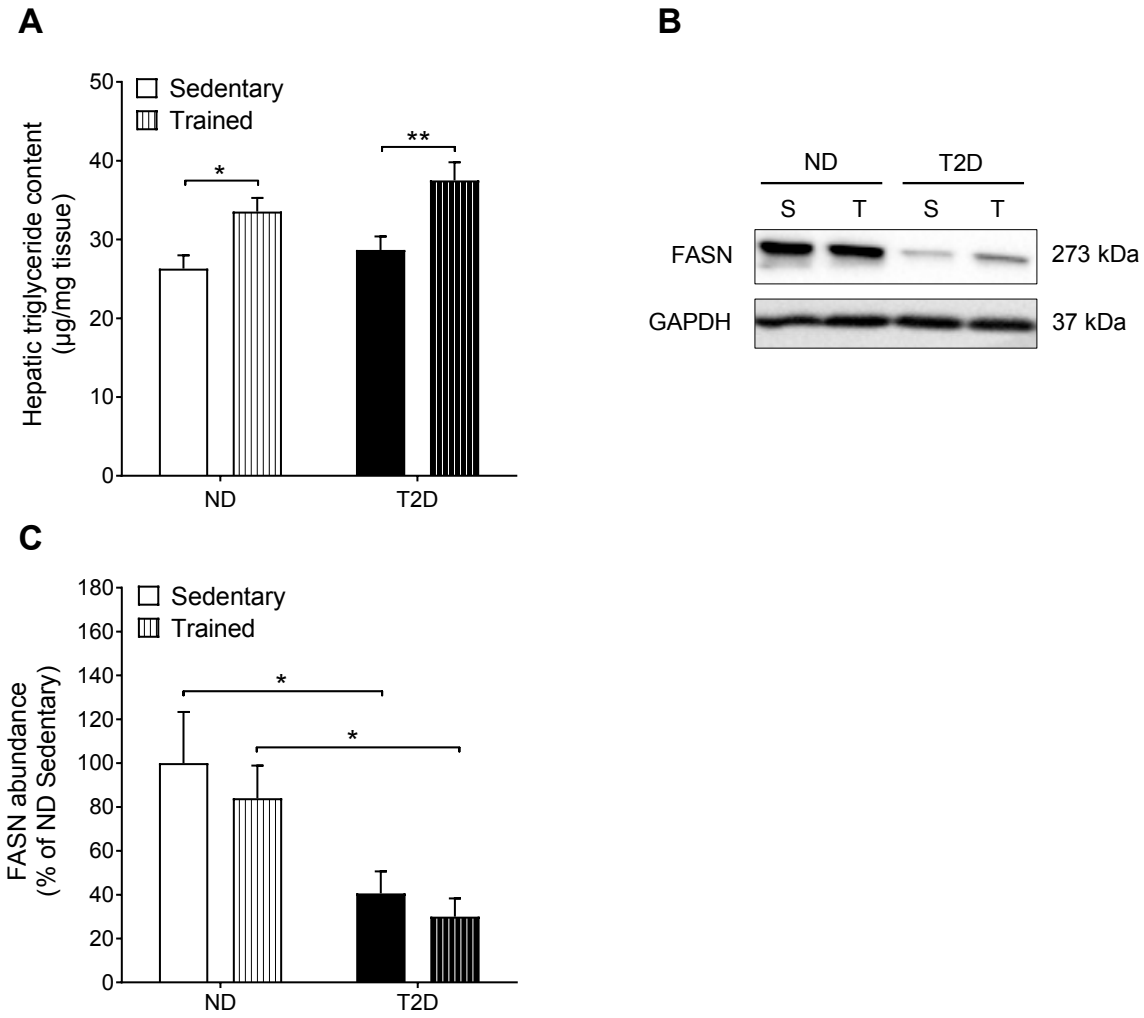

Figure 33: Hepatic triglyceride content and protein abundance of FASN in liver of ND and T2D mice after chronic interval training. Triglyceride content (**A**), representative Western Blot of FASN (**B**) and quantification of FASN (**C**) in liver of sedentary and trained ND and T2D NZO mice. Protein abundance was normalized to GAPDH and given as percentage of the ND sedentary group. Data are presented as mean ± SEM (n = 6-11). Data were analysed using two-way ANOVA with Bonferroni's multiple comparisons test. *, $p < 0.05$; **, $p < 0.01$ between indicated groups. S, sedentary; T, trained.

In conclusion, six weeks of chronic interval training only mildly improved physical capacity and insulin tolerance in the non-diabetic subgroup of NZO mice. However, these improvements were not due to increased glucose uptake in either skeletal muscle or WAT. In fact, skeletal muscle and WAT appeared insulin-resistant to a greater extend in trained mice compared to sedentary controls. Furthermore, elevated hepatic triglyceride content indicated abnormal lipid storage in NZO mice in response to exercise training.

4. Discussion

Regular exercise is considered as an efficient intervention for the treatment of impaired insulin sensitivity, but the response to a certain training bout is heterogeneous among different individuals, presumably dependent on genetic and environmental factors. Here, the impact of chronic exercise was investigated in (1) D4KO mice, a monogenic model for insulin resistance and (2) in NZO mice, a polygenic model for insulin resistance and T2DM, following the question if exercise would improve glycaemia in these models.

The present study shows that chronic exercise improved whole-body glycaemia in D4KO mice, presumably due to restored glucose uptake in adipose tissue, thereby compensating for the impaired skeletal muscle glucose uptake due to the lack of TBC1D4. Conversely, chronic exercise did not improve glycaemia in polygenic NZO mice, but even exaggerated peripheral and hepatic insulin resistance in general. Moreover, it was shown that NZO mice are rather non-responders to exercise-mediated improvements of glycaemia. In summary, the diverse exercise-response in the two mouse models confirm the impact of the genetic predisposition that determines the exercise capacity.

4.1 The role of TBC1D4 in exercise-mediated metabolism

The role of TBC1D4 in insulin- and contraction-mediated skeletal muscle and adipose tissue glucose uptake has been studied intensively in the last years. Several studies using D4KO mice have shown that the lack of TBC1D4 leads to postprandial hyperglycaemia, impaired skeletal muscle and adipose tissue glucose uptake, whole-body insulin resistance and impaired hepatic insulin sensitivity (Wang et al. 2013, Chadt et al. 2015, Xie et al. 2016). However, the impact of a chronic exercise intervention on TBC1D4 function has not been investigated so far. For the first time, this thesis examined the impact of regular treadmill training in D4KO mice in order to investigate whether this would restore glycaemia and improve peripheral glucose uptake.

4.1.1 Lack of TBC1D4 impairs exercise capacity, probably due to impaired skeletal muscle glucose uptake

The previously reported impaired glycaemia in mice deficient for TBC1D4 could be confirmed in the present thesis, as sedentary D4KO mice clearly exhibited an abrogated skeletal muscle and adipose tissue glucose uptake. The first new main finding was that lack of TBC1D4 additionally impairs physical capacity, reflected in a significantly reduced time to exhaustion in

D4KO mice during exhaustion running tests. This impaired performance can mainly be attributed to the reduced skeletal muscle GLUT4 protein content and glucose uptake, since glucose serves as the predominant substrate fuel during exercise (Richter & Hargreaves 2013). However, in this study only the impact of *Tbc1d4*-deficiency on insulin-, but not contraction-mediated glucose uptake was measured. It was previously shown in our group that lack of TBC1D4 impaired glucose uptake in the oxidative *Soleus* muscle, stimulated by the AMP analogue AICAR (5'-aminoimidazole-4-carboxyamide-ribonucleoside), which mimics muscular contraction (Chadt et al. 2015). Therefore, it is likely that the contraction-mediated glucose uptake is concomitantly decreased in the D4KO mice used for this study and thereby affects the endurance capacity.

In addition to glucose uptake, skeletal muscle and hepatic glycogenolysis serve as important contributors to skeletal muscle energy supply and thus, diminished glycogen stores in these tissues may further impair the endurance capacity during running. Indeed, a reduced hepatic glycogen content was previously reported for D4KO mice (Chadt et al. 2015). In the present study, neither skeletal muscle nor hepatic glycogen content was considerably reduced compared to WT controls. However, glycogen content was only measured at the end of the experiment after tissue harvest and thus does not reflect the acute state during the exhaustion running test that may be altered due to the lack of TBC1D4. Nevertheless, these findings show that skeletal muscle and hepatic glycogen content were probably not contributing to the impaired exercise performance. Similar findings were found in global KO mice for TBC1D1 (D1KO), the close homologue of TBC1D4. D1KO mice showed a reduced endurance performance and impaired exercise-mediated glucose uptake in glycolytic muscles. These findings were independent of changes of skeletal muscle glycogen content, as well as plasma lactate and plasma NEFA levels, suggesting that the impaired skeletal muscle glucose uptake was causative for the impaired exercise capacity (Stöckli et al. 2015). Consistently, plasma lactate and NEFA concentrations were not different in D4KO mice compared to WT littermates. Thus, it can be assumed that the impaired skeletal muscle glucose uptake in D4KO mice was causative for the impaired running performance, similar to D1KO mice.

Altogether, these findings indicate a crucial role of TBC1D4 in regulating the exercise-mediated glucose uptake to maintain endurance capacity. However, it was already speculated whether the impaired capacity was the direct cause of the lack of the respective RabGAP or due to the concomitant loss of GLUT4 protein (Stöckli et al. 2015). Deletion of GLUT4 has been shown to deteriorate skeletal muscle contractile function and to impair running performance in mice (Gorselink et al. 2002, Fueger et al. 2007), suggesting that the lack of GLUT4 would be the

primary cause for the reduced exercise capacity. On the other hand, disrupting the more upstream AMPK in the glucose uptake-pathway has been reported to equally impair endurance performance and skeletal muscle glucose uptake, independent of changes in GLUT4 protein content (O'Neill et al. 2011). In conclusion, this shows that disruption of either one of the proteins of the AMPK-RabGAP-GLUT4-axis can impair the physical capacity, highlighting the importance of each functional protein in maintaining exercise-regulated metabolism.

4.1.2 Chronic exercise improves exercise capacity and whole-body insulin sensitivity in D4KO mice, independent of skeletal muscle glucose uptake

In order to elucidate whether the endurance capacity and glycaemia would be improved after exercise, D4KO mice were subjected to a moderate treadmill training intervention. Four weeks of regular exercise rescued the exercise capacity in D4KO mice, reflected in a substantially elevated time to exhaustion. Moreover, whole-body insulin sensitivity was improved in trained D4KO mice, demonstrated by increased glucose and insulin tolerance. Since skeletal muscle determines the exercise performance and, together with the liver, represents the primary organ for glucose disposal during the i.p. ITT (Bowe et al. 2014), these observations indicate an improved skeletal muscle glucose uptake in D4KO mice after exercise. Although trained D4KO mice exhibited an increased glucose uptake compared to sedentary controls, the insulin-stimulated glucose uptake was not additionally increased compared to basal conditions and thereby not restored to the levels of the WT mice. In addition, the initially reduced gene expression and protein abundance of GLUT4 were not increased in trained D4KO mice. Apart from GLUT4, the phosphorylation of glucose to G6P by the HK-II has been considered to be a rate-limiting step for glucose uptake (Heikkinen et al. 1999). More importantly, exercise performance was impaired in partial HK-II-KO mice, but improved in transgenic mice with HK-II overexpression, suggesting an important role for this protein to determine the exercise capacity (Fueger et al. 2005). Similar to the ablated GLUT4, HK-II protein content was reduced in *Soleus* muscle of D4KO mice, but not elevated after chronic exercise (Figure S1). Collectively, the improvements of exercise capacity and insulin sensitivity were independent of skeletal muscle GLUT4 protein and glucose uptake.

This raises the question, which alternative metabolites or pathways are contributing to skeletal muscle energy supply during the exhaustion running test. Skeletal muscle glycogen was reported to be increased after regular exercise to counteract the rapid depletion during running (Manabe et al. 2013, Gurley et al. 2016). Moreover, hepatic glycogenolysis and gluconeogenesis represent other contributors to skeletal muscle glucose supply (Gonzalez et al. 2015, Shephard & Johnson 2015). In D4KO mice, both skeletal muscle and hepatic

glycogen content as well as the abundance of the hepatic gluconeogenic enzyme PCK remained unchanged after chronic exercise. Furthermore, plasma lactate that could serve as a possible gluconeogenic substrate for the liver was unaffected by exercise in D4KO mice. Conclusively, skeletal muscle glycogen content and hepatic glucose output were not contributing to skeletal muscle energy supply at exercising conditions.

In addition to glucose, the oxidation of lipids derived from intracellular triglyceride stores has long been known to serve as an important substrate fuel for the working skeletal muscle during exercise (Hurley et al. 1986). Previous studies have shown that deletion of either TBC1D1 or TBC1D4 in mice leads to increased skeletal muscle FAO associated with reduced whole-body RER, suggesting a RabGAP-dependent switch of substrate preference (Chadt et al. 2015, Hargett et al. 2015). Here, the RER was measured during indirect calorimetry and during exhausting running tests, which gives a reliable estimator of whole-body substrate utilization. Contrary to the previously reported findings, the RER was not reduced in D4KO mice compared to WT controls, neither at steady state (Table S4), nor at exercising conditions during the physical capacity test. Moreover, the RER was unchanged between sedentary and trained D4KO mice, thus not pointing towards altered whole-body substrate preference. Nevertheless, increased skeletal muscle FAO of D4KO mice could contribute to energy supply during running, which may not be reflected in whole-body measurements. Skeletal muscle FAO can be assessed *ex vivo* by measuring the oxidation of tritium-labelled [^{3}H] palmitate in isolated muscles. Unfortunately, this assay could not yet be performed with this cohort due to technichal issues. In order to clarify whether skeletal muscle FAO was affected by the genotype or the training intervention, further experiments are required after re-establishing the *ex vivo* FAO assay.

Interestingly, the reported findings for the substrate utilization of D4KO mice fed a HFD in the present study are considerably different from the previously reported study using D4KO mice on a SD (Chadt et al. 2015). Besides the reduced RER, D4KO mice fed a SD represented a slightly reduced body weight and fat mass compared to WT controls. Conversely, D4KO mice fed a HFD from the present thesis showed elevated body weight and fat mass, as well as elevated hepatic triglyceride content. Lack of TBC1D4 presumably drives whole-body and skeletal muscle FAO due to the impaired disposal and utilization of glucose. Upon HFD-feeding, D4KO mice presumably cannot cope with the excess availability of lipids derived from the HFD, leading to increased ectopic lipid accumulation such as in the liver (Green & Hodson 2014). These findings further confirm the importance of TBC1D4 to regulate substrate utilization in states of overnutrition.

4.1.3 Increased adipose tissue glucose uptake accounts for the improved insulin sensitivity in D4KO mice

Since skeletal muscle glucose uptake was unchanged, the question remained, which alternative tissues might account for the improved insulin sensitivity in trained D4KO mice. Unexpectedly, the abrogated GLUT4 protein content in white adipose tissue of D4KO mice was restored to WT levels after four weeks of chronic exercise. Moreover, regular exercise substantially improved the initially impaired insulin-stimulated glucose uptake in isolated adipocytes. Interestingly, chronic exercise did not only affect glucose transport in the white fat depot, but also increased GLUT4 protein content in the BAT of trained D4KO mice, suggesting that glucose uptake might be altered in brown fat as well. Taken together, these findings provide strong evidence for the adipose tissue accounting for the overall improved insulin sensitivity in trained D4KO mice, thereby compensating for the impaired glycaemia in skeletal muscle.

So far, the ability of exercise to restore initially impaired GLUT4 protein levels has only been described to occur in skeletal muscle, as presented in a study using voluntary running wheel exercise that rescued the HFD-induced reduction of muscular GLUT4 (Gurley et al. 2016). Furthermore, a few studies have reported increases of GLUT4 protein and glucose uptake in WAT of rats or mice after treadmill running (Stephenson et al. 2013, Marcinko et al. 2015). However, this thesis demonstrates for the first time that the former abrogated GLUT4 protein and glucose uptake in WAT due to the deletion of an essential glucose uptake-regulating protein (TBC1D4) can be rescued by chronic exercise. Interestingly, Stephenson et al. showed that GLUT4 protein content was only increased in rats with high- but not low-intrinsic running capacity, suggesting a direct association of increased adipose tissue GLUT4 with increased exercise capacity (Stephenson et al. 2013). Thus, the enhanced GLUT4 protein content and glucose uptake in WAT of trained D4KO mice may have contributed to the enhanced running performance during the exhaustion running test. Since GLUT4 was substantially increased in both WAT and BAT despite the lack of TBC1D4, this points towards a novel TBC1D4-independent mechanism regulating glucose uptake in these tissues. A recent study performed in our institute showed that deletion of both RabGAPs abrogates the exercise-induced increase of GLUT4 in WAT (Grieß-Osowski 2018, Master thesis). Since TBC1D1 has been shown to be a putative regulator of exercise-induced glucose uptake (Stöckli et al. 2015), these findings could indicate a compensatory role of the functional RabGAP TBC1D1 in mediating the exercise-dependent upregulation of glucose uptake in D4KO mice. However, TBC1D1 is only marginally expressed in white and brown fat (Chadt et al. 2008), implicating a rather nonrelevant role for this RabGAP to regulate exercise-mediated glycaemia in these adipose

depots. Consequentially, the improved glycaemia in adipose tissue of trained D4KO mice suggests a fully RabGAP-independent mechanism to regulate exercise-induced glucose uptake.

A previous study has shown that the deficiency of TBC1D4 leads to a substantially reduced GLUT4 gene expression in adipocytes (Lansey et al. 2012). In accordance to this study, *Slc2a4* mRNA content was found to be significantly reduced in WAT of D4KO mice compared to WT littermates, implicating a transcriptional regulation of GLUT4 protein content. More importantly, *Slc2a4* mRNA levels tended to be elevated after exercise intervention. This would suggest an exercise-mediated increase of GLUT4 gene expression, resulting in increased GLUT4 protein content that enables the enhanced glucose uptake. A variety of transcription factors have been discovered to regulate GLUT4 gene expression in muscle and adipose tissue, such as myocyte enhancer factor 2 (MEF-2) and GLUT4 enhancer factor, which regulate the transcription of GLUT4 through interaction with the GLUT4 promoter (Knight et al. 2003). Interestingly, PGC-1α has been found to be a coactivator of MEF-2 and thereby controls GLUT4 expression in skeletal muscle (Michael et al. 2001). In D4KO mice, *Ppargc1a* mRNA expression was elevated in scWAT after chronic exercise. Although primarily measured in the context of browning, this result suggests a possible regulatory function of PGC-1α on GLUT4 gene expression in adipose tissue. Moreover, transcription of GLUT4 can be regulated by epigenetic DNA modifications such as histone acetylation by histone deacetylases (HDACs). Among the HDACs, HDAC5 was shown to modulate skeletal muscle GLUT4 transcription by interaction with MEF-2, dependent on AMPK phosphorylation (Ntanasis-Stathopoulos et al. 2013). Thus, this AMPK-dependent regulation represents a possible mechanism to increase GLUT4 expression by exercise. Whether adipose tissue consists of a similar pathway and which exercise-dependent factors may regulate the transcription of GLUT4 in D4KO mice remains to be further investigated.

However, the hypothesis for a transcriptional regulation of GLUT4 on glucose uptake does not hold true for the WT controls of this cohort. Although the WT mice showed no change of *Slc2a4* mRNA content and only a mildly elevated GLUT4 protein content, they exhibited a remarkably increased insulin-stimulated glucose uptake in the WAT that was even more pronounced compared to D4KO mice. In line with these findings, Gurley et al. reported that the rescue of GLUT4 in obese mice after voluntary running was independent of GLUT4 gene expression, indicating a posttranscriptional mechanism that regulates GLUT4 abundance (Gurley et al. 2016). Consequentially, not increased transcription but the increased translocation of intracellular GLUT4 storage vesicles to the plasma membrane might explain the improved

glucose uptake seen in WT mice. In the present thesis, only total GLUT4 protein content was measured by regular Western Blot analysis, which is not able to distinguish between the amount of intracellular and plasma membrane-bound GLUT4. Therefore, GLUT4 translocation could be evaluated by preparing plasma membrane fractions or by cell surface labelling using specific biotinylated compounds (Nishiumi & Ashida 2007, Chadt et al. 2015). This would clarify whether an increased GLUT4 translocation accounts for the improved glucose uptake in WT and D4KO mice. Furthermore, the WT data point towards an additional exercise-induced pathway to control glycaemia in WAT completely independent of GLUT4, which may also contribute to the improved glucose uptake in trained D4KO mice. Trevellin et al. have shown that the increase of glucose uptake in scWAT of mice after swimming was independent of GLUT4 protein content. The authors further propose a role for the endothelial nitric oxide synthase (eNOS) to regulate exercise-dependent glycaemia in scWAT. The exercise-induced increase of eNOS is known to increase the production of nitric oxide (NO), which in turn induces mitochondrial biogenesis and glucose uptake. This exercise-induced glucose uptake was abrogated in scWAT of eNOS-KO mice, while the application of an NO donor led to an elevated glucose uptake in isolated adipocytes (Trevellin et al. 2014). Thus, yet unknown pathways independent of, or alternative to GLUT4 may account for the improved exercise-induced glycaemia in the adipose tissue of D4KO mice.

4.1.4 Increased browning contributes to adipose tissue insulin sensitivity in D4KO mice

Mitochondrial biogenesis has been shown to be elevated in scWAT of mice after performing exercise (Trevellin et al. 2014). In accordance to this study, the expression of genes related to enhanced mitochondrial activity and browning was significantly elevated in scWAT of trained D4KO mice. In addition, elevated *Ucp-1* mRNA content was associated with significantly elevated UCP-1 protein abundance, further confirming the presence of increased browning processes in scWAT of D4KO mice. Several studies have confirmed the occurrence of browning in scWAT of mice in response to endurance exercise (Boström et al. 2012, Stanford, Middelbeek, & Goodyear 2015). Moreover, elevated browning of scWAT in trained B6 mice was associated with improved glycaemia, implicating a role for the trained adipose tissue in transferring the beneficial effects of exercise to other tissues in order to improve whole-body glucose homeostasis (Stanford, Middelbeek, Townsend, et al. 2015). In accordance to this study, the increased browning in scWAT of trained D4KO mice probably contributed to the improved adipose tissue and whole-body insulin sensitivity after chronic exercise. Interestingly, the abundance of UCP-1 as well as the expression of almost all browning markers tended to be reduced in sedentary D4KO mice compared to WT controls, indicating a dysregulated mitochondrial function upon lack of TBC1D4 that was rescued after regular exercise. Similar

findings were reported in a study using B6 mice with a HFD-induced metabolic dysfunction. While *Ucp-1* and *Ppargc1a* mRNA content was diminished in response to the HFD, chronic treadmill training was able to increase the expression of both genes, as well as to increase the abundance of UCP-1 protein (Xu et al. 2011). In addition, recent data of our working group have shown that the exercise-induced browning of scWAT was more pronounced in HFD-fed mice compared to mice fed a SD (Crepcia-Pevzner 2017, Master thesis). Thus, these results implicate a stronger effect of browning processes to mediate improvements in primary states of metabolic dysfunction.

How exactly exercise induces and regulates the browning of white adipocytes still remains unclear. Most prominently, it is hypothesized that the working skeletal muscle releases specific proteins during exercise, namely myokines, which interact with the adipose tissue to increase mitochondrial activity. For instance, the myokines myostatin (gene name *MSTN*) and irisin (gene name *FNDC5*) have been described to be secreted from skeletal muscle and to stimulate browning in white adipocytes, associated with improved insulin sensitivity (Feldman et al. 2006, Boström et al. 2012). More recently, increased plasma levels of the myokine fibroblast growth factor-21 (FGF-21) were associated with increased brown adipocyte-specific gene expression (Jelenik et al. 2018). Thus, the skeletal muscle of D4KO mice may release known or yet unknown myokines during exercise that act on adipose tissue to induce browning and increase insulin sensitivity.

4.1.5 Reduced whole-body and hepatic fat content contribute to the improved insulin sensitivity in trained D4KO mice

In addition to the improved glycaemia of the adipose tissue, another important finding was that four weeks of exercise substantially reduced whole-body fat mass as well as hepatic triglyceride content in D4KO mice. Regular exercise has been shown to efficiently reduce both visceral and hepatic fat content in obese humans. Moreover, reduction of hepatic fat content has been reported to be associated with improved insulin sensitivity (van der Heijden et al. 2010, Hafstad et al. 2013). Thus, the reduced whole-body and hepatic fat content in trained D4KO mice presumably contributed to the overall improved insulin sensitivity. The reduction of whole-body fat mass can probably be attributed to increased adipose tissue lipolysis, as evident from the mildly increased plasma NEFA concentrations in trained D4KO mice. The increased plasma NEFA levels could in turn further supply the skeletal muscle with lipids during running (Karpe et al. 2011). Furthermore, increased adipose tissue insulin sensitivity was associated with increased numbers of small adipocytes that exhibit elevated expression levels of GLUT4 (Hallakou et al. 1997, Hammarstedt et al. 2005). Thus, the reduced whole-body fat

mass could be additionally explained by a reduced adipocyte size in trained D4KO mice, which would also go in line with the slightly elevated *Slc2a4* mRNA content of the scWAT. Concerning the hepatic fat content, either elevated fatty acid turnover and/ or reduced DNL might account for the exercise-mediated reduction of triglycerides in the liver of D4KO mice. Indeed, preliminary experiments suggest a blunted insulin-stimulated DNL in liver of trained D4KO mice to be responsible for the reduction of hepatic triglycerides (data not shown).

In conclusion, the present data shows that four weeks of chronic exercise restored the initially impaired physical capacity and improved whole-body insulin sensitivity in D4KO mice, due to a remarkably improved adipose tissue glycaemia, independent of skeletal muscle glucose uptake. Reduction of whole-body as well as hepatic fat content contributed to the increased insulin sensitivity. The findings suggest that the lack of TBC1D4 in adipose tissue is compensated by alternative exercise-responsive pathways, presumably affecting transcription or translocation of GLUT4 and mitochondrial activity. Moreover, secretion of skeletal muscle-specific myokines represents a possible mechanism to mediate the improved insulin sensitivity of adipose tissue (Figure 34).

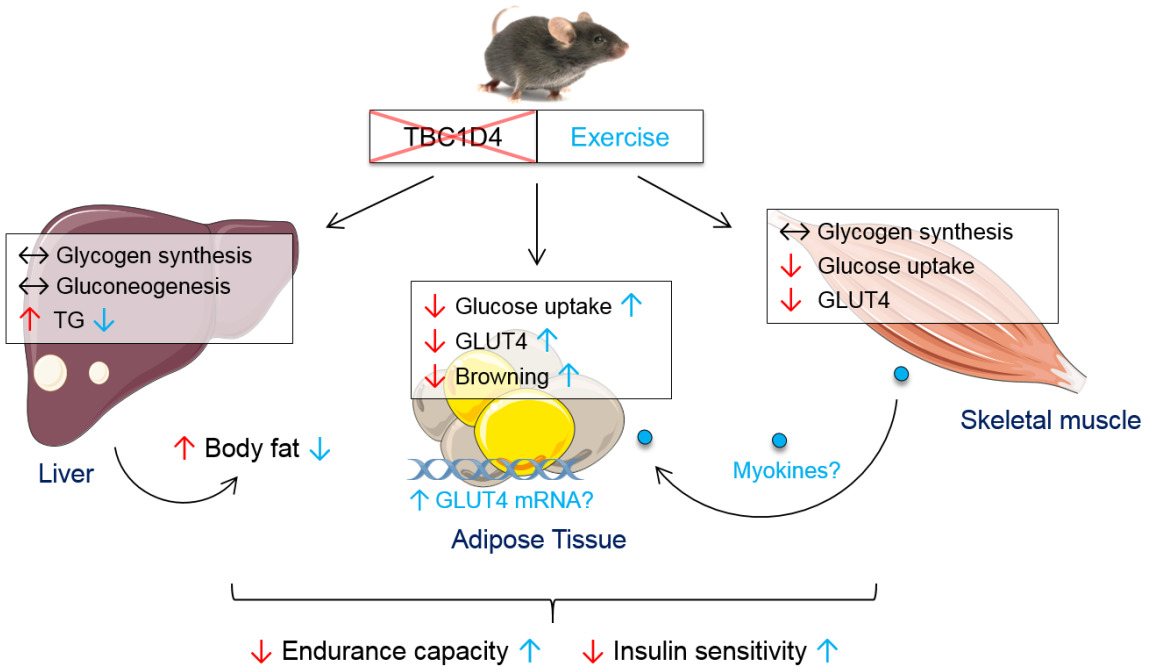

Figure 34: Restored adipose tissue glycaemia accounts for the improved insulin sensitivity in trained D4KO mice. TBC1D4 deficiency (red arrows) leads to impaired glucose uptake in skeletal muscle and adipose tissue, as well as impaired endurance capacity. Chronic exercise (blue arrows) improves endurance capacity and restores GLUT4 protein content and glucose uptake in adipose tissue, while skeletal muscle glycaemia is not rescued. Elevated whole-body and hepatic fat content is reduced after exercise, contributing to improved insulin sensitivity in D4KO mice. RabGAP-independent pathways such as secretion of muscle-specific myokines or transcription factors regulating GLUT4 gene expression might account for the improved glycaemia and increased browning in adipose tissue.

4.2 The impact of exercise on glycaemia of NZO mice

The diabetic NZO mouse has previously been shown to be associated with reduced energy expenditure and impaired voluntary running activity (Jürgens et al. 2006). For the first time, this study investigated the impact of a regular training intervention on physical capacity and development of T2DM in NZO mice. The first finding was that chronic treadmill training was able to improve the physical capacity of NZO mice that were initially rendered normoglycaemic by feeding a SD. However, glucose tolerance was not improved in these mice, leading to the question whether chronic exercise would affect glycaemia in NZO mice challenged with a HFD to initiate the onset of T2DM.

4.2.1 HFD-feeding leads to hyperglycaemia and clustering of blood glucose, which is not prevented by chronic exercise

Subjecting NZO mice to a HFD has been reported to induce hyperglycaemia in NZO mice (Jürgens et al. 2007, Kluth et al. 2011). Consistently, feeding the NZO mice with the 30 % HFD-RS in week 6 resulted in the development of hyperglycaemia, reflected by markedly increased FBG concentrations in week 11. However, six weeks of chronic interval training were not able to prevent the HFD-induced onset of hyperglycaemia in NZO mice. Interestingly, the blood glucose values clustered, subdividing the sedentary and trained group into either normoglycaemic (ND) or hyperglycaemic (T2D) animals, respectively. Thus, the response to the HFD is highly heterogeneous within the NZO mice, independent of exercise.

A similar clustering of blood glucose concentrations was observed in NZO mice fed a HFD with 45 % fat from calories (Schallschmidt 2018, Dissertation). Since NZO mice can be considered as genetically identical, these findings implicate a possible role of epigenetic modifications affecting glycaemia of the NZO mice in response to environmental factors, such as HFD-feeding. Epigenetic modifications describe the changes of gene expression induced by environmental signals or soluble factors, independent of the primary DNA sequence, including histone modifications via methylation or acetylation, non-coding RNA activity or DNA methylation (Ntanasis-Stathopoulos et al. 2013, Dos Santos et al. 2015). Feeding a HFD has been shown to cause epigenetic responses through altered genome-wide or skeletal muscle-specific DNA methylation in mice (Laker et al. 2017, Yoon et al. 2017). Thus, a diverse epigenetic mechanism in NZO mice may determine the development of glycaemia in response to the HFD, independent of physical activity. Moreover, several studies have provided evidence for a maternal impact that determines the development of obesity and T2DM in the progeny, particularly the maternal nutrition (Königsdorf et al. 2012). For instance, female B6 offspring of HFD-fed dams exhibited elevated whole-body and hepatic fat content although

raised on a regular chow diet, indicating that the maternal HFD consumption predisposed the offspring to develop this impaired phenotype (Elahi et al. 2009). In addition, a crossbreeding study with NZO mice and a lean control strain showed that the diabetes prevalence was higher in the progeny deriving from the obese mother compared to mice that had a lean mother. The authors propose that specific factors in the milk of the obese dams may affect the early growth and phenotype of the progeny (Reifsnyder et al. 2000). In accordance to these findings, it is likely that the maternal phenotype and nutritional state have caused the diverse development of glycaemia in the NZO mice of the present study, since the offspring was generated using different parental breeding partners. Further investigations addressing the maternal impact on the progeny are required in order to exactly clarify the mechanisms that drive the heterogeneous T2DM development in NZO mice.

4.2.2 Exercise capacity is only improved in the non-diabetic NZO subgroup, independent of skeletal muscle glucose uptake

Although chronic exercise did not prevent the NZO mice from developing hyperglycaemia, it remained to be investigated whether physical capacity and insulin sensitivity were affected in the non-diabetic (ND) or diabetic (T2D) subgroup. The analysis of exercise capacity in NZO mice showed that six weeks of chronic exercise significantly improved the time to exhaustion of the ND subgroup compared to sedentary controls. Similar to the previous D4KO study, the increase in endurance time was not associated with changes of maximal oxygen uptake, as VO_{2max} remained unchanged between the groups. In addition, ND mice exhibited a mildly improved glucose tolerance and a significantly improved insulin tolerance. Thus, the improved whole-body insulin sensitivity in trained ND mice may have contributed to the enhanced exercise capacity. In contrast, T2D mice did not show an improved exercise capacity. Moreover, the glucose tolerance that was severely abrogated in sedentary T2D mice, as well as insulin tolerance were not improved in T2D mice. Since the insulin content of T2D mice was almost depleted compared to the ND subgroup, this suggests that pancreatic beta cell destruction had already occurred due to the development of severe insulin resistance, resulting in hypoinsulinemia and further progression of an overt diabetic phenotype (Kluge et al. 2012). In accordance to a previously reported association of hypoinsulinemia with reductions in body weight (Cerf et al. 2007), T2D mice exhibited reduced body weight and body fat content, further highlighting the severity of the diabetic phenotype in this group.

A previous study presented that the exercise capacity was concomitantly reduced with increased severity of the diabetic phenotype in *db/db* mice, a monogenic model for T2DM (Ostler et al. 2014). However, within the same study, a second mouse model for polygenic

T2DM (*TallyHo* mice) maintained the exercise capacity despite progression of T2DM development, presumably due to preserved skeletal muscle function. The results for the exercise capacity of the diabetic NZO subgroup are somewhat similar to these findings. Although the time to exhaustion did not show an additional increase after chronic exercise, it was in fact not considerably different compared to the ND group. More surprisingly, the *ex vivo* skeletal muscle insulin-stimulated glucose uptake was not impaired in T2D mice despite reduced GLUT4 protein content, suggesting that the skeletal muscle did not yet become completely insulin-resistant. Thus, the preserved skeletal muscle insulin sensitivity in T2D mice may partially compensate for the hyperglycaemic phenotype to maintain the exercise capacity during exhaustion running.

However, the improved time to exhaustion in ND mice was not associated with improved skeletal muscle GLUT4 protein content and glucose uptake. Furthermore, exercise did not lead to elevated phosphorylation of skeletal muscle AMPK at steady state, neither in the ND nor in the T2D subgroup, indicating that chronic exercise failed to activate the muscular AMPK-GLUT4-axis in NZO mice. Although an elevated skeletal muscle GLUT4 protein content was observed in *db/db* mice performing HIT training, muscular AMPK abundance and PGC-1α expression remained unchanged (Chavanelle et al. 2017). Another exercise study that compared the effects of voluntary and forced treadmill running on glycaemia of *db/db* mice showed that glycaemia and skeletal muscle GLUT4 protein content were not improved after forced exercise (Sennott et al. 2008). Consistent with the NZO results, these findings suggest that chronic treadmill training is rather ineffective to substantially improve skeletal muscle glucose uptake in mouse models for severe T2DM. In addition to glucose uptake, availability of muscular and hepatic glycogen content is known to limit the endurance capacity (Coggan et al. 1995, Manabe et al. 2013). While hepatic glycogen content was reduced in both trained groups, skeletal muscle glycogen concentrations were only reduced in the T2D subgroup. Thus, the rapid exercise-induced depletion of glycogen was prevented in skeletal muscle of trained ND mice, presumably explaining the additional increase of endurance capacity in ND compared to T2D mice. Taken together, these findings show that the diabetic state limits the exercise capacity in NZO mice.

4.2.3 Increased rates of whole-body FAO compensate for the impaired glycaemia in diabetic NZO mice

In order to estimate the effects of HFD-feeding and exercise on substrate utilization, RER was measured during the exhaustion running test and during indirect calorimetry measurements at steady state conditions in metabolic cages. In both groups, the RER was not significantly

changed after chronic exercise. However, diabetic NZO mice exhibited an overall reduced RER compared to the non-diabetic controls during exhaustion running. Similar findings were observed during indirect calorimetry measurements, reflected by reduced calculated rates of whole-body CHO and elevated rates of FAO, indicating a shift towards increased use of lipids for substrate utilization. This shift towards whole-body FAO likely represents a compensatory mechanism to fuel the skeletal muscle with lipids. Although the *ex vivo* skeletal muscle glucose uptake was not abrogated, diabetic NZO mice might be incapable of further utilizing the glucose for substrate oxidation. This would be consistent with the reduced plasma lactate concentrations after treadmill running in both ND and T2D mice, which points towards an overall impaired ability to further metabolize the incorporated glucose that is compensated by increased skeletal muscle FAO. Interestingly, trained T2D mice exhibited an increased food intake compared to sedentary controls, suggesting that exercise further raised the animals' energy demand due to the T2DM-dependent reduction of body weight. Consequently, higher consumption and oxidation of HFD-derived lipids would contribute to skeletal muscle energy supply during treadmill running and compensate for the impaired glycaemia.

However, it is known that increased FAO in insulin-resistant states promotes the further impairment of skeletal muscle function. This phenomenon is referred to as "incomplete FAO," in which insulin-resistant skeletal muscles utilize high amounts of fatty acids, leading to excessive β-oxidation but only partially processing via the mitochondrial citric acid cycle and oxidative phosphorylation pathway. This metabolic overload of mitochondria with excessive fatty acids in turn impairs skeletal muscle insulin sensitivity and its ability to switch to carbohydrate utilization (Koves et al. 2008). Very recently, higher rates of incomplete FAO were associated with impaired skeletal muscle insulin sensitivity in poorly controlled compared to well-controlled T2DM patients (Gavin et al. 2018). Conclusively, the increased whole-body FAO in diabetic NZO mice might be indicative of an incomplete lipid oxidation that probably further contributes to the development of hyperglycaemia and insulin resistance. Further analyses of *ex vivo* skeletal muscle FAO and abundance or activity of β-oxidation- and citric acid cycle-regulating enzymes in NZO mice could be performed in order to analyse the contribution of skeletal muscle FAO to whole-body substrate utilization.

4.2.4 Chronic exercise further aggravates adipose tissue and hepatic insulin resistance in NZO mice

The chronic exercise intervention only mildly improved exercise capacity and insulin sensitivity in the ND subgroup, which could not be explained by elevated skeletal muscle glucose uptake. This raised the question whether exercise may have improved hepatic or adipose tissue

glucose metabolism to compensate for the lack of response in skeletal muscle. Unexpectedly, the insulin-stimulated glucose uptake in WAT was markedly abrogated in both ND and T2D mice in response to exercise. Moreover, hepatic glycolysis was reduced in exercised and diabetic conditions, while hepatic gluconeogenesis was upregulated, as evident by reduced GCK and elevated PCK-1 abundance, respectively. Furthermore, hepatic fat content was not reduced but markedly increased after chronic exercise in both NZO subgroups. In summary, these results indicate that regular exercise did not improve but further aggravated adipose tissue and hepatic insulin resistance in NZO mice.

This raises the question, which (lack of) pathways did promote rather than prevent against the development of insulin resistance in NZO mice that performed regular exercise. In the D4KO cohort, it was shown that increased adipose tissue glycaemia was related to increased browning of adipose tissue. In contrast, reduced browning has been reported to be associated with reduced insulin sensitivity in isolated human adipocytes (Rajan et al. 2016). Unfortunately, qPCR analysis of genes related to browning in scWAT of NZO mice could not be quantified reliably, but overall pointed towards a reduction of browning markers in trained and diabetic mice (data not shown). This would suggest that a lack of browning in WAT of NZO mice may contribute to the impaired adipose tissue insulin sensitivity. Apart from its function to regulate glucose uptake and lipolysis, the adipose tissue is an endocrine organ that secretes specific polypeptides. These the so-called adipokines have been shown to act on other tissues to regulate glucose and lipid metabolism and thereby contribute to tissue communication (Stern et al. 2016). Besides leptin, the adipokine adiponectin was linked to obesity and T2DM. Plasma levels of adiponectin have been shown to be inversely related to visceral obesity and insulin resistance, with increased T2DM prevalence apparent in patients with adiponectin deficiency (Machado et al. 2012, Stern et al. 2016). Regular exercise has been shown to increase plasma adiponectin concentrations, associated with improved insulin sensitivity in humans and diabetic *db/db* mice (Kriketos et al. 2004, Lee et al. 2011). In contrast to these findings, NZO mice showed a trend towards reduced plasma adiponectin concentrations after chronic exercise (Figure S7). Thus, the reduction of adiponectin indicates a dysregulated adipose tissue secretory function that may have contributed to the impaired adipose tissue and whole-body insulin-sensitivity in diabetic NZO mice in response to exercise.

In liver of NZO mice, chronic exercise apparently further increased insulin resistance, reflected by reduced glycolysis, elevated gluconeogenesis and abnormal fat storage. The accumulation of intrahepatic triglycerides was shown to be associated with hepatic insulin resistance (Gastaldelli et al. 2007). Moreover, the same study reported significant associations of

increased rates of hepatic gluconeogenesis with increased visceral fat content. In addition, elevated adipose tissue lipolysis leads to elevated NEFA concentrations, resulting in excess transport of NEFA into skeletal muscle and liver (Gastaldelli 2011). Although the plasma NEFA concentrations of NZO mice were not significantly different, sedentary T2D mice exhibited a tendency for increased plasma NEFA, which was further increased after exercise. Thus, elevated adipose tissue lipolysis may contribute to an increased influx of fatty acids into the liver, leading to increased hepatic fat accumulation that further impaired glycaemic control in trained NZO mice. Additional evidence for the adipose tissue affecting the hepatic triglyceride accumulation is provided by the adiponectin data. Plasma adiponectin levels have been shown to be inversely related to hepatic fat content in mouse and human studies, while delivery of recombinant adiponectin into mice led to a reduction of hepatic triglycerides (Xu et al. 2003, Bugianesi et al. 2005). Moreover, *ob/ob* mice overexpressing adiponectin exhibited improved glycaemia despite developing morbid obesity. The data suggested that adiponectin promoted the storage of triglycerides in the adipose tissue, leading to reduced hepatic triglyceride content associated with improved insulin sensitivity (Kim et al. 2007). Conclusively, the reduced adiponectin of trained NZO mice presumably promoted the enhanced accumulation of triglycerides in the liver instead of storing them in the adipose tissue.

In T2DM states, elevated hepatic DNL is the main cause of increased hepatic fat content (Sanders & Griffin 2016). Moreover, expression of DNL-regulating genes was shown to be highly upregulated in NZO mice compared to a non-diabetic control strain (Knebel et al. 2018). However, the hepatic abundance of FASN was not concomitantly elevated with liver fat content in trained NZO mice, but reduced in the T2D subgroup, indicating that the accumulation of hepatic triglycerides was not due to an elevated DNL. Instead, these results point towards an impaired FAO to be responsible for the increased hepatic fat content. Preliminary measurements of mitochondrial oxidative capacity in the liver of sedentary and trained NZO mice revealed an increased β-oxidation-linked but decreased citric acid cycle-linked maximal respiratory capacity in trained NZO mice (Figure S8). Thus, these findings may be indicative of only partial degradation of hepatic fatty acids in trained NZO mice, leading to increased accumulation of lipids in the liver.

4.2.5 NZO mice are rather non-responders to exercise

In summary, chronic exercise failed to reduce hyperglycaemia in NZO mice and rather impaired peripheral and hepatic insulin resistance. Although no studies performing regular exercise with NZO mice were reported, various studies using alternative mouse models for T2DM are available. Most of the studies report improvements of glycaemia in mice that

performed regular exercise, e.g. in the monogenic *db/db* mice or the polygenic *KK* and *TallyHo* mice (Nascimento et al. 2016, Chavanelle et al. 2017, Takagi et al. 2017). Nevertheless, a few studies showed that exercise did not lead to improved glycaemia (Sennott et al. 2008, Shearer et al. 2011). In the latter, exercise training even worsened the accumulation of cardiac glycogen in hearts of *db/db* mice, showing a similar deterioration of metabolism in response to exercise as in the NZO mice. In humans, this phenomenon of exercise resistance is referred to as "non-response" (Böhm et al. 2016). First evidence for a non-response to exercise was found in a chronic exercise study from the late 90s, in which some individuals exhibited only minor or no increases of VO_{2max} after twenty weeks of cycling exercise (Bouchard et al. 1999). Subsequent studies further reported the occurrence of non-responders to exercise-induced improvements of glycaemia in both healthy and obese or T2DM patients (Boule et al. 2005, Borel et al. 2012, Stephens et al. 2015). Additionally, it was shown that exercise can further deteriorate insulin sensitivity, i.e. leading to an adverse training response (Bouchard et al. 2012). Although the exact pathways leading to this inability to respond to exercise have not been elucidated, several studies clearly indicate that the genetic predisposition confers the non-response. For instance, the non-response in humans was shown to be associated with variants in the genes encoding for PPAR-δ, PGC-1α or NDUFB6, which is a subunit of the mitochondrial NADH dehydrogenase (Stefan et al. 2007, Ruchat et al. 2010, Kacerovsky-Bielesz et al. 2012). Especially the altered expression of genes involved in skeletal muscle mitochondrial function is considered to determine the exercise response (Stephens et al. 2018). Thus, the non-response of NZO mice to improve their glycaemia after exercise might be due to a distinct genetic pattern that regulates peripheral and hepatic insulin sensitivity.

However, it is highly debated whether such non-response truly exists or if the response to exercise is only dependent on the mode or intensity of the used training protocol. Indeed, subjecting initially identified non-responders to a subsequent exercise intervention with increased workload did eliminate the percentage of non-responders, suggesting that the response to exercise is only dose-dependent (Montero & Lundby 2017). Interestingly, *KK* mice that were subjected to different exercise protocols with either high or low intensity showed an improved glycaemia when exclusively performing the low-intensity training (Takagi et al. 2017). This suggests that increasing the dose may not necessarily lead to an increased exercise performance. Instead, modifying the protocol to the individual performance may compensate for the non-response. Of note, the intensity of the interval protocol was already attenuated in the NZO mice compared to the B6 cohort, in order to be able to fulfil the running protocol despite T2DM development. Thus, further reducing the intensity might be more beneficial for the NZO mice to respond to exercise with improved glycaemia.

4.3 Reduced hepatic triglyceride content determines the response to exercise

Investigating the impact of chronic exercise on glucose homeostasis in D4KO and NZO mice revealed two extremes of “exercise-responders”. When summarizing the main findings, D4KO mice can be considered as responders to exercise-mediated improvements of insulin sensitivity. In contrast, diabetic NZO mice are rather non-responders to exercise, since peripheral and whole-body glycaemia were not restored in the diabetic subgroup (Table 14).

Table 14: Comparison of the exercise-response in D4KO and diabetic NZO mice.

Parameter	D4KO mice	NZO mice (T2D)
Physical capacity (Time to exhaustion)	↑	↔
Whole-body insulin sensitivity (GTT, ITT)	↑	↓
Skeletal muscle glucose uptake	↔	↔
Adipose Tissue glucose uptake	↑	↓
Hepatic triglyceride content	↓	↑

Arrows indicate improved, unchanged or impaired observation of respective parameter.

Interestingly, skeletal muscle glucose uptake remained unaffected in both models. However, D4KO mice were able to compensate for the unchanged skeletal muscle glycaemia by a markedly elevated adipose tissue glucose uptake. In NZO mice, the adipose tissue failed to compensate for the skeletal muscle, contributing to the impaired whole-body insulin sensitivity. More importantly, the ability to improve whole-body insulin sensitivity in response to exercise seems to be associated with the reduction of hepatic triglyceride content, as evident from the D4KO study. In addition, intensifying the exercise protocol in B6 mice also led to an improved glucose tolerance associated with a significant reduction of hepatic triglycerides. Taken together, these findings suggest that exercise-mediated improvements of insulin sensitivity are to some extend dependent on the reduction of hepatic fat content, which may represent a possible new readout for a successful exercise response.

Several studies have already reported that the improved insulin sensitivity of T2DM patients that have performed regular exercise is associated with a reduced hepatic triglyceride content (Bacchi et al. 2013, Cheng et al. 2017). Although the exact mechanisms that reduce hepatic fat content in response to exercise remain unclear, both human and rodent studies give some evidence on possible pathways, as reviewed by van der Windt et al. Regular exercise has

been shown to reduce the concentration of plasma NEFA derived from elevated adipose tissue lipolysis, resulting in reduced transport of lipids to the liver. Secondly, a reduced DNL was considered to account for the reduction of hepatic triglycerides. Indeed, animal studies showed that chronic exercise decreased the expression of DNL-regulating enzymes such as FASN or stearoyl-CoA desaturase 1 (SCD1). Finally, exercise studies in rodents showed increased abundance of several enzymes regulating mitochondrial FAO, e.g. palmitoyl-CoA transferases (CPTs), as well as increased expression of transcription factors regulating hepatic β-oxidation such as peroxisome proliferator-activated receptor-α (PPAR-α; van der Windt et al. 2018). Thus, it is likely that D4KO mice were highly amenable to these exercise-induced pathways to reduce hepatic triglycerides, while these mechanisms seem to be disturbed in NZO mice, as already discussed previously. However, the exact pathways that drive the diverse hepatic metabolism in response to exercise in these mouse models remain to be elucidated.

Finally, the two interventions in D4KO and NZO mice highlight that the response to exercise is highly heterogeneous between individuals and probably depends on the genetic predisposition. The findings for the NZO mice additionally point towards the need of a personalized T2DM therapy that consists of alternative treatments for individuals that do not greatly benefit from exercise (Stephens et al. 2018).

4.4 Conclusion and future perspectives

Regular exercise has been shown to improve glycaemia in D4KO mice, presumably via targeting pathways in the adipose tissue that enhanced mitochondrial activity and insulin sensitivity. It was speculated that the skeletal muscle may secrete specific myokines that mediate the improvements in adipose tissue. To further validate this hypothesis, measurements of plasma myokines such as irisin, myostatin, FGF-21 and different interleukines will be performed using a specific magnetic bead-based immunofluorescent assay kit. Furthermore, our cooperation partners from the Max Planck Institute for Molecular Genetics in Berlin are conducting high-throughput RNA-sequencing analysis in RNA samples from skeletal muscle and adipose tissue of sedentary and trained D4KO mice. Using this approach, expression of genes and transcription factors that might be involved in the exercise-mediated regulation of glucose uptake and mitochondrial activity in the adipose tissue of trained D4KO mice might be identified.

Deficiency of TBC1D4 is not only affecting glycaemia in mice but has also been shown to be relevant in humans. Homozygous carriers of a loss-of-function variant in the *TBC1D4* gene

that was identified in a Greenlandic Inuit population exhibited postprandial hyperglycaemia and increased T2DM prevalence (Moltke et al. 2014). Interestingly, increased moderate physical activity has recently been shown to improve glucose clearance during an oral GTT in homozygous allele carriers of the *TBC1D4* variant, even to a greater extent than in non-carriers. These findings are surprisingly identical to the present murine D4KO study, in which D4KO mice showed a greater benefit from chronic exercise to improve glycaemia compared to WT controls, thereby phenocopying the human Inuit situation (Schnurr et al., Manuscript in preparation). Future translational research will focus on the analysis of adipose tissue from the human Inuit cohort in order to elucidate whether a compensatory mechanism similar to D4KO mice improves insulin sensitivity in trained individuals.

In contrast to D4KO mice, chronic exercise did not improve glycaemia, but instead further impaired peripheral and hepatic insulin resistance in polygenic NZO mice. Furthermore, hepatic triglycerides were not reduced but considerably increased in trained NZO mice, presumably contributing to the non-response to exercise. RNA-sequencing of skeletal muscle and liver as well as the analysis of the hepatic fatty acid composition (lipodomics) will give further evidence on the respective pathways that confer the adverse response to exercise in NZO mice.

Another important finding was the heterogeneous development of hyperglycaemia in response to the HFD in NZO mice, independent of exercise. Therefore, epigenetic pathways or the maternal nutritional state might affect the onset of T2DM in NZO mice. To investigate the impact of epigenetic modifications on glycaemia in NZO mice, future experiments may include methylated DNA immunoprecipitation (MeDIP) analysis. This technique detects methylated DNA fragments using specific antibodies and would help to clarify whether DNA methylation might be altered in skeletal muscle, adipose tissue or liver of NZO mice.

5. Literature

5.1 Scientific publications

Adams LA, Angulo P, Lindor KD (2005). Nonalcoholic fatty liver disease. *CMAJ* 172: 899-905.

Aguirre V, Uchida T, Yenush L, Davis R, White MF (2000). The c-Jun NH(2)-terminal kinase promotes insulin resistance during association with insulin receptor substrate-1 and phosphorylation of Ser(307). *J Biol Chem* 275: 9047-54.

Al-Goblan AS, Al-Alfi MA, Khan MZ (2014). Mechanism linking diabetes mellitus and obesity. *Diabetes Metab Syndr Obes* 7: 587-91.

Alex S, Boss A, Heerschap A, Kersten S (2015). Exercise training improves liver steatosis in mice. *Nutr Metab* 12: 29.

Ameer F, Scandiuzzi L, Hasnain S, Kalbacher H, Zaidi N (2014). De novo lipogenesis in health and disease. *Metabolism* 63: 895-902.

American Diabetes Association (2010). Diagnosis and classification of diabetes mellitus. *Diabetes Care* 33 Suppl 1: S62-9.

Arany Z (2008). PGC-1 coactivators and skeletal muscle adaptations in health and disease. *Curr Opin Genet Dev* 18: 426-34.

Baar K, Wende AR, Jones TE, Marison M, Nolte LA, Chen M, Kelly DP, Holloszy JO (2002). Adaptations of skeletal muscle to exercise: rapid increase in the transcriptional coactivator PGC-1. *FASEB J* 16: 1879-86.

Bacchi E, Negri C, Targher G, Faccioli N, Lanza M, Zoppini G, Zanolin E, Schena F, Bonora E, Moghetti P (2013). Both resistance training and aerobic training reduce hepatic fat content in type 2 diabetic subjects with nonalcoholic fatty liver disease (the RAED2 Randomized Trial). *Hepatology* 58: 1287-95.

Bassett DR, Jr., Howley ET (2000). Limiting factors for maximum oxygen uptake and determinants of endurance performance. *Med Sci Sports Exerc* 32: 70-84.

Baumeier C, Kaiser D, Heeren J, Scheja L, John C, Weise C, Eravci M, Lagerpusch M, Schulze G, Joost HG, Schwenk RW, Schürmann A (2015). Caloric restriction and intermittent fasting alter hepatic lipid droplet proteome and diacylglycerol species and prevent diabetes in NZO mice. *Biochim Biophys Acta* 1851: 566-76.

Bielschowsky F, Bielschowsky M (1956). The New Zealand strain of obese mice; their response to stilboestrol and to insulin. *Aust J Exp Biol Med Sci* 34: 181-98.

Binsch C, Jelenik T, Pfitzer A, Dille M, Müller-Lühlhoff S, Hartwig S, Karpinski S, Lehr S, Kabra DG, Chadt A, Roden M, Al-Hasani H, Castaneda TR (2017). Absence of the kinase S6k1 mimics the effect of chronic endurance exercise on glucose tolerance and muscle oxidative stress. *Mol Metab* 6: 1443-53.

Boden G, Lebed B, Schatz M, Homko C, Lemieux S (2001). Effects of acute changes of plasma free fatty acids on intramyocellular fat content and insulin resistance in healthy subjects. *Diabetes* 50: 1612-7.

Böhm A, Weigert C, Staiger H, Häring HU (2016). Exercise and diabetes: relevance and causes for response variability. *Endocrine* 51: 390-401.

Bonnefond A, Froguel P (2015). Rare and common genetic events in type 2 diabetes: what should biologists know? *Cell Metab* 21: 357-68.

Booth FW, Roberts CK, Laye MJ (2012). Lack of exercise is a major cause of chronic diseases. *Compr Physiol* 2: 1143-211.

Borel AL, Nazare JA, Smith J, Almeras N, Tremblay A, Bergeron J, Poirier P, Despres JP (2012). Improvement in insulin sensitivity following a 1-year lifestyle intervention program in viscerally obese men: contribution of abdominal adiposity. *Metabolism* 61: 262-72.

Boström P, Wu J, Jedrychowski MP, Korde A, Ye L, Lo JC, Rasbach KA, Bostrom EA, Choi JH, Long JZ, Kajimura S, Zingaretti MC, Vind BF, Tu H, Cinti S, Hojlund K, Gygi SP, Spiegelman BM (2012). A PGC1-alpha-dependent myokine that drives brown-fat-like development of white fat and thermogenesis. *Nature* 481: 463-8.

Bouchard C, An P, Rice T, Skinner JS, Wilmore JH, Gagnon J, Perusse L, Leon AS, Rao DC (1999). Familial aggregation of VO(2max) response to exercise training: results from the HERITAGE Family Study. *J Appl Physiol (1985)* 87: 1003-8.

Bouchard C, Blair SN, Church TS, Earnest CP, Hagberg JM, Hakkinen K, Jenkins NT, Karavirta L, Kraus WE, Leon AS, Rao DC, Sarzynski MA, Skinner JS, Slentz CA, Rankinen T (2012). Adverse metabolic response to regular exercise: is it a rare or common occurrence? *PLoS One* 7: e37887.

Boule NG, Weisnagel SJ, Lakka TA, Tremblay A, Bergman RN, Rankinen T, Leon AS, Skinner JS, Wilmore JH, Rao DC, Bouchard C, Study HF (2005). Effects of exercise training on glucose homeostasis: the HERITAGE Family Study. *Diabetes Care* 28: 108-14.

Bowe JE, Franklin ZJ, Hauge-Evans AC, King AJ, Persaud SJ, Jones PM (2014). Metabolic phenotyping guidelines: assessing glucose homeostasis in rodent models. *J Endocrinol* 222: G13-25.

Brouwers B, Hesselink MK, Schrauwen P, Schrauwen-Hinderling VB (2016). Effects of exercise training on intrahepatic lipid content in humans. *Diabetologia* 59: 2068-79.

Bugianesi E, Pagotto U, Manini R, Vanni E, Gastaldelli A, de Iasio R, Gentilcore E, Natale S, Cassader M, Rizzetto M, Pasquali R, Marchesini G (2005). Plasma adiponectin in nonalcoholic fatty liver is related to hepatic insulin resistance and hepatic fat content, not to liver disease severity. *J Clin Endocrinol Metab* 90: 3498-504.

Casey A, Mann R, Banister K, Fox J, Morris PG, Macdonald IA, Greenhaff PL (2000). Effect of carbohydrate ingestion on glycogen resynthesis in human liver and skeletal muscle, measured by (13)C MRS. *Am J Physiol Endocrinol Metab* 278: E65-75.

Ceddia RB (2013). The role of AMP-activated protein kinase in regulating white adipose tissue metabolism. *Mol Cell Endocrinol* 366: 194-203.

Cerf ME, Williams K, Chapman CS, Louw J (2007). Compromised beta-cell development and beta-cell dysfunction in weanling offspring from dams maintained on a high-fat diet during gestation. *Pancreas* 34: 347-53.

Chadt A, Immisch A, de Wendt C, Springer C, Zhou Z, Stermann T, Holman GD, Loffing-Cueni D, Loffing J, Joost HG, Al-Hasani H (2015). Deletion of both Rab-GTPase-activating proteins TBC1D1 and TBC1D4 in mice eliminates insulin- and AICAR-stimulated glucose transport [corrected]. *Diabetes* 64: 746-59.

Chadt A, Leicht K, Deshmukh A, Jiang LQ, Scherneck S, Bernhardt U, Dreja T, Vogel H, Schmolz K, Kluge R, Zierath JR, Hultschig C, Hoeben RC, Schürmann A, Joost HG, Al-Hasani H (2008). Tbc1d1 mutation in lean mouse strain confers leanness and protects from diet-induced obesity. *Nat Genet* 40: 1354-9.

Chang SP, Chen YH, Chang WC, Liu IM, Cheng JT (2006). Merit of physical exercise to reverse the higher gene expression of hepatic phosphoenolpyruvate carboxykinase in obese Zucker rats. *Life Sci* 79: 240-6.

Chavanelle V, Boisseau N, Otero YF, Combaret L, Dardevet D, Montaurier C, Delcros G, Peltier SL, Sirvent P (2017). Effects of high-intensity interval training and moderate-intensity continuous training on glycaemic control and skeletal muscle mitochondrial function in db/db mice. *Sci Rep* 7: 204.

Cheng S, Ge J, Zhao C, Le S, Yang Y, Ke D, Wu N, Tan X, Zhang X, Du X, Sun J, Wang R, Shi Y, Borra RJH, Parkkola R, Wiklund P, Lu D (2017). Effect of aerobic exercise and diet on liver fat in pre-diabetic patients with non-alcoholic-fatty-liver-disease: A randomized controlled trial. *Sci Rep* 7: 15952.

Cho YS, Chen CH, Hu C, Long J, Ong RT, Sim X, Takeuchi F, Wu Y, Go MJ, Yamauchi T, Chang YC, Kwak SH, Ma RC, Yamamoto K, Adair LS, Aung T, Cai Q, Chang LC, Chen YT, Gao Y, Hu FB, Kim HL, Kim S, Kim YJ, Lee JJ, Lee NR, Li Y, Liu JJ, Lu W, Nakamura J, Nakashima E, Ng DP, Tay WT, Tsai FJ, Wong TY, Yokota M, Zheng W, Zhang R, Wang C, So WY, Ohnaka K, Ikegami H, Hara K, Cho YM, Cho NH, Chang TJ, Bao Y, Hedman AK, Morris AP, McCarthy MI, et al. (2011). Meta-analysis of genome-wide association studies identifies eight new loci for type 2 diabetes in east Asians. *Nat Genet* 44: 67-72.

Coggan AR, Swanson SC, Mendenhall LA, Habash DL, Kien CL (1995). Effect of endurance training on hepatic glycogenolysis and gluconeogenesis during prolonged exercise in men. *Am J Physiol* 268: E375-83.

Colberg SR, Sigal RJ, Yardley JE, Riddell MC, Dunstan DW, Dempsey PC, Horton ES, Castorino K, Tate DF (2016). Physical activity/exercise and diabetes: a position statement of the American Diabetes Association. *Diabetes Care* 39: 2065-79.

Cozzone D, Frojdo S, Disse E, Debard C, Laville M, Pirola L, Vidal H (2008). Isoform-specific defects of insulin stimulation of Akt/protein kinase B (PKB) in skeletal muscle cells from type 2 diabetic patients. *Diabetologia* 51: 512-21.

Cypess AM, Lehman S, Williams G, Tal I, Rodman D, Goldfine AB, Kuo FC, Palmer EL, Tseng YH, Doria A, Kolodny GM, Kahn CR (2009). Identification and importance of brown adipose tissue in adult humans. *N Engl J Med* 360: 1509-17.

Damsbo P, Vaag A, Hother-Nielsen O, Beck-Nielsen H (1991). Reduced glycogen synthase activity in skeletal muscle from obese patients with and without type 2 (non-insulin-dependent) diabetes mellitus. *Diabetologia* 34: 239-45.

Daval M, Foufelle F, Ferre P (2006). Functions of AMP-activated protein kinase in adipose tissue. *J Physiol* 574: 55-62.

Deeb SS, Fajas L, Nemoto M, Pihlajamaki J, Mykkanen L, Kuusisto J, Laakso M, Fujimoto W, Auwerx J (1998). A Pro12Ala substitution in PPARgamma2 associated with decreased receptor activity, lower body mass index and improved insulin sensitivity. *Nat Genet* 20: 284-7.

DeFronzo RA, Jacot E, Jequier E, Maeder E, Wahren J, Felber JP (1981). The effect of insulin on the disposal of intravenous glucose. Results from indirect calorimetry and hepatic and femoral venous catheterization. *Diabetes* 30: 1000-7.

Dimitriadis G, Mitrou P, Lambadiari V, Maratou E, Raptis SA (2011). Insulin effects in muscle and adipose tissue. *Diabetes Res Clin Pract* 93 Suppl 1: S52-9.

Dos Santos JM, Moreli ML, Tewari S, Benite-Ribeiro SA (2015). The effect of exercise on skeletal muscle glucose uptake in type 2 diabetes: An epigenetic perspective. *Metabolism* 64: 1619-28.

Dunaif A, Xia J, Book CB, Schenker E, Tang Z (1995). Excessive insulin receptor serine phosphorylation in cultured fibroblasts and in skeletal muscle. A potential mechanism for insulin resistance in the polycystic ovary syndrome. *J Clin Invest* 96: 801-10.

E L, Lu J, Burns JM, Swerdlow RH (2013). Effect of exercise on mouse liver and brain bioenergetic infrastructures. *Exp Physiol* 98: 207-19.

Egan B, Carson BP, Garcia-Roves PM, Chibalin AV, Sarsfield FM, Barron N, McCaffrey N, Moyna NM, Zierath JR, O'Gorman DJ (2010). Exercise intensity-dependent regulation of peroxisome proliferator-activated receptor coactivator-1 mRNA abundance is associated with differential activation of upstream signalling kinases in human skeletal muscle. *J Physiol* 588: 1779-90.

Egan B, Zierath JR (2013). Exercise metabolism and the molecular regulation of skeletal muscle adaptation. *Cell Metab* 17: 162-84.

Elahi MM, Cagampang FR, Mukhtar D, Anthony FW, Ohri SK, Hanson MA (2009). Long-term maternal high-fat feeding from weaning through pregnancy and lactation predisposes offspring to hypertension, raised plasma lipids and fatty liver in mice. *Br J Nutr* 102: 514-9.

Evans CC, LePard KJ, Kwak JW, Stancukas MC, Laskowski S, Dougherty J, Moulton L, Glawe A, Wang Y, Leone V, Antonopoulos DA, Smith D, Chang EB, Ciancio MJ (2014). Exercise prevents weight gain and alters the gut microbiota in a mouse model of high fat diet-induced obesity. *PLoS One* 9: e92193.

Feldman BJ, Streeper RS, Farese RV, Jr., Yamamoto KR (2006). Myostatin modulates adipogenesis to generate adipocytes with favorable metabolic effects. *Proc Natl Acad Sci U S A* 103: 15675-80.

Ferreira JC, Rolim NP, Bartholomeu JB, Gobatto CA, Kokubun E, Brum PC (2007). Maximal lactate steady state in running mice: effect of exercise training. *Clin Exp Pharmacol Physiol* 34: 760-5.

Ford ES, Li C, Sattar N (2008). Metabolic syndrome and incident diabetes: current state of the evidence. *Diabetes Care* 31: 1898-904.

Frayling TM, Timpson NJ, Weedon MN, Zeggini E, Freathy RM, Lindgren CM, Perry JR, Elliott KS, Lango H, Rayner NW, Shields B, Harries LW, Barrett JC, Ellard S, Groves CJ, Knight B, Patch AM, Ness AR, Ebrahim S, Lawlor DA, Ring SM, Ben-Shlomo Y, Jarvelin MR, Sovio U,

Bennett AJ, Melzer D, Ferrucci L, Loos RJ, Barroso I, Wareham NJ, Karpe F, Owen KR, Cardon LR, Walker M, Hitman GA, Palmer CN, Doney AS, Morris AD, Smith GD, Hattersley AT, McCarthy MI (2007). A common variant in the FTO gene is associated with body mass index and predisposes to childhood and adult obesity. *Science* 316: 889-94.

Frayn KN, Arner P, Yki-Jarvinen H (2006). Fatty acid metabolism in adipose tissue, muscle and liver in health and disease. *Essays Biochem* 42: 89-103.

Froguel P, Vaxillaire M, Sun F, Velho G, Zouali H, Butel MO, Lesage S, Vionnet N, Clement K, Fougerousse F, et al. (1992). Close linkage of glucokinase locus on chromosome 7p to early-onset non-insulin-dependent diabetes mellitus. *Nature* 356: 162-4.

Frosig C, Jorgensen SB, Hardie DG, Richter EA, Wojtaszewski JF (2004). 5'-AMP-activated protein kinase activity and protein expression are regulated by endurance training in human skeletal muscle. *Am J Physiol Endocrinol Metab* 286: E411-7.

Fueger PT, Li CY, Ayala JE, Shearer J, Bracy DP, Charron MJ, Rottman JN, Wasserman DH (2007). Glucose kinetics and exercise tolerance in mice lacking the GLUT4 glucose transporter. *J Physiol* 582: 801-12.

Fueger PT, Shearer J, Krueger TM, Posey KA, Bracy DP, Heikkinen S, Laakso M, Rottman JN, Wasserman DH (2005). Hexokinase II protein content is a determinant of exercise endurance capacity in the mouse. *J Physiol* 566: 533-41.

Fukuda M (2011). TBC proteins: GAPs for mammalian small GTPase Rab? *Biosci Rep* 31: 159-68.

Garcia RA, Roemmich JN, Claycombe KJ (2016). Evaluation of markers of beige adipocytes in white adipose tissue of the mouse. *Nutr Metab* 13: 24.

Garvey WT, Maianu L, Zhu JH, Brechtel-Hook G, Wallace P, Baron AD (1998). Evidence for defects in the trafficking and translocation of GLUT4 glucose transporters in skeletal muscle as a cause of human insulin resistance. *J Clin Invest* 101: 2377-86.

Gastaldelli A (2011). Role of beta-cell dysfunction, ectopic fat accumulation and insulin resistance in the pathogenesis of type 2 diabetes mellitus. *Diabetes Res Clin Pract* 93 Suppl 1: S60-5.

Gastaldelli A, Cusi K, Pettiti M, Hardies J, Miyazaki Y, Berria R, Buzzigoli E, Sironi AM, Cersosimo E, Ferrannini E, Defronzo RA (2007). Relationship between hepatic/visceral fat and hepatic insulin resistance in nondiabetic and type 2 diabetic subjects. *Gastroenterology* 133: 496-506.

Gavin TP, Ernst JM, Kwak HB, Caudill SE, Reed MA, Garner RT, Nie Y, Weiss JA, Pories WJ, Dar M, Lin CT, Hubal MJ, Neufer PD, Kuang S, Dohm GL (2018). High incomplete skeletal muscle fatty acid oxidation explains low muscle insulin sensitivity in poorly controlled T2D. *J Clin Endocrinol Metab* 103: 882-89.

Gimenez-Cassina A, Garcia-Haro L, Choi CS, Osundiji MA, Lane EA, Huang H, Yildirim MA, Szlyk B, Fisher JK, Polak K, Patton E, Wiwczar J, Godes M, Lee DH, Robertson K, Kim S, Kulkarni A, Distefano A, Samuel V, Cline G, Kim YB, Shulman GI, Danial NN (2014). Regulation of hepatic energy metabolism and gluconeogenesis by BAD. *Cell Metab* 19: 272-84.

Gonzalez JT, Fuchs CJ, Smith FE, Thelwall PE, Taylor R, Stevenson EJ, Trenell MI, Cermak NM, van Loon LJ (2015). Ingestion of glucose or sucrose prevents liver but not muscle glycogen depletion during prolonged endurance-type exercise in trained cyclists. *Am J Physiol Endocrinol Metab* 309: E1032-9.

Goodwin ML, Harris JE, Hernandez A, Gladden LB (2007). Blood lactate measurements and analysis during exercise: a guide for clinicians. *J Diabetes Sci Technol* 1: 558-69.

Gormley SE, Swain DP, High R, Spina RJ, Dowling EA, Kotipalli US, Gandrakota R (2008). Effect of intensity of aerobic training on VO2max. *Med Sci Sports Exerc* 40: 1336-43.

Gorovits N, Charron MJ (2003). What we know about facilitative glucose transporters: lessons from cultured cells, animal models, and human studies. *Biochem Mol Biol Educ* 31: 163-172.

Gorselink M, Drost MR, de Brouwer KF, Schaart G, van Kranenburg GP, Roemen TH, van Bilsen M, Charron MJ, van der Vusse GJ (2002). Increased muscle fatigability in GLUT-4-deficient mice. *Am J Physiol Endocrinol Metab* 282: E348-54.

Grarup N, Moltke I, Albrechtsen A, Hansen T (2015). Diabetes in population isolates: lessons from Greenland. *Rev Diabet Stud* 12: 320-9.

Green CJ, Hodson L (2014). The influence of dietary fat on liver fat accumulation. *Nutrients* 6: 5018-33.

Guo X, Honggui L, Xu H, Woo S, Dong H, Lu F, Lange AJ, Wu C (2012). Glycolysis in the control of blood glucose homeostasis. *Acta Pharm Sin B* 2: 358-367.

Gurley JM, Griesel BA, Olson AL (2016). Increased skeletal muscle GLUT4 expression in obese mice after voluntary wheel running exercise is posttranscriptional. *Diabetes* 65: 2911-9.

Hafstad AD, Lund J, Hadler-Olsen E, Hoper AC, Larsen TS, Aasum E (2013). High- and moderate-intensity training normalizes ventricular function and mechanoenergetics in mice with diet-induced obesity. *Diabetes* 62: 2287-94.

Hallakou S, Doare L, Foufelle F, Kergoat M, Guerre-Millo M, Berthault MF, Dugail I, Morin J, Auwerx J, Ferre P (1997). Pioglitazone induces in vivo adipocyte differentiation in the obese Zucker fa/fa rat. *Diabetes* 46: 1393-9.

Hammarstedt A, Sopasakis VR, Gogg S, Jansson PA, Smith U (2005). Improved insulin sensitivity and adipose tissue dysregulation after short-term treatment with pioglitazone in non-diabetic, insulin-resistant subjects. *Diabetologia* 48: 96-104.

Hanson RL, Muller YL, Kobes S, Guo T, Bian L, Ossowski V, Wiedrich K, Sutherland J, Wiedrich C, Mahkee D, Huang K, Abdussamad M, Traurig M, Weil EJ, Nelson RG, Bennett PH, Knowler WC, Bogardus C, Baier LJ (2014). A genome-wide association study in American Indians implicates DNER as a susceptibility locus for type 2 diabetes. *Diabetes* 63: 369-76.

Hardy OT, Czech MP, Corvera S (2012). What causes the insulin resistance underlying obesity? *Curr Opin Endocrinol Diabetes Obes* 19: 81-7.

Hargett SR, Walker NN, Hussain SS, Hoehn KL, Keller SR (2015). Deletion of the Rab GAP Tbc1d1 modifies glucose, lipid, and energy homeostasis in mice. *Am J Physiol Endocrinol Metab* 309: E233-45.

He L, Sabet A, Djedjos S, Miller R, Sun X, Hussain MA, Radovick S, Wondisford FE (2009). Metformin and insulin suppress hepatic gluconeogenesis through phosphorylation of CREB binding protein. *Cell* 137: 635-46.

Heikkinen S, Pietila M, Halmekyto M, Suppola S, Pirinen E, Deeb SS, Janne J, Laakso M (1999). Hexokinase II-deficient mice. Prenatal death of homozygotes without disturbances in glucose tolerance in heterozygotes. *J Biol Chem* 274: 22517-23.

Heikkinen S, Suppola S, Malkki M, Deeb SS, Janne J, Laakso M (2000). Mouse hexokinase II gene: structure, cDNA, promoter analysis, and expression pattern. *Mamm Genome* 11: 91-6.

Honka MJ, Latva-Rasku A, Bucci M, Virtanen KA, Hannukainen JC, Kalliokoski KK, Nuutila P (2018). Insulin-stimulated glucose uptake in skeletal muscle, adipose tissue and liver: a positron emission tomography study. *Eur J Endocrinol* 178: 523-31.

Hurley BF, Nemeth PM, Martin WH, 3rd, Hagberg JM, Dalsky GP, Holloszy JO (1986). Muscle triglyceride utilization during exercise: effect of training. *J Appl Physiol (1985)* 60: 562-7.

Hussey SE, McGee SL, Garnham A, Wentworth JM, Jeukendrup AE, Hargreaves M (2011). Exercise training increases adipose tissue GLUT4 expression in patients with type 2 diabetes. *Diabetes Obes Metab* 13: 959-62.

Igel M, Becker W, Herberg L, Joost HG (1997). Hyperleptinemia, leptin resistance, and polymorphic leptin receptor in the New Zealand obese mouse. *Endocrinology* 138: 4234-9.

Ishibashi J, Seale P (2010). Medicine. Beige can be slimming. *Science* 328: 1113-4.

Jelenik T, Dille M, Müller-Lühlhoff S, Kabra DG, Zhou Z, Binsch C, Hartwig S, Lehr S, Chadt A, Peters EMJ, Kruse J, Roden M, Al-Hasani H, Castaneda TR (2018). FGF21 regulates insulin sensitivity following long-term chronic stress. *Mol Metab* 16: 126-38.

Jeon SM (2016). Regulation and function of AMPK in physiology and diseases. *Exp Mol Med* 48: e245.

Joost HG, Schürmann A (2014). The genetic basis of obesity-associated type 2 diabetes (diabesity) in polygenic mouse models. *Mamm Genome* 25: 401-12.

Jung ME, Bourne JE, Little JP (2014). Where does HIT fit? An examination of the affective response to high-intensity intervals in comparison to continuous moderate- and continuous vigorous-intensity exercise in the exercise intensity-affect continuum. *PLoS One* 9: e114541.

Junger E, Herberg L, Jeruschke K, Leiter EH (2002). The diabetes-prone NZO/Hl strain. II. Pancreatic immunopathology. *Lab Invest* 82: 843-53.

Jürgens H, Haass W, Castaneda TR, Schürmann A, Koebnick C, Dombrowski F, Otto B, Nawrocki AR, Scherer PE, Spranger J, Ristow M, Joost HG, Havel PJ, Tschöp MH (2005). Consuming fructose-sweetened beverages increases body adiposity in mice. *Obes Res* 13: 1146-56.

Jürgens HS, Neschen S, Ortmann S, Scherneck S, Schmolz K, Schuler G, Schmidt S, Bluher M, Klaus S, Perez-Tilve D, Tschöp MH, Schürmann A, Joost HG (2007). Development of diabetes in obese, insulin-resistant mice: essential role of dietary carbohydrate in beta cell destruction. *Diabetologia* 50: 1481-9.

Jürgens HS, Schürmann A, Kluge R, Ortmann S, Klaus S, Joost HG, Tschöp MH (2006). Hyperphagia, lower body temperature, and reduced running wheel activity precede development of morbid obesity in New Zealand obese mice. *Physiol Genomics* 25: 234-41.

Kacerovsky-Bielesz G, Kacerovsky M, Chmelik M, Farukuoye M, Ling C, Pokan R, Tschan H, Szendroedi J, Schmid AI, Gruber S, Herder C, Wolzt M, Moser E, Pacini G, Smekal G, Groop L, Roden M (2012). A single nucleotide polymorphism associates with the response of muscle ATP synthesis to long-term exercise training in relatives of type 2 diabetic humans. *Diabetes Care* 35: 350-7.

Karpe F, Dickmann JR, Frayn KN (2011). Fatty acids, obesity, and insulin resistance: time for a reevaluation. *Diabetes* 60: 2441-9.

Kasumov T, Solomon TP, Hwang C, Huang H, Haus JM, Zhang R, Kirwan JP (2015). Improved insulin sensitivity after exercise training is linked to reduced plasma C14:0 ceramide in obesity and type 2 diabetes. *Obesity (Silver Spring)* 23: 1414-21.

Kennedy JW, Hirshman MF, Gervino EV, Ocel JV, Forse RA, Hoenig SJ, Aronson D, Goodyear LJ, Horton ES (1999). Acute exercise induces GLUT4 translocation in skeletal muscle of normal human subjects and subjects with type 2 diabetes. *Diabetes* 48: 1192-7.

Kim JY, van de Wall E, Laplante M, Azzara A, Trujillo ME, Hofmann SM, Schraw T, Durand JL, Li H, Li G, Jelicks LA, Mehler MF, Hui DY, Deshaies Y, Shulman GI, Schwartz GJ, Scherer PE (2007). Obesity-associated improvements in metabolic profile through expansion of adipose tissue. *J Clin Invest* 117: 2621-37.

King AJ (2012). The use of animal models in diabetes research. *Br J Pharmacol* 166: 877-94.

Kluge R, Scherneck S, Schürmann A, Joost HG (2012). Pathophysiology and genetics of obesity and diabetes in the New Zealand obese mouse: a model of the human metabolic syndrome. *Methods Mol Biol* 933: 59-73.

Kluth O, Mirhashemi F, Scherneck S, Kaiser D, Kluge R, Neschen S, Joost HG, Schürmann A (2011). Dissociation of lipotoxicity and glucotoxicity in a mouse model of obesity associated diabetes: role of forkhead box O1 (FOXO1) in glucose-induced beta cell failure. *Diabetologia* 54: 605-16.

Knebel B, Göddeke S, Hartwig S, Hörbelt T, Fahlbusch P, Al-Hasani H, Jacob S, Koellmer C, Nitzgen U, Schiller M, Lehr S, Kotzka J (2018). Alteration of liver peroxisomal and mitochondrial functionality in the NZO mouse model of metabolic syndrome. *Proteomics Clin Appl* 12.

Knight JB, Eyster CA, Griesel BA, Olson AL (2003). Regulation of the human GLUT4 gene promoter: interaction between a transcriptional activator and myocyte enhancer factor 2A. *Proc Natl Acad Sci U S A* 100: 14725-30.

Knowler WC, Barrett-Connor E, Fowler SE, Hamman RF, Lachin JM, Walker EA, Nathan DM, Diabetes Prevention Program Research G (2002). Reduction in the incidence of type 2 diabetes with lifestyle intervention or metformin. *N Engl J Med* 346: 393-403.

Knudsen JG, Bienso RS, Hassing HA, Jakobsen AH, Pilegaard H (2015). Exercise-induced regulation of key factors in substrate choice and gluconeogenesis in mouse liver. *Mol Cell Biochem* 403: 209-17.

Kobayashi K, Forte TM, Taniguchi S, Ishida BY, Oka K, Chan L (2000). The db/db mouse, a model for diabetic dyslipidemia: molecular characterization and effects of Western diet feeding. *Metabolism* 49: 22-31.

Königsdorf CA, Navarrete Santos A, Schmidt JS, Fischer S, Fischer B (2012). Expression profile of fatty acid metabolism genes in preimplantation blastocysts of obese and non-obese mice. *Obes Facts* 5: 575-86.

Koves TR, Ussher JR, Noland RC, Slentz D, Mosedale M, Ilkayeva O, Bain J, Stevens R, Dyck JR, Newgard CB, Lopaschuk GD, Muoio DM (2008). Mitochondrial overload and incomplete fatty acid oxidation contribute to skeletal muscle insulin resistance. *Cell Metab* 7: 45-56.

Kramer HF, Witczak CA, Taylor EB, Fujii N, Hirshman MF, Goodyear LJ (2006). AS160 regulates insulin- and contraction-stimulated glucose uptake in mouse skeletal muscle. *J Biol Chem* 281: 31478-85.

Kriketos AD, Gan SK, Poynten AM, Furler SM, Chisholm DJ, Campbell LV (2004). Exercise increases adiponectin levels and insulin sensitivity in humans. *Diabetes Care* 27: 629-30.

Laker RC, Garde C, Camera DM, Smiles WJ, Zierath JR, Hawley JA, Barres R (2017). Transcriptomic and epigenetic responses to short-term nutrient-exercise stress in humans. *Sci Rep* 7: 15134.

Lansey MN, Walker NN, Hargett SR, Stevens JR, Keller SR (2012). Deletion of Rab GAP AS160 modifies glucose uptake and GLUT4 translocation in primary skeletal muscles and adipocytes and impairs glucose homeostasis. *Am J Physiol Endocrinol Metab* 303: E1273-86.

Lao XQ, Deng HB, Liu X, Chan TC, Zhang Z, Chang LY, Yeoh EK, Tam T, Wong MCS, Thomas GN (2018). Increased leisure-time physical activity associated with lower onset of diabetes in 44 828 adults with impaired fasting glucose: a population-based prospective cohort study. *Br J Sports Med*.

Lee S, Deldin AR, White D, Kim Y, Libman I, Rivera-Vega M, Kuk JL, Sandoval S, Boesch C, Arslanian S (2013). Aerobic exercise but not resistance exercise reduces intrahepatic lipid content and visceral fat and improves insulin sensitivity in obese adolescent girls: a randomized controlled trial. *Am J Physiol Endocrinol Metab* 305: E1222-9.

Lee S, Park Y, Dellsperger KC, Zhang C (2011). Exercise training improves endothelial function via adiponectin-dependent and independent pathways in type 2 diabetic mice. *Am J Physiol Heart Circ Physiol* 301: H306-14.

Leney SE, Tavare JM (2009). The molecular basis of insulin-stimulated glucose uptake: signalling, trafficking and potential drug targets. *J Endocrinol* 203: 1-18.

Lindstrom P (2007). The physiology of obese-hyperglycemic mice [ob/ob mice]. *ScientificWorldJournal* 7: 666-85.

Lowell BB, Spiegelman BM (2000). Towards a molecular understanding of adaptive thermogenesis. *Nature* 404: 652-60.

Machado MV, Coutinho J, Carepa F, Costa A, Proenca H, Cortez-Pinto H (2012). How adiponectin, leptin, and ghrelin orchestrate together and correlate with the severity of nonalcoholic fatty liver disease. *Eur J Gastroenterol Hepatol* 24: 1166-72.

MacInnis MJ, Nugent SF, MacLeod KE, Lohse KR (2015). Methods to estimate VO2max upon acute hypoxia exposure. *Med Sci Sports Exerc* 47: 1869-76.

Mackrell JG, Cartee GD (2012). A novel method to measure glucose uptake and myosin heavy chain isoform expression of single fibers from rat skeletal muscle. *Diabetes* 61: 995-1003.

Madsen SM, Thorup AC, Overgaard K, Jeppesen PB (2015). High intensity interval training improves glycaemic control and pancreatic beta cell function of type 2 diabetes patients. *PLoS One* 10: e0133286.

Mafakheri S, Chadt A, Al-Hasani H (2018). Regulation of RabGAPs involved in insulin action. *Biochem Soc Trans* 46: 683-90.

Magkos F (2012). Putative factors that may modulate the effect of exercise on liver fat: insights from animal studies. *J Nutr Metab* 2012: 827417.

Magnusson I, Rothman DL, Katz LD, Shulman RG, Shulman GI (1992). Increased rate of gluconeogenesis in type II diabetes mellitus. A 13C nuclear magnetic resonance study. *J Clin Invest* 90: 1323-7.

Maillard F, Rousset S, Pereira B, Traore A, de Pradel Del Amaze P, Boirie Y, Duclos M, Boisseau N (2016). High-intensity interval training reduces abdominal fat mass in postmenopausal women with type 2 diabetes. *Diabetes Metab* 42: 433-41.

Manabe Y, Gollisch KS, Holton L, Kim YB, Brandauer J, Fujii NL, Hirshman MF, Goodyear LJ (2013). Exercise training-induced adaptations associated with increases in skeletal muscle glycogen content. *FEBS J* 280: 916-26.

Marcinko K, Sikkema SR, Samaan MC, Kemp BE, Fullerton MD, Steinberg GR (2015). High intensity interval training improves liver and adipose tissue insulin sensitivity. *Mol Metab* 4: 903-15.

Mbata O, Abo El-Magd NF, El-Remessy AB (2017). Obesity, metabolic syndrome and diabetic retinopathy: Beyond hyperglycemia. *World J Diabetes* 8: 317-29.

Meigs JB, Cupples LA, Wilson PW (2000). Parental transmission of type 2 diabetes: the Framingham Offspring Study. *Diabetes* 49: 2201-7.

Methenitis S (2018). A brief review on concurrent training: from laboratory to the field. *Sports (Basel)* 6.

Michael LF, Wu Z, Cheatham RB, Puigserver P, Adelmant G, Lehman JJ, Kelly DP, Spiegelman BM (2001). Restoration of insulin-sensitive glucose transporter (GLUT4) gene expression in muscle cells by the transcriptional coactivator PGC-1. *Proc Natl Acad Sci U S A* 98: 3820-5.

Middelbeek RJ, Chambers MA, Tantiwong P, Treebak JT, An D, Hirshman MF, Musi N, Goodyear LJ (2013). Insulin stimulation regulates AS160 and TBC1D1 phosphorylation sites in human skeletal muscle. *Nutr Diabetes* 3: e74.

Miura T, Suzuki W, Ishihara E, Arai I, Ishida H, Seino Y, Tanigawa K (2001). Impairment of insulin-stimulated GLUT4 translocation in skeletal muscle and adipose tissue in the Tsumura Suzuki obese diabetic mouse: a new genetic animal model of type 2 diabetes. *Eur J Endocrinol* 145: 785-90.

Moltke I, Grarup N, Jorgensen ME, Bjerregaard P, Treebak JT, Fumagalli M, Korneliussen TS, Andersen MA, Nielsen TS, Krarup NT, Gjesing AP, Zierath JR, Linneberg A, Wu X, Sun G, Jin X, Al-Aama J, Wang J, Borch-Johnsen K, Pedersen O, Nielsen R, Albrechtsen A, Hansen T (2014). A common Greenlandic TBC1D4 variant confers muscle insulin resistance and type 2 diabetes. *Nature* 512: 190-3.

Montero D, Lundby C (2017). Refuting the myth of non-response to exercise training: 'non-responders' do respond to higher dose of training. *J Physiol* 595: 3377-87.

Mooradian AD (2009). Dyslipidemia in type 2 diabetes mellitus. *Nat Clin Pract Endocrinol Metab* 5: 150-9.

Mora-Rodriguez R, Ortega JF, Hamouti N, Fernandez-Elias VE, Canete Garcia-Prieto J, Guadalupe-Grau A, Saborido A, Martin-Garcia M, Guio de Prada V, Ara I, Martinez-Vizcaino V (2014). Time-course effects of aerobic interval training and detraining in patients with metabolic syndrome. *Nutr Metab Cardiovasc Dis* 24: 792-8.

Motiani P, Virtanen KA, Motiani KK, Eskelinen JJ, Middelbeek RJ, Goodyear LJ, Savolainen AM, Kemppainen J, Jensen J, Din MU, Saunavaara V, Parkkola R, Loyttyniemi E, Knuuti J, Nuutila P, Kalliokoski KK, Hannukainen JC (2017). Decreased insulin-stimulated brown adipose tissue glucose uptake after short-term exercise training in healthy middle-aged men. *Diabetes Obes Metab* 19: 1379-88.

Muoio DM, Newgard CB (2008). Mechanisms of disease: Molecular and metabolic mechanisms of insulin resistance and beta-cell failure in type 2 diabetes. *Nat Rev Mol Cell Biol* 9: 193-205.

Murakami T, Shimomura Y, Fujitsuka N, Sokabe M, Okamura K, Sakamoto S (1997). Enlargement glycogen store in rat liver and muscle by fructose-diet intake and exercise training. *J Appl Physiol (1985)* 82: 772-5.

Nalbandian M, Takeda M (2016). Lactate as a signaling molecule that regulates exercise-induced adaptations. *Biology (Basel)* 5: E38.

Nascimento NF, Hicks JA, Carlson KN, Hatzidis A, Amaral DN, Logan RW, Seggio JA (2016). Long-term wheel-running and acute 6-h advances alter glucose tolerance and insulin levels in TALLYHO/JngJ mice. *Chronobiol Int* 33: 108-16.

Nedergaard J, Bengtsson T, Cannon B (2007). Unexpected evidence for active brown adipose tissue in adult humans. *Am J Physiol Endocrinol Metab* 293: E444-52.

Nishida Y, Tokuyama K, Nagasaka S, Higaki Y, Shirai Y, Kiyonaga A, Shindo M, Kusaka I, Nakamura T, Ishibashi S, Tanaka H (2004). Effect of moderate exercise training on peripheral glucose effectiveness, insulin sensitivity, and endogenous glucose production in healthy humans estimated by a two-compartment-labeled minimal model. *Diabetes* 53: 315-20.

Nishiumi S, Ashida H (2007). Rapid preparation of a plasma membrane fraction from adipocytes and muscle cells: application to detection of translocated glucose transporter 4 on the plasma membrane. *Biosci Biotechnol Biochem* 71: 2343-6.

Ntanasis-Stathopoulos J, Tzanninis JG, Philippou A, Koutsilieris M (2013). Epigenetic regulation on gene expression induced by physical exercise. *J Musculoskelet Neuronal Interact* 13: 133-46.

Nybo L, Sundstrup E, Jakobsen MD, Mohr M, Hornstrup T, Simonsen L, Bulow J, Randers MB, Nielsen JJ, Aagaard P, Krustrup P (2010). High-intensity training versus traditional exercise interventions for promoting health. *Med Sci Sports Exerc* 42: 1951-8.

O'Neill HM (2013). AMPK and exercise: glucose uptake and insulin sensitivity. *Diabetes Metab J* 37: 1-21.

O'Neill HM, Maarbjerg SJ, Crane JD, Jeppesen J, Jorgensen SB, Schertzer JD, Shyroka O, Kiens B, van Denderen BJ, Tarnopolsky MA, Kemp BE, Richter EA, Steinberg GR (2011). AMP-activated protein kinase (AMPK) beta1beta2 muscle null mice reveal an essential role for AMPK in maintaining mitochondrial content and glucose uptake during exercise. *Proc Natl Acad Sci U S A* 108: 16092-7.

Olsen JM, Sato M, Dallner OS, Sandstrom AL, Pisani DF, Chambard JC, Amri EZ, Hutchinson DS, Bengtsson T (2014). Glucose uptake in brown fat cells is dependent on mTOR complex 2-promoted GLUT1 translocation. *J Cell Biol* 207: 365-74.

Ortlepp JR, Kluge R, Giesen K, Plum L, Radke P, Hanrath P, Joost HG (2000). A metabolic syndrome of hypertension, hyperinsulinaemia and hypercholesterolaemia in the New Zealand obese mouse. *Eur J Clin Invest* 30: 195-202.

Ostler JE, Maurya SK, Dials J, Roof SR, Devor ST, Ziolo MT, Periasamy M (2014). Effects of insulin resistance on skeletal muscle growth and exercise capacity in type 2 diabetic mouse models. *Am J Physiol Endocrinol Metab* 306: E592-605.

Peronnet F, Massicotte D (1991). Table of nonprotein respiratory quotient: an update. *Can J Sport Sci* 16: 23-29.

Pesta DH, Goncalves RLS, Madiraju AK, Strasser B, Sparks LM (2017). Resistance training to improve type 2 diabetes: working toward a prescription for the future. *Nutr Metab (Lond)* 14: 24.

Phielix E, Meex R, Ouwens DM, Sparks L, Hoeks J, Schaart G, Moonen-Kornips E, Hesselink MK, Schrauwen P (2012). High oxidative capacity due to chronic exercise training attenuates lipid-induced insulin resistance. *Diabetes* 61: 2472-8.

Prasad RB, Groop L (2015). Genetics of type 2 diabetes-pitfalls and possibilities. *Genes (Basel)* 6: 87-123.

Rajan S, Shankar K, Beg M, Varshney S, Gupta A, Srivastava A, Kumar D, Mishra RK, Hussain Z, Gayen JR, Gaikwad AN (2016). Chronic hyperinsulinemia reduces insulin sensitivity and metabolic functions of brown adipocyte. *J Endocrinol* 230: 275-90.

Reifsnyder PC, Churchill G, Leiter EH (2000). Maternal environment and genotype interact to establish diabesity in mice. *Genome Res* 10: 1568-78.

Reusch JE, Bridenstine M, Regensteiner JG (2013). Type 2 diabetes mellitus and exercise impairment. *Rev Endocr Metab Disord* 14: 77-86.

Richter EA, Hargreaves M (2013). Exercise, GLUT4, and skeletal muscle glucose uptake. *Physiol Rev* 93: 993-1017.

Ritchie IR, Wright DC, Dyck DJ (2014). Adiponectin is not required for exercise training-induced improvements in glucose and insulin tolerance in mice. *Physiol Rep* 2.

Roberts DJ, Miyamoto S (2015). Hexokinase II integrates energy metabolism and cellular protection: Akting on mitochondria and TORCing to autophagy. *Cell Death Differ* 22: 364.

Roden M (2012). Exercise in type 2 diabetes: to resist or to endure? *Diabetologia* 55: 1235-9.

Ruchat SM, Rankinen T, Weisnagel SJ, Rice T, Rao DC, Bergman RN, Bouchard C, Perusse L (2010). Improvements in glucose homeostasis in response to regular exercise are influenced by the PPARG Pro12Ala variant: results from the HERITAGE Family Study. *Diabetologia* 53: 679-89.

Rui L (2014). Energy metabolism in the liver. *Compr Physiol* 4: 177-97.

Rung J, Cauchi S, Albrechtsen A, Shen L, Rocheleau G, Cavalcanti-Proenca C, Bacot F, Balkau B, Belisle A, Borch-Johnsen K, Charpentier G, Dina C, Durand E, Elliott P, Hadjadj S, Jarvelin MR, Laitinen J, Lauritzen T, Marre M, Mazur A, Meyre D, Montpetit A, Pisinger C, Posner B, Poulsen P, Pouta A, Prentki M, Ribel-Madsen R, Ruokonen A, Sandbaek A, Serre D, Tichet J, Vaxillaire M, Wojtaszewski JF, Vaag A, Hansen T, Polychronakos C, Pedersen O, Froguel P, Sladek R (2009). Genetic variant near IRS1 is associated with type 2 diabetes, insulin resistance and hyperinsulinemia. *Nat Genet* 41: 1110-5.

Sakamoto K, Holman GD (2008). Emerging role for AS160/TBC1D4 and TBC1D1 in the regulation of GLUT4 traffic. *Am J Physiol Endocrinol Metab* 295: E29-37.

Samaan MC, Marcinko K, Sikkema S, Fullerton MD, Ziafazeli T, Khan MI, Steinberg GR (2014). Endurance interval training in obese mice reduces muscle inflammation and macrophage content independently of weight loss. *Physiol Rep* 2: E12012.

Samuel VT, Shulman GI (2012). Mechanisms for insulin resistance: common threads and missing links. *Cell* 148: 852-71.

Sanders FW, Griffin JL (2016). De novo lipogenesis in the liver in health and disease: more than just a shunting yard for glucose. *Biol Rev Camb Philos Soc* 91: 452-68.

Sano H, Kane S, Sano E, Miinea CP, Asara JM, Lane WS, Garner CW, Lienhard GE (2003). Insulin-stimulated phosphorylation of a Rab GTPase-activating protein regulates GLUT4 translocation. *J Biol Chem* 278: 14599-602.

Sattar N, McConnachie A, Shaper AG, Blauw GJ, Buckley BM, de Craen AJ, Ford I, Forouhi NG, Freeman DJ, Jukema JW, Lennon L, Macfarlane PW, Murphy MB, Packard CJ, Stott DJ, Westendorp RG, Whincup PH, Shepherd J, Wannamethee SG (2008). Can metabolic syndrome usefully predict cardiovascular disease and diabetes? Outcome data from two prospective studies. *Lancet* 371: 1927-35.

Schnurr TM, Springer C, Jørsboe E, Toska L, Dahl-Petersen IK, Grieß A, Carstensen B, Karpinski S, de Wendt C, Kristensen JM, Wojtaszewski JFP, Dille M, Bjerregaard P, Backes H, Brage S, Cremer AL, Brüning JC, Pedersen O, Hartwig S, Moltke I, Lehr S, Grarup N, Albrechtsen A, Chadt A, Jørgensen ME, Hansen T, Al-Hasani H. Physical activity can restore glucose tolerance in homozygous carriers of a muscle-specific TBC1D4 loss-of-function mutation. *Manuscript in preparation*.

Sennott J, Morrissey J, Standley PR, Broderick TL (2008). Treadmill exercise training fails to reverse defects in glucose, insulin and muscle GLUT4 content in the db/db mouse model of diabetes. *Pathophysiology* 15: 173-9.

Sharabi K, Tavares CD, Rines AK, Puigserver P (2015). Molecular pathophysiology of hepatic glucose production. *Mol Aspects Med* 46: 21-33.

Shearer J, Ross KD, Hughey CC, Johnsen VL, Hittel DS, Severson DL (2011). Exercise training does not correct abnormal cardiac glycogen accumulation in the db/db mouse model of type 2 diabetes. *Am J Physiol Endocrinol Metab* 301: E31-9.

Shephard RJ, Johnson N (2015). Effects of physical activity upon the liver. *Eur J Appl Physiol* 115: 1-46.

Smith U, Kahn BB (2016). Adipose tissue regulates insulin sensitivity: role of adipogenesis, de novo lipogenesis and novel lipids. *J Intern Med* 280: 465-75.

Softic S, Gupta MK, Wang GX, Fujisaka S, O'Neill BT, Rao TN, Willoughby J, Harbison C, Fitzgerald K, Ilkayeva O, Newgard CB, Cohen DE, Kahn CR (2017). Divergent effects of glucose and fructose on hepatic lipogenesis and insulin signaling. *J Clin Invest* 127: 4059-74.

Stanford KI, Middelbeek RJ, Goodyear LJ (2015). Exercise effects on white adipose tissue: beiging and metabolic adaptations. *Diabetes* 64: 2361-68.

Stanford KI, Middelbeek RJ, Townsend KL, An D, Nygaard EB, Hitchcox KM, Markan KR, Nakano K, Hirshman MF, Tseng YH, Goodyear LJ (2013). Brown adipose tissue regulates glucose homeostasis and insulin sensitivity. *J Clin Invest* 123: 215-23.

Stanford KI, Middelbeek RJ, Townsend KL, Lee MY, Takahashi H, So K, Hitchcox KM, Markan KR, Hellbach K, Hirshman MF, Tseng YH, Goodyear LJ (2015). A novel role for subcutaneous adipose tissue in exercise-induced improvements in glucose homeostasis. *Diabetes* 64: 2002-14.

Stark R, Kibbey RG (2014). The mitochondrial isoform of phosphoenolpyruvate carboxykinase (PEPCK-M) and glucose homeostasis: has it been overlooked? *Biochim Biophys Acta* 1840: 1313-30.

Stefan N, Thamer C, Staiger H, Machicao F, Machann J, Schick F, Venter C, Niess A, Laakso M, Fritsche A, Häring HU (2007). Genetic variations in PPARD and PPARGC1A determine mitochondrial function and change in aerobic physical fitness and insulin sensitivity during lifestyle intervention. *J Clin Endocrinol Metab* 92: 1827-33.

Stenmark H (2009). Rab GTPases as coordinators of vesicle traffic. *Nat Rev Mol Cell Biol* 10: 513-25.

Stephens NA, Brouwers B, Eroshkin AM, Yi F, Cornnell HH, Meyer C, Goodpaster BH, Pratley RE, Smith SR, Sparks LM (2018). Exercise response variations in skeletal muscle PCr recovery rate and insulin sensitivity relate to muscle epigenomic profiles in individuals with type 2 diabetes. *Diabetes Care* 41: 2245-54.

Stephens NA, Sparks LM (2015). Resistance to the beneficial effects of exercise in type 2 diabetes: are some individuals programmed to fail? *J Clin Endocrinol Metab* 100: 43-52.

Stephens NA, Xie H, Johannsen NM, Church TS, Smith SR, Sparks LM (2015). A transcriptional signature of "exercise resistance" in skeletal muscle of individuals with type 2 diabetes mellitus. *Metabolism* 64: 999-1004.

Stephenson EJ, Lessard SJ, Rivas DA, Watt MJ, Yaspelkis BB, 3rd, Koch LG, Britton SL, Hawley JA (2013). Exercise training enhances white adipose tissue metabolism in rats

selectively bred for low- or high-endurance running capacity. *Am J Physiol Endocrinol Metab* 305: E429-38.

Stern JH, Rutkowski JM, Scherer PE (2016). Adiponectin, leptin, and fatty acids in the maintenance of metabolic homeostasis through adipose tissue crosstalk. *Cell Metab* 23: 770-84.

Stoa EM, Meling S, Nyhus LK, Glenn S, Mangerud KM, Helgerud J, Bratland-Sanda S, Storen O (2017). High-intensity aerobic interval training improves aerobic fitness and HbA1c among persons diagnosed with type 2 diabetes. *Eur J Appl Physiol* 117: 455-67.

Stöckli J, Meoli CC, Hoffman NJ, Fazakerley DJ, Pant H, Cleasby ME, Ma X, Kleinert M, Brandon AE, Lopez JA, Cooney GJ, James DE (2015). The RabGAP TBC1D1 plays a central role in exercise-regulated glucose metabolism in skeletal muscle. *Diabetes* 64: 1914-22.

Stuart CA, Howell ME, Baker JD, Dykes RJ, Duffourc MM, Ramsey MW, Stone MH (2010). Cycle training increased GLUT4 and activation of mammalian target of rapamycin in fast twitch muscle fibers. *Med Sci Sports Exerc* 42: 96-106.

Suzuki Y, Lanner C, Kim JH, Vilardo PG, Zhang H, Yang J, Cooper LD, Steele M, Kennedy A, Bock CB, Scrimgeour A, Lawrence JCJ, DePaoli-Roach AA (2001). Insulin control of glycogen metabolism in knockout mice lacking the muscle-specific protein phosphatase PP1G/RGL. *Mol Cell Biol* 21: 2683-94.

Takagi S, Yamashita T, Miura T (2017). Does a treadmill running exercise contribute to preventing deterioration of bone mineral density and bone quality of the femur in KK-Ay mice, a type 2 diabetic animal model? *Calcif Tissue Int* 101: 631-40.

Thong FS, Bilan PJ, Klip A (2007). The Rab GTPase-activating protein AS160 integrates Akt, protein kinase C, and AMP-activated protein kinase signals regulating GLUT4 traffic. *Diabetes* 56: 414-23.

Trefts E, Williams AS, Wasserman DH (2015). Exercise and the regulation of hepatic metabolism. *Prog Mol Biol Transl Sci* 135: 203-25.

Trevellin E, Scorzeto M, Olivieri M, Granzotto M, Valerio A, Tedesco L, Fabris R, Serra R, Quarta M, Reggiani C, Nisoli E, Vettor R (2014). Exercise training induces mitochondrial biogenesis and glucose uptake in subcutaneous adipose tissue through eNOS-dependent mechanisms. *Diabetes* 63: 2800-11.

Tuomilehto J, Lindstrom J, Eriksson JG, Valle TT, Hamalainen H, Ilanne-Parikka P, Keinanen-Kiukaanniemi S, Laakso M, Louheranta A, Rastas M, Salminen V, Uusitupa M, Finnish Diabetes Prevention Study G (2001). Prevention of type 2 diabetes mellitus by changes in lifestyle among subjects with impaired glucose tolerance. *N Engl J Med* 344: 1343-50.

van der Heijden GJ, Wang ZJ, Chu ZD, Sauer PJ, Haymond MW, Rodriguez LM, Sunehag AL (2010). A 12-week aerobic exercise program reduces hepatic fat accumulation and insulin resistance in obese, Hispanic adolescents. *Obesity (Silver Spring)* 18: 384-90.

van der Windt DJ, Sud V, Zhang H, Tsung A, Huang H (2018). The effects of physical exercise on fatty liver disease. *Gene Expr* 18: 89-101.

van Dijk JW, Manders RJ, Tummers K, Bonomi AG, Stehouwer CD, Hartgens F, van Loon LJ (2012). Both resistance- and endurance-type exercise reduce the prevalence of

hyperglycaemia in individuals with impaired glucose tolerance and in insulin-treated and non-insulin-treated type 2 diabetic patients. *Diabetologia* 55: 1273-82.

Vogel H, Kamitz A, Hallahan N, Lebek S, Schallschmidt T, Jonas W, Jahnert M, Gottmann P, Zellner L, Kanzleiter T, Damen M, Altenhofen D, Burkhardt R, Renner S, Dahlhoff M, Wolf E, Muller TD, Bluher M, Joost HG, Chadt A, Al-Hasani H, Schürmann A (2018). A collective diabetes cross in combination with a computational framework to dissect the genetics of human obesity and Type 2 diabetes. *Hum Mol Genet* 27: 3099-112.

Vogel H, Mirhashemi F, Liehl B, Taugner F, Kluth O, Kluge R, Joost HG, Schürmann A (2013). Estrogen deficiency aggravates insulin resistance and induces beta-cell loss and diabetes in female New Zealand obese mice. *Horm Metab Res* 45: 430-5.

Voigt A, Katterle Y, Kahle M, Kluge R, Schürmann A, Joost HG, Klaus S (2015). Skeletal muscle mitochondrial uncoupling prevents diabetes but not obesity in NZO mice, a model for polygenic diabesity. *Genes Nutr* 10: 57.

Wang HY, Ducommun S, Quan C, Xie B, Li M, Wasserman DH, Sakamoto K, Mackintosh C, Chen S (2013). AS160 deficiency causes whole-body insulin resistance via composite effects in multiple tissues. *Biochem J* 449: 479-89.

Waterston RH, Lindblad-Toh K, Birney E, Rogers J, Abril JF, Agarwal P, Agarwala R, Ainscough R, Alexandersson M, An P, Antonarakis SE, Attwood J, Baertsch R, Bailey J, Barlow K, Beck S, Berry E, Birren B, Bloom T, Bork P, Botcherby M, Bray N, Brent MR, Brown DG, Brown SD, Bult C, Burton J, Butler J, Campbell RD, Carninci P, Cawley S, Chiaromonte F, Chinwalla AT, Church DM, Clamp M, Clee C, Collins FS, Cook LL, Copley RR, Coulson A, Couronne O, Cuff J, Curwen V, Cutts T, Daly M, David R, Davies J, Delehaunty KD, Deri J, Dermitzakis ET, et al. (2002). Initial sequencing and comparative analysis of the mouse genome. *Nature* 420: 520-62.

Watson RT, Pessin JE (2001). Intracellular organization of insulin signaling and GLUT4 translocation. *Recent Prog Horm Res* 56: 175-93.

Watt MJ, Hoy AJ (2012). Lipid metabolism in skeletal muscle: generation of adaptive and maladaptive intracellular signals for cellular function. *Am J Physiol Endocrinol Metab* 302: E1315-28.

Wilcox G (2005). Insulin and insulin resistance. *Clin Biochem Rev* 26: 19-39.

Xie B, Chen Q, Chen L, Sheng Y, Wang HY, Chen S (2016). The inactivation of RabGAP function of AS160 promotes lysosomal degradation of GLUT4 and causes postprandial hyperglycemia and hyperinsulinemia. *Diabetes* 65: 3327-40.

Xu A, Wang Y, Keshaw H, Xu LY, Lam KS, Cooper GJ (2003). The fat-derived hormone adiponectin alleviates alcoholic and nonalcoholic fatty liver diseases in mice. *J Clin Invest* 112: 91-100.

Xu X, Ying Z, Cai M, Xu Z, Li Y, Jiang SY, Tzan K, Wang A, Parthasarathy S, He G, Rajagopalan S, Sun Q (2011). Exercise ameliorates high-fat diet-induced metabolic and vascular dysfunction, and increases adipocyte progenitor cell population in brown adipose tissue. *Am J Physiol Regul Integr Comp Physiol* 300: R1115-25.

Yoon A, Tammen SA, Park S, Han SN, Choi SW (2017). Genome-wide hepatic DNA methylation changes in high-fat diet-induced obese mice. *Nutr Res Pract* 11: 105-13.

Zhang J, Liu F (2014). Tissue-specific insulin signaling in the regulation of metabolism and aging. *IUBMB Life* 66: 485-95.

5.2 Additional references

Crepcia-Pevzner A (2017). Analysis of the training effect on the browning in subcutaneous white adipose tissue in mice and humans. *Master thesis.* Heinrich-Heine Universität Düsseldorf.

Fox JG, Davisson MT, Quimby FW, Barthold SW, Newcomer CE, Smith AL (2006). The Mouse in Biomedical Research: Normative Biology, Husbandry, and Models. Academic Press, 2nd edition, 816 pp.

Grieß-Osowski A (2018). Analysis of glucose and lipid metabolism in insulin-responsive tissues of *Tbc1d1/Tbc1d4*-deficient mice on high-fat diet with training intervention. *Master thesis.* Heinrich-Heine Universität Düsseldorf.

International Diabetes Federation (2017). IDF Diabetes Atlas, 8th edition. Brussels, Belgium. *Online*: http://www.diabetesatlas.org

Joost HG, Al-Hasani H, Schürmann A (2012). Animal Models in Diabetes Research. Humana Press, 325 pp.

Karpinski S (2014). Impact of physical activity on the metabolism of a mouse model with altered substrate utilization. *Master thesis*. Heinrich-Heine Universität Düsseldorf.

Köbberling J, Tillil H (1982). Empirical risk figures for first degree relatives of non-insulin dependent diabetics. *In*: The Genetics of Diabetes Mellitus (editors: Köbberling J, Tattersall R). Academic Press, pp. 201-209.

Manore M, Meyer NL, Thompson J (2009). Sport Nutrition for Health and Performance. Human Kinetics, 2nd edition, 542 pp.

Schallschmidt T (2018). Identification of novel susceptibility genes for diabetes-related traits in a backcross of obese NZO with lean C3H mice. *Dissertation*. Heinrich-Heine Universität Düsseldorf.

World Health Organization (2016). Global Report on Diabetes. *Online:* http://www.who.int/iris/handle/10665/204871

World Health Organization (2018). Obesity and overweight. *Online:* http://www.who.int/news-room/fact-sheets/detail/obesity-and-overweight

6. Supplement

6.1 Contribution to manuscripts

1) Chadt A, Immisch A, de Wendt C, **Springer C**, Zhou Z, Stermann T, Holman GD, Loffing-Cueni D, Loffing J, Joost HG, Al-Hasani H (2015). Deletion of both Rab-GTPase-activating proteins TBC1D1 and TBC1D4 in mice eliminates insulin- and AICAR-stimulated glucose transport [corrected]. *Diabetes* 64: 746-59.

Contribution: Measurement and analysis of plasma lipids (Supplemental Figure 3) was performed by myself.

In addition, parts of the present thesis are included in the following manuscripts to whom I have contributed significantly:

2) Görgens SW, Benninghoff T, Eckardt K, **Springer C**, Chadt A, Melior A, Wefers J, Cramer A, Jensen J, Birkeland KI, Drevon CA, Al-Hasani H, Eckel J (2017). Hypoxia in combination with muscle contraction improves insulin action and glucose metabolism in human skeletal muscle via the HIF-1α pathway. *Diabetes* 66: 2800-2807.

Contribution: The treadmill training of the mice used for this publication was performed by myself. *Gastrocnemius* muscle of sedentary and trained mice was used for the generation of the following figures: Figure 3 H - J and Figure 4 I - K. In addition, I drafted the respective method section (mice exercise study), which therefore exhibits similar or identical wording to the following parts of the methods section of the present thesis: *Treadmill training (2.2.2.2)* and *Dissection of animal tissues (2.2.2.12).*

3) Schnurr TM, **Springer C**, Jørsboe E, Toska L, Dahl-Petersen IK, Grieß A, Carstensen B, Karpinski S, de Wendt C, Kristensen JM, Wojtaszewski JFP, Dille M, Bjerregaard P, Backes H, Brage S, Cremer AL, Brüning JC, Pedersen O, Hartwig S, Moltke I, Lehr S, Grarup N, Albrechtsen A, Chadt A, Jørgensen ME, Hansen T, Al-Hasani H. Physical activity can restore glucose tolerance in homozygous carriers of a muscle-specific TBC1D4 loss-of-function mutation. *Manuscript in preparation*.

Contribution: Shared first author (Schnurr, Springer and Jørsboe). The main findings of the D4KO results are part of this manuscript. The animal experiments were performed in large parts by myself, and in part with the help of collaborators. Furthermore, I analysed and interpreted the animal data. For the manuscript, the following figures from the present thesis were adapted: *Figure 7 - 10, Figure 11 A, Figure 14 - 18 and Figure S1*. In addition, large parts

of the animal methods section were written by myself. Therefore, passages of the manuscript exhibit similar or identical wording to the following parts of the methods section of the present thesis: *General animal housing (2.2.2.1), Treadmill training (2.2.2.2), Physical capacity test* (*2.2.2.3)*, *Body composition (2.2.2.5)*, *Blood lactate measurement (*2.2.2.7) and *Statistical analysis (2.2.5)*.

6.2 Abbreviations

2-DOG	[^{3}H]-2-deoxyglucose
a.u.	arbitrary unit
ACLY	ATP-citrate lyase
ADA	American Diabetes Association
AICAR	5'-aminoimidazole-4-carboxyamide-ribonucleoside
AKT	Protein kinase B
AMP	Adenosine monophosphate
AMPK	5'-AMP-activated protein kinase
ANOVA	Analysis of variance
APS	Ammonium persulfate
Arg	Arginine
ATP	Adenosine triphosphate
AUC	Area under curve
B6	C57BL/6J mice
BAT	Brown adipose tissue
BCA	Bicinchoninic acid
BMI	Body mass index
BSA	Bovine serum albumin
Ca^{2+}	Calcium
$CaCl_2$	Calcium chloride
cal	calories
CBD	Calmodulin-binding domain
CD36	Cluster of differentiation 36
cDNA	complementary DNA
CHO	Carbohydrate oxidation
Ci	Curie
CO_2	Carbon dioxide
CoA	Coenzyme A
cpm	counts per minutes
CPT	Palmitoyl-CoA transferase
Ct	Amplification threshold
D1KO	*Tbc1d1*-knockout mice
D4KO	*Tbc1d4*-knockout mice
ddH_2O	*aqua purificata*
DDZ	Deutsches Diabetes-Zentrum (German Diabetes Center)

DNA	Deoxyribonucleic acid
DNL	*de novo* lipogenesis
dNTP	deoxynucleoside triphosphate
DTT	Dithiothreitol
ECL	Enhanced Chemiluminescence
EDL	*Extensor digitorum longus*
EDTA	Ethylenediaminetetraacetic acid
EGTA	Ethylene glycol bis(2-aminoethylether)-N, N, N', N'-tetra acetic acid
ELISA	Enzyme-linked immunosorbent assay
eNOS	endothelial nitric oxide synthase
ER	Endoplasmic reticulum
EtOH	Ehtanol
FAO	Fatty acid oxidation
FASN	Fatty acid synthase
FAT/CD36	Fatty acid translocase
FATP	Fatty acid transport protein
FBG	Fasting blood glucose
FPI	Fasting plasma insulin
FTO	Fat mass and obesity-associated protein
Fwd	Forward
G1P	Glucose-1-phosphate
G6P	Glucose-6-phosphate
GAP	GTPase-activating protein
GAPDH	Glyceraldehyde 3-phosphate dehydrogenase
GCK	Glucokinase
GDP	Guanosine diphosphate
GEF	Guanine nucleotide exchange factor
GLUT	Glucose transporter
GS	Glycogen synthase
GTP	Guanosine triphosphate
GTT	Glucose tolerance test
GWAs	Genome-wide association studies
HCl	Hydrochloric acid
HDAC	Histone deacetylase
HEPES	4-(2-hydroxyethyl)-1-piperazineethanesulfonic acid
HFD	High-fat diet

HFD-RS	High-fat diet with reduced sucrose content
HIT	High-intensity training
HK	Hexokinase
HRP	Horse radish-peroxidase
i.p.	intraperitoneal
IDF	International Diabetes Federation
IgG	Immunoglobulin G
IMCL	Intramyocellular lipids
IR	Insulin receptor
IRS	Insulin receptor substrate
ITT	Insulin tolerance test
KCl	Potassium chloride
kDa	kilodaltons
KH_2PO_4	Potassium dihydrogen phosphate
KHB	Krebs-Henseleit buffer
KO	Knockout
KOH	Potassium hydroxide
KRBH	Krebs-Ringer-Bicarbonate HEPES
LSB	Laemmli sample buffer
MeDIP	Methylated DNA immunoprecipitation
MEF-2	Myocyte enhancer factor 2
$MgSO_4$	Magnesium sulfate
MODY	Maturity-onset diabetes of the young
mRNA	messenger RNA
Na_2SO_4	Sodium sulfate
NaCl	Sodium chloride
NADH	Nicotinamide adenine dinucleotide hydrogen
$NaHCO_3$	Sodium hydrogen carbonate
ND	Non-diabetic NZO subgroup
NDUFB6	NADH dehydrogenase (ubiquinone) 1 beta subcomplex 6
NEFA	Non-esterified free fatty acids
NMR	Nuclear magnetic resonance
Nob1	New Zealand obese 1
NZB	New Zealand Black
NZO	New Zealand Obese
O_2	Oxygen

OAA	Oxaloacetate
PAGE	Polyacrylamide gel electrophoresis
PCK	Phosphoenolpyruvate carboxylase
PCR	Polymerase chain reaction
PI3K	Phosphatidylinositol-3-kinase
PGC-1α	Peroxisome proliferator-activated receptor γ coactivator-1α
PPAR-α	Peroxisome proliferator-activated receptor-α
PPAR-δ	Peroxisome proliferator-activated receptor-δ
PTB	Phosphotyrosine-binding
PVDF	Polyvinylidene difluoride
qPCR	Quantitative Real-Time PCR
Rab	Ras-related in brain
RCS	Recombinant congenic strain
RER	Respiratory exchange ratio
Rev	Reverse
RM-ANOVA	Repeated measurements ANOVA
RNA	Ribonucleic acid
RT	Room temperature
SCD1	Stearoyl-CoA desaturase 1
scWAT	subcutaneous white adipose tissue
SD	Standard diet
SDS	Sodium dodecyl sulfate
SEM	Standard error of the mean
Ser	Serine
SJL	Swiss Jim Lambert mice
T1DM	Type 1 diabetes mellitus
T2D	Diabetic NZO subgroup
T2DM	Type 2 diabetes mellitus
TBC1D1	Tre-2/USP6, BUB2, Cdc16 Domain Family, Member 1
TBC1D4	Tre-2/USP6, BUB2, Cdc16 Domain Family, Member 4
TBS-T	Tris-buffered saline-Tween 20
TCA	Citric acid cycle
TEMED	N, N, N’, N’-Tetramethylendiamine
Ter	Termination codon
TG	Triglycerides
Thr	Threonine

TMB	3, 3', 5, 5'-tetramethylbenzidine
Tris	Tris(hydroxymethyl)aminomethane
UCP-1	Uncoupling protein 1
UDP	Uridine diphosphate
VO_{2max}	Maximal oxygen consumption
WAT	White adipose tissue
WHO	World Health Organization
WT	Wildtype

6.3 Supplemental Tables

Table S1: Treadmill training protocol used for D4KO mice. Left column indicates respective week of training. Inclination of the treadmill was set at constant 5° inclination or was increased to 10° within the exercise session (marked in bold). The physical capacity tests were performed instead of a regular exercise bout and mice did not perform training at days of measuring i.p. GTT or i.p. ITT.

Week 1	**Day**	**Mon**	**Tue**	**Wed**	**Thu**	**Fri**
	Warm-up	5 min 6-7 m/min	5 min 6-9 m/min		5 min 6-9 m/min	5 min 6-9 m/min
	Training	5 min 7 m/min	5 min 9-10 m/min 10 min 10 m/min	**Physical capacity test**	5 min 9-10 m/min 5 min 10 m/min 5 min 10-12 m/min 10 min 12 m/min	5 min 9-10 m/min 5 min 10 m/min 5 min 10-12 m/min 10 min 12 m/min
	Duration	10 min	20 min		30 min	30 min
Week 2	**Day**	**Mon**	**Tue**	**Wed**	**Thu**	**Fri**
	Warm-up	5 min 6-10 m/min	5 min 6-10 m/min	5 min 6-10 m/min	5 min 6-10 m/min	5 min 6-10 m/min
	Training	5 min 10 m/min 5 min 10-12 m/min 10 min 12 m/min 5 min 12-15 m/min 5 min 15 m/min	5 min 10 m/min 5 min 10-12 m/min 10 min 12 m/min 5 min 12-15 m/min 5 min 15 m/min	5 min 10 m/min 5 min 10-12 m/min 10 min 12 m/min 5 min 12-15 m/min 10 min 15 m/min	5 min 10 m/min 5 min 10-12 m/min 10 min 12 m/min 5 min 12-15 m/min **10 min 15 m/min**	5 min 10 m/min 5 min 10-12 m/min 10 min 12-13 m/min 5 min 13 m/min **5 min 13-15 m/min** **10 min 15 m/min**
	Duration	35 min	35 min	40 min	40 min	45 min
Week 3	**Day**	**Mon**	**Tue**	**Wed**	**Thu**	**Fri**
	Warm-up	5 min 6-10 m/min	5 min 6-10 m/min	5 min 6-10 m/min	5 min 6-10 m/min	5 min 6-10 m/min
	Training	5 min 10 m/min 5 min 10-12 m/min 10 min 12-13 m/min 5 min 13 m/min **5 min 13-15 m/min** **10 min 15 m/min**	5 min 10 m/min 5 min 10-12 m/min 10 min 12-13 m/min 5 min 13 m/min **5 min 13-15 m/min** **10 min 15 m/min** **5 min 15-18 m/min**	5 min 10 m/min 5 min 10-12 m/min 10 min 12-13 m/min 5 min 13 m/min **5 min 13-15 m/min** **10 min 15 m/min** **5 min 15-18 m/min**	5 min 10 m/min 5 min 10-12 m/min 10 min 12-13 m/min 5 min 13 m/min **5 min 13-15 m/min** **10 min 15 m/min** **5 min 15-18 m/min** **5 min 18 m/min**	5 min 10 m/min 5 min 10-12 m/min 10 min 12-13 m/min 5 min 13 m/min **5 min 13-15 m/min** **10 min 15 m/min** **5 min 15-18 m/min** **5 min 18 m/min**
	Duration	45 min	50 min	50 min	55 min	55 min
Week 4	**Day**	**Mon**	**Tue**	**Wed**	**Thu**	**Fri**
	Warm-up	5 min 6-10 m/min	5 min 6-10 m/min		5 min 6-10 m/min	
	Training	5 min 10 m/min 5 min 10-12 m/min 10 min 12-13 m/min 5 min 13 m/min **5 min 13-15 m/min** **10 min 15 m/min** **5 min 15-18 m/min** **5 min 18 m/min**	5 min 10 m/min 5 min 10-12 m/min 10 min 12-13 m/min 5 min 13 m/min **5 min 13-15 m/min** **10 min 15 m/min** **5 min 15-18 m/min** **10 min 18 m/min**	**i.p. GTT/ i.p. ITT**	5 min 10 m/min 5 min 10-12 m/min 10 min 12-13 m/min 5 min 13 m/min **5 min 13-15 m/min** **10 min 15 m/min** **5 min 15-18 m/min** **10 min 18 m/min**	**Physical capacity test**
	Duration	55 min	60 min		60 min	
Week 5	**Day**	**Mon**	**Tue**			
	Warm-up	5 min 6-10 m/min				
	Training	5 min 10 m/min 5 min 10-12 m/min 10 min 12-13 m/min 5 min 13 m/min **5 min 13-15 m/min** **10 min 15 m/min** **5 min 15-18 m/min** **10 min 18 m/min**	***Ex vivo* glucose uptake/ Tissue harvest**			
	Duration	60 min				

Table S2: Treadmill interval training protocol used for B6 mice. Left column indicates respective week of training. Inclination of the treadmill was set at constant 5°. From week 3 on, the protocol consisted of alternating 5-minutes intervals with moderate to high (15, 18 m/min) or low running intensity (10 m/min). The physical capacity tests were performed instead of a regular exercise bout and mice did not perform training at days of measuring i.p. GTT.

Week 1	**Day**	**Mon**	**Tue**	**Wed**	**Thu**	**Fri**
	Warm-up	5 min 6-9 m/min	5 min 6-9 m/min		5 min 6-9 m/min	5 min 6-9 m/min
	Training	5 min 9-10 m/min 10 min 10 m/min	5 min 9-10 m/min 5 min 10 m/min 5 min 10-12 m/min 10 min 12 m/min	**Physical capacity test**	5 min 9-10 m/min 10 min 10-13 m/min 10 min 13 m/min 5 min 13-15 m/min	5 min 9-10 m/min 10 min 10-13 m/min 10 min 13-15 m/min 5 min 15 m/min
	Duration	20 min	30 min		35 min	35 min
Week 2	**Day**	**Mon**	**Tue**	**Wed**	**Thu**	**Fri**
	Warm-up	5 min 6-9 m/min	5 min 6-9 m/min	5 min 6-10 m/min	5 min 6-10 m/min	5 min 6-10 m/min
	Training	5 min 9-10 m/min 10 min 10-13 m/min 10 min 13-15 m/min 5 min 15 m/min	5 min 9-10 m/min 10 min 10-13 m/min 5 min 13-15 m/min 10 min 15 m/min	3 min 9-10 m/min 3 min 10-13 m/min 2 min 13-15 m/min 10 min 15 m/min 5 min 15-18 m/min 10 min 18 m/min	3 min 9-10 m/min 3 min 10-13 m/min 2 min 13-15 m/min 10 min 15 m/min 5 min 15-18 m/min 10 min 18 m/min	3 min 9-10 m/min 3 min 10-13 m/min 2 min 13-15 m/min 10 min 15 m/min 5 min 15-18 m/min 10 min 18 m/min
	Duration	35 min	35 min	38 min	38 min	38 min
Week 3	**Day**	**Mon**	**Tue**	**Wed**	**Thu**	**Fri**
	Warm-up	5 min 6-10 m/min	5 min 6-10 m/min	5 min 6-10 m/min	5 min 6-10 m/min	5 min 6-10 m/min
	Training	5 min 15 m/min 5 min 10 m/min **(2x)** 5 min 18 m/min 5 min 10 m/min 5 min 18 m/min	5 min 15 m/min 5 min 10 m/min **(3x)** 5 min 18 m/min 5 min 10 m/min **(3x)**	5 min 15 m/min 5 min 10 m/min **(3x)** 5 min 18 m/min 5 min 10 m/min **(3x)**	5 min 15 m/min 5 min 10 m/min **(3x)** 5 min 18 m/min 5 min 10 m/min **(3x)**	5 min 15 m/min 5 min 10 m/min **(3x)** 5 min 18 m/min 5 min 10 m/min **(3x)**
	Duration	40 min	65 min	65 min	65 min	65 min
Week 4	**Day**	**Mon**	**Tue**	**Wed**	**Thu**	**Fri**
	Warm-up	5 min 6-10 m/min	5 min 6-10 m/min	5 min 6-10 m/min	5 min 6-10 m/min	5 min 6-10 m/min
	Training	5 min 15 m/min 5 min 10 m/min **(3x)** 5 min 18 m/min 5 min 10 m/min **(3x)**	5 min 15 m/min 5 min 10 m/min **(2x)** 5 min 18 m/min 5 min 10 m/min **(4x)**	5 min 15 m/min 5 min 10 m/min **(2x)** 5 min 18 m/min 5 min 10 m/min **(4x)**	5 min 15 m/min 5 min 10 m/min **(2x)** 5 min 18 m/min 5 min 10 m/min **(4x)**	5 min 15 m/min 5 min 10 m/min **(1x)** 5 min 18 m/min 5 min 10 m/min **(5x)**
	Duration	65 min	65 min	65 min	65 min	65 min
Week 5	**Day**	**Mon**	**Tue**	**Wed**	**Thu**	**Fri**
	Warm-up	5 min 6-10 m/min	5 min 6-10 m/min	5 min 6-10 m/min	5 min 6-10 m/min	5 min 6-10 m/min
	Training	5 min 15 m/min 5 min 10 m/min **(1x)** 5 min 18 m/min 5 min 10 m/min **(5x)**	5 min 15 m/min 5 min 10 m/min **(1x)** 5 min 18 m/min 5 min 10 m/min **(5x)**	5 min 15 m/min 5 min 10 m/min **(1x)** 5 min 18 m/min 5 min 10 m/min **(5x)**	5 min 15 m/min 5 min 10 m/min **(1x)** 5 min 18 m/min 5 min 10 m/min **(5x)**	5 min 15 m/min 5 min 10 m/min **(1x)** 5 min 18 m/min 5 min 10 m/min **(5x)**
	Duration	65 min	65 min	65 min	65 min	65 min
Week 6	**Day**	**Mon**	**Tue**	**Wed**	**Thu**	**Fri**
	Warm-up	5 min 6-10 m/min	5 min 6-10 m/min		5 min 6-10 m/min	
	Training	5 min 15 m/min 5 min 10 m/min **(1x)** 5 min 18 m/min 5 min 10 m/min **(5x)**	5 min 15 m/min 5 min 10 m/min **(1x)** 5 min 18 m/min 5 min 10 m/min **(5x)**	**i.p. GTT**	5 min 15 m/min 5 min 10 m/min **(1x)** 5 min 18 m/min 5 min 10 m/min **(5x)**	**Physical capacity test**
	Duration	65 min	65 min		65 min	
Week 7	**Day**	**Mon**	**Tue**	**Wed**		
	Warm-up	5 min 6-10 m/min	5 min 6-10 m/min			
	Training	5 min 15 m/min 5 min 10 m/min **(1x)** 5 min 18 m/min 5 min 10 m/min **(5x)**	5 min 15 m/min 5 min 10 m/min **(1x)** 5 min 18 m/min 5 min 10 m/min **(5x)**	**Tissue harvest**		
	Duration	65 min	65 min			

Table S3: Treadmill interval training protocol used for NZO mice fed a 30 % HFD-RS. Left column indicates respective week of training. Inclination of the treadmill was set at constant 5°. From week 2 on, the protocol consisted of alternating 5-minutes intervals with moderate to high (13, 15, 18 m/min) or low running intensity (10 m/min). The physical capacity tests were performed instead of a regular exercise bout and mice did not perform training at days of measuring i.p. GTT or i.p. ITT.

Week 1	**Day**	**Mon**	**Tue**	**Wed**	**Thu**	**Fri**
	Warm-up	5 min 6-9 m/min	5 min 6-9 m/min	5 min 6-10 m/min	5 min 6-10 m/min	
	Training		5 min 9-10 m/min 5 min 10 m/min	5 min 10 m/min 5 min 12 m/min **(2x)**	5 min 10 m/min 5 min 12 m/min **(2x)**	**Physical capacity test**
	Duration	5 min	15 min	25 min	25 min	
Week 2	**Day**	**Mon**	**Tue**	**Wed**	**Thu**	**Fri**
	Warm-up	5 min 6-10 m/min	5 min 6-10 m/min	5 min 6-10 m/min	5 min 6-10 m/min	5 min 6-10 m/min
	Training	5 min 12 m/min 5 min 10 m/min 5 min 13 m/min 5 min 10 m/min 5 min 15 m/min	5 min 12 m/min 5 min 10 m/min 5 min 13 m/min 5 min 10 m/min **5 min 15 m/min** **5 min 10 m/min** **(2x)**	5 min 12 m/min 5 min 10 m/min 5 min 13 m/min 5 min 10 m/min **5 min 15 m/min** **5 min 10 m/min** **(2x)**	5 min 12 m/min 5 min 10 m/min **5 min 15 m/min** **5 min 10 m/min** **(2x)** 5 min 13 m/min 5 min 10 m/min 5 min 18 m/min	5 min 12 m/min 5 min 10 m/min **5 min 15 m/min** **5 min 10 m/min** **(2x)** 5 min 13 m/min 5 min 10 m/min 5 min 18 m/min
	Duration	30 min	45 min	45 min	50 min	50 min
Week 3	**Day**	**Mon**	**Tue**	**Wed**	**Thu**	**Fri**
	Warm-up	5 min 6-10 m/min	5 min 6-10 m/min	5 min 6-10 m/min	5 min 6-10 m/min	5 min 6-10 m/min
	Training	5 min 13 m/min 5 min 10 m/min 5 min 15 m/min 5 min 10 m/min 5 min 18 m/min **(2x)**	5 min 13 m/min 5 min 10 m/min 5 min 15 m/min 5 min 10 m/min 5 min 18 m/min **(2x)**	5 min 13 m/min 5 min 10 m/min 5 min 15 m/min 5 min 10 m/min 5 min 18 m/min **(2x)**	5 min 13 m/min 5 min 10 m/min 5 min 15 m/min 5 min 10 m/min 5 min 18 m/min **(2x)**	5 min 13 m/min 5 min 10 m/min 5 min 15 m/min 5 min 10 m/min 5 min 18 m/min **(2x)**
	Duration	60 min	60 min	60 min	60 min	60 min
Week 4	**Day**	**Mon**	**Tue**	**Wed**	**Thu**	**Fri**
	Warm-up	5 min 6-10 m/min	5 min 6-10 m/min	5 min 6-10 m/min	5 min 6-10 m/min	5 min 6-10 m/min
	Training	5 min 13 m/min 5 min 10 m/min **5 min 15 m/min** **5 min 10 m/min** **(3x)** 5 min 18 m/min 5 min 10 m/min **(2x)**	5 min 13 m/min 5 min 10 m/min **5 min 15 m/min** **5 min 10 m/min** **(3x)** 5 min 18 m/min 5 min 10 m/min **(2x)**	5 min 13 m/min 5 min 10 m/min **5 min 15 m/min** **5 min 10 m/min** **(3x)** 5 min 18 m/min 5 min 10 m/min **(2x)**	5 min 13 m/min 5 min 10 m/min **5 min 15 m/min** **5 min 10 m/min** **(3x)** 5 min 18 m/min 5 min 10 m/min **(2x)**	5 min 13 m/min 5 min 10 m/min **5 min 15 m/min** **5 min 10 m/min** **(3x)** 5 min 18 m/min 5 min 10 m/min **(2x)**
	Duration	65 min	65 min	65 min	65 min	65 min
Week 5	**Day**	**Mon**	**Tue**	**Wed**	**Thu**	**Fri**
	Warm-up	5 min 6-10 m/min	5 min 6-10 m/min		5 min 6-10 m/min	5 min 6-10 m/min
	Training	5 min 15 m/min 5 min 10 m/min **(3x)** 5 min 18 m/min 5 min 10 m/min **(3x)**	5 min 15 m/min 5 min 10 m/min **(3x)** 5 min 18 m/min 5 min 10 m/min **(3x)**	**i.p. ITT**	5 min 15 m/min 5 min 10 m/min **(3x)** 5 min 18 m/min 5 min 10 m/min **(3x)**	5 min 15 m/min 5 min 10 m/min **(3x)** 5 min 18 m/min 5 min 10 m/min **(3x)**
	Duration	65 min	65 min	65 min	65 min	65 min
Week 6	**Day**	**Mon**	**Tue**	**Wed**	**Thu**	**Fri**
	Warm-up	5 min 6-10 m/min	5 min 6-10 m/min		5 min 6-10 m/min	
	Training	5 min 15 m/min 5 min 10 m/min **(2x)** 5 min 18 m/min 5 min 10 m/min **(4x)**	5 min 15 m/min 5 min 10 m/min **(2x)** 5 min 18 m/min 5 min 10 m/min **(4x)**	**i.p. GTT**	5 min 15 m/min 5 min 10 m/min **(2x)** 5 min 18 m/min 5 min 10 m/min **(4x)**	**Physical capacity test**
	Duration	65 min	65 min		65 min	
Week 7	**Day**	**Mon**	**Tue**	**Wed**		
	Warm-up	5 min 6-10 m/min	5 min 6-10 m/min			
	Training	5 min 15 m/min 5 min 10 m/min **(2x)** 5 min 18 m/min 5 min 10 m/min **(4x)**	5 min 15 m/min 5 min 10 m/min **(2x)** 5 min 18 m/min 5 min 10 m/min **(4x)**	***Ex vivo* glucose uptake/ Tissue harvest**		
	Duration	65 min	65 min			

Table S4: Whole-body energy expenditure of WT and D4KO mice measured by indirect calorimetry.

Parameter	WT Sedentary	WT Trained	D4KO Sedentary	D4KO Trained
RER average (VCO_2/VO_2)	0.789 ± 0.006	0.780 ± 0.005	0.790 ± 0.006	0.784 ± 0.007
Voluntary activity (x/y-total beam breaks)	414.6 ± 95.2	516.4 ± 84.6	396 ± 85.4	463.5 ± 105.6
VO_2 average ($ml/min/kg^{0.75}$)	22.1 ± 0.5	20.9 ± 0.5	**20 ± 0.6#**	21.5 ± 0.8
Food Intake (kcal/g body weight)	0.77 ± 0.08	0.65 ± 0.05	0.67 ± 0.05	0.73 ± 0.08

Data are presented as mean ± SEM (n = 7-8). Data were analysed using two-way ANOVA with Bonferroni's multiple comparisons test. #, $p < 0.05$ D4KO vs respective WT group.

Table S5: Body composition, plasma parameters and RER of NZO mice fed a SD after six weeks of chronic interval training.

Parameter	Sedentary	Trained
Body weight (g)	42.2 ± 1.0	40.0 ± 1.5
Fat mass (g)	12.8 ± 0.8	12.1 ± 0.9
Lean mass (g)	27.2 ± 0.5	**25.2 ± 0.7 ***
FBG (mg/dl)	84.8 ± 5.7	74.3 ± 4.5
FPI (ng/ml)	1.4 ± 0.2	2.2 ± 0.4
RER (VCO_2/VO_2)	0.83 ± 0.02	0.80 ± 0.02

Data are presented as mean ± SEM (n = 5-8). Data were analysed using unpaired student's t-test. *, $p < 0.05$ sedentary vs. trained.

6.4 Supplemental Figures

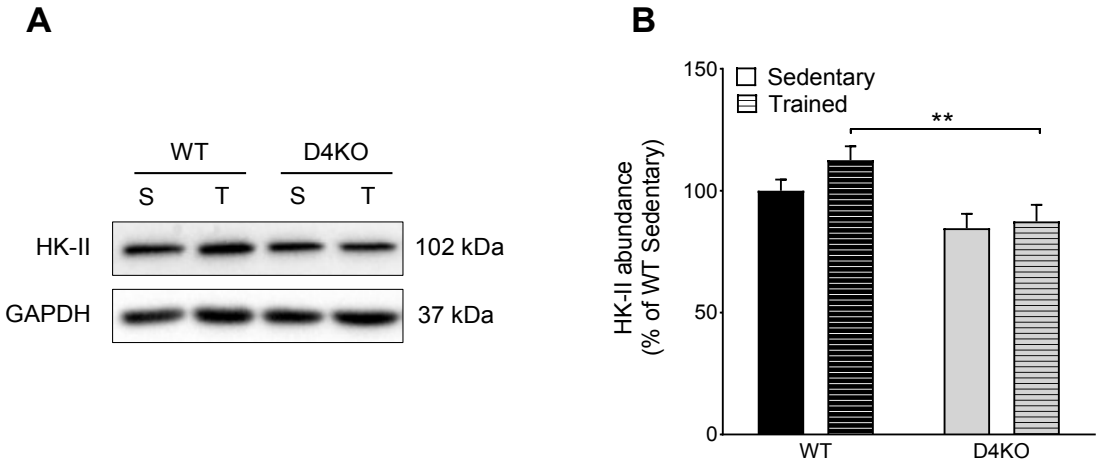

Figure S1: Protein abundance of HK-II in skeletal muscle of WT and D4KO mice. Representative Western Blot of HK-II (**A**) and quantification of HK-II (**B**) in *Soleus* muscle of WT and D4KO mice. Protein abundance was normalized to GAPDH and given as percentage of the WT sedentary group. Data are presented as mean ± SEM (n = 7-9). Data were analysed using two-way ANOVA with Bonferroni's multiple comparisons test. **, $p < 0.01$ between indicated groups. S, sedentary; T; trained.

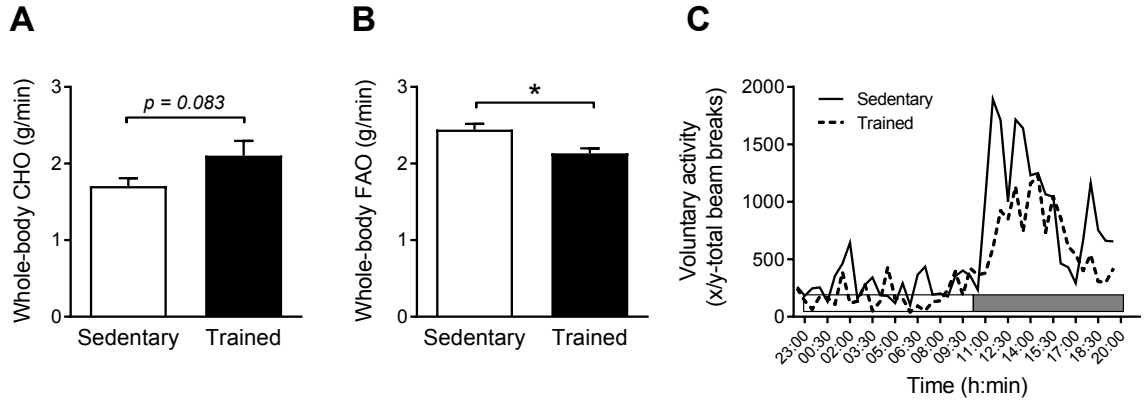

Figure S2: Whole-body CHO, FAO and voluntary activity of B6 mice after chronic interval training. Whole-body CHO (**A**), whole-body FAO (**B**) and voluntary activity (**C**) of sedentary and trained B6 mice were measured during indirect calorimetry for 24 hours. White and grey horizontal bar represents light and dark phase, respectively. Data are presented as mean ± SEM (n = 6-7). Data were analysed using unpaired student's t-test. *, $p < 0.05$.

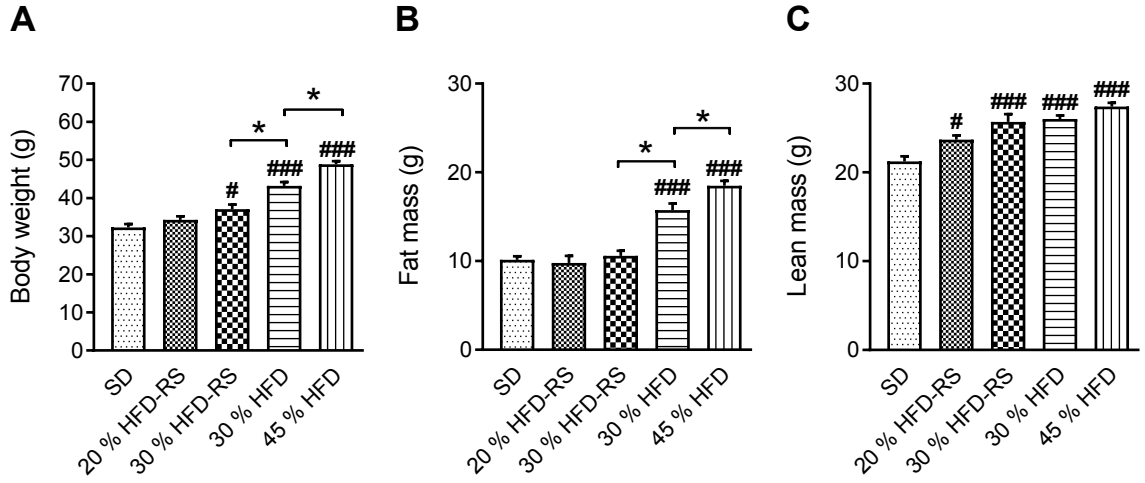

Figure S3: Body composition of NZO mice fed with four different HFDs. With 3 weeks of age, sedentary NZO mice were either fed a 45 % HFD, 30 % HFD, 30 % HFD with reduced sucrose (RS) or a 20 % HFD-RS. Body weight (**A**), fat mass (**B**) and lean mass (**C**) were measured in week 6 and compared to SD-fed mice. Body composition was gradually increased with increasing fat and sucrose content of the diet. Data are presented as mean ± SEM (n = 5-11). Data were analysed using one-way ANOVA with Tukey's multiple comparisons test. *, $p < 0.05$ between indicated HFD groups; #, $p < 0.05$; ###, $p < 0.001$ between indicated HFD and SD group.

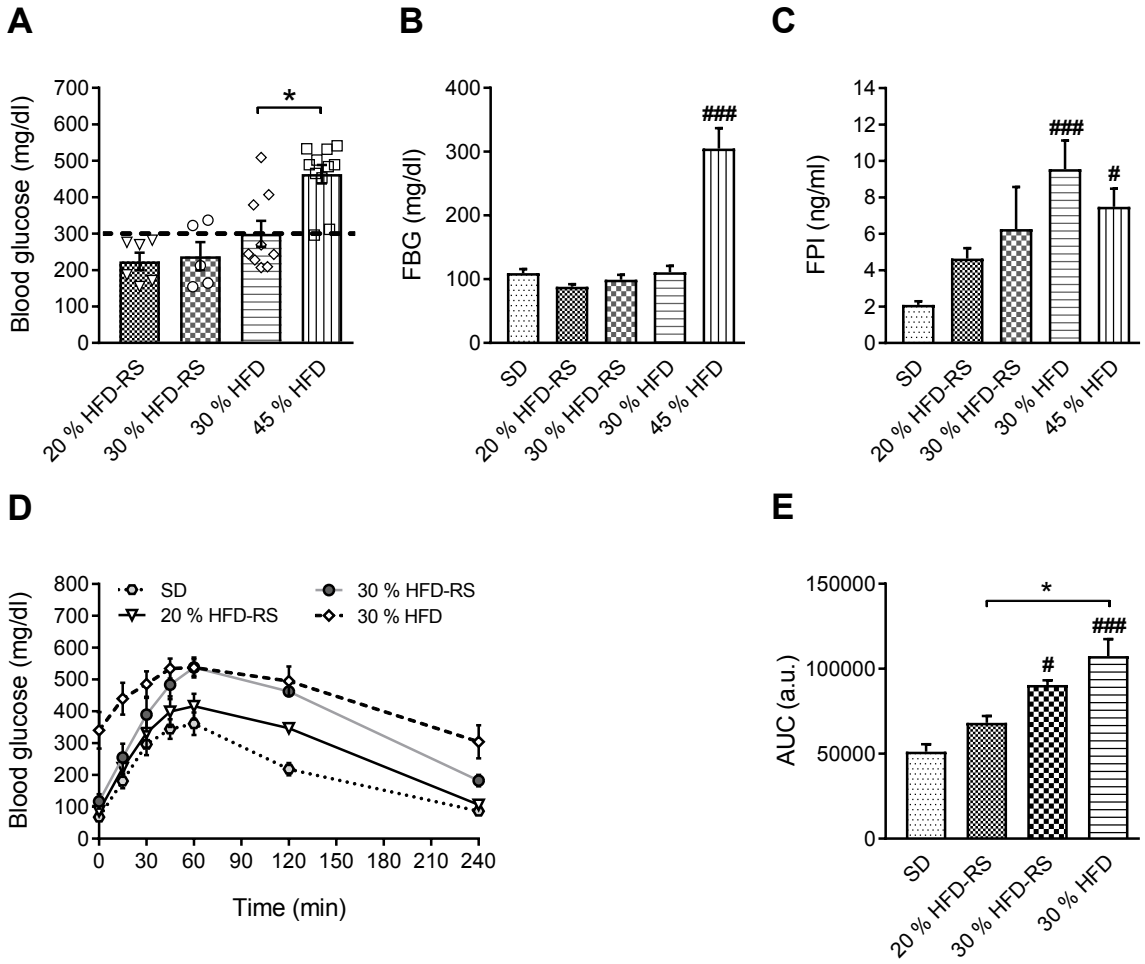

Figure S4: Whole-body glycaemia of NZO mice fed with four different HFDs. Random fed blood glucose (**A**), FBG (**B**) and FPI (**C**) of sedentary NZO mice fed with the different diets was measured in week 6, respectively. Dashed line in **A** illustrates the diabetic threshold of 300 mg/dl. For the SD group, no random fed blood glucose data in week 6 was obtained. The 20 % HFD-RS remained below the diabetic threshold, whereas 90 % of the 45 % HFD group was hyperglycaemic (**A**). FBG was significantly impaired in the 45 % HFD group (**B**), whereas FPI content was increased in all HFD groups (**C**). Glucose tolerance (**D**) was measured in week 10-12 during i.p. GTTs. AUC was determined for quantification of glucose tolerance (**E**). Since almost half of the animals fed with the 45 % HFD had died until week 10, no GTTs were performed with these mice. Glucose tolerance was incrementally impaired with increasing sucrose and fat content of the HFD (**D**, **E**). Data are presented as mean ± SEM (n = 3-11). Data were analysed using one-way ANOVA with Tukey's multiple comparisons test. *, $p < 0.05$ between indicated HFD groups; #, $p < 0.05$; ###, $p < 0.001$ between indicated HFD and SD group.

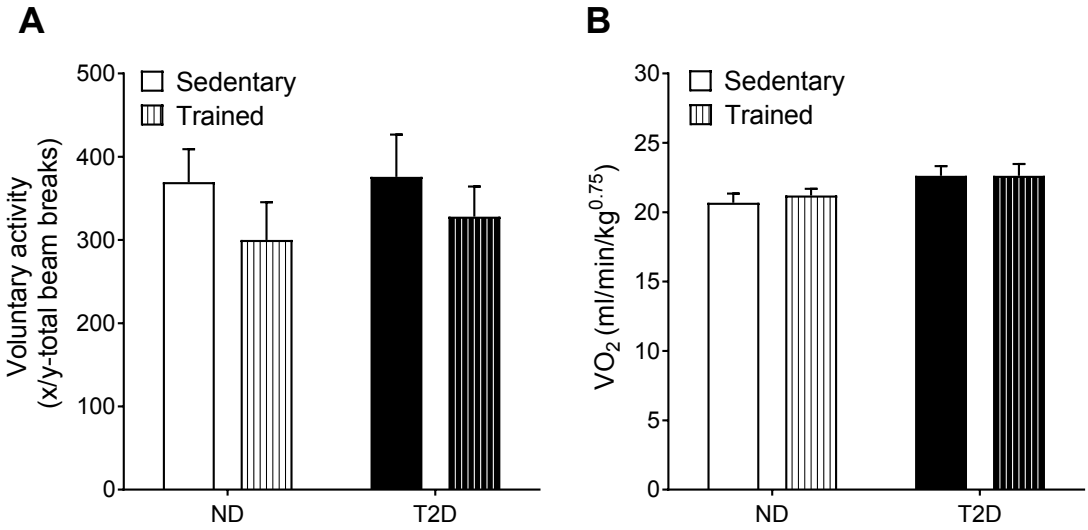

Figure S5: Voluntary activity and VO_2 consumption of ND and T2D NZO mice after chronic interval training. Voluntary activity (**A**) and mean VO_2 consumption (**B**) were measured during indirect calorimetry for 24 hours. Data are presented as mean ± SEM (n = 6-7). Data were analysed using two-way ANOVA with Bonferroni's multiple comparisons test.

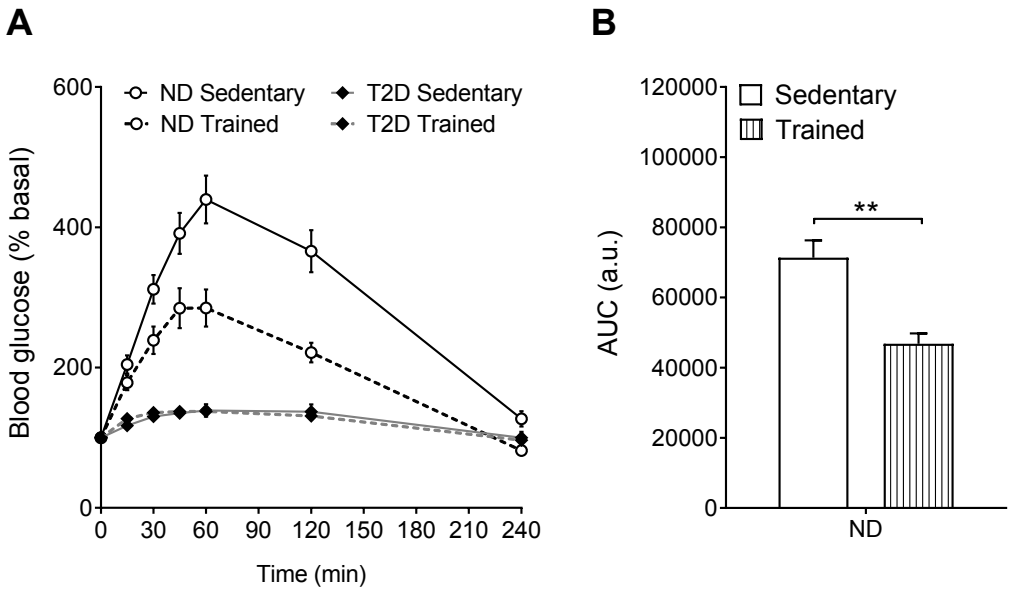

Figure S6: Glucose tolerance of ND and T2D NZO mice normalized to basal values. Glucose tolerance (**A**) was measured after intraperitoneal injection of glucose. AUC was determined for

quantification of glucose tolerance (**B**). Blood glucose concentrations were normalized to basal values. Normalisation of glucose clearance of T2D mice resulted in a flat curve, since blood glucose concentrations rapidly reached values beyond detection level (FBG > 600 mg/dl). Therefore, AUC could not be calculated for T2D mice. Data are presented as mean ± SEM (n = 7-12). Data were analysed using unpaired student's t-test. **, p < 0.01 between indicated groups.

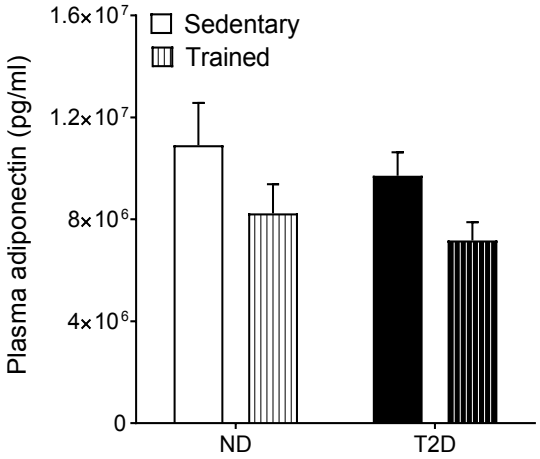

Figure S7: Plasma adiponectin concentrations of ND and T2D NZO mice after chronic interval training. Plasma concentrations of adiponectin were measured using the magnetic bead-based immunofluorescent Adiponectin All-in-One Bio-Plex assay (Bio-Rad, Hercules, CA, USA). Measurements were performed by Sonja Hartwig and Waltraud Passlack from the Proteome Analysis Unit of the Institute for Pathobiochemistry at the DDZ. Data are presented as mean ± SEM (n = 5-7). Data were analysed using two-way ANOVA with Bonferroni's multiple comparisons test.

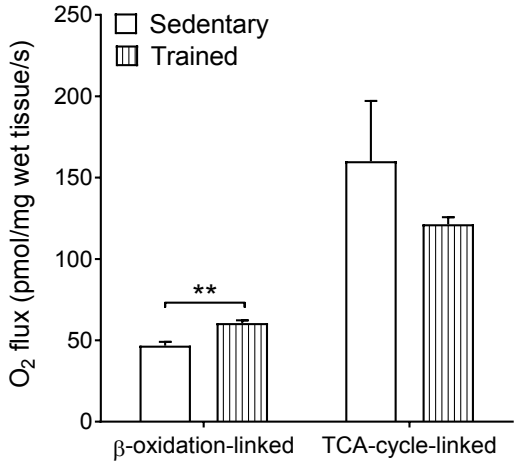

Figure S8: Hepatic β-oxidation- and citric acid (TCA)-cycle-linked maximal respiratory capacity of sedentary and trained NZO mice after chronic interval training. *Ex vivo* mitochondrial respiration analysis was performed in freshly isolated liver samples of sedentary and trained NZO mice using the Oxygraph-2k (Oroborus Instruments, Innsbruck, Austria). β-oxidation- as well as TCA-cycle-linked respiration was measured by adding the specific substrates for each pathway as described elsewhere (Binsch et al. 2017). The data shows the fluoro-carbonyl cyanide phenylhydrazone (fccp)-induced maximal respiratory capacity of the oroborus measurements. Measurements were performed by Tomas Jelenik from the Energy Metabolism Unit of the Institute for Clinical Diabetology at the DDZ. Data are presented as mean ± SEM (n = 2-3). Data were analysed using unpaired student's t-test. **, p < 0.01 between indicated groups.

6.5 List of Figures

Figure 1: Insulin- and contraction-mediated glucose uptake in skeletal muscle. 13
Figure 2: Disturbed glucose and lipid metabolism in T2DM. 16
Figure 3: Improved glucose and lipid metabolism after chronic exercise. 22
Figure 4: Structure and function of the RabGAP TBC1D4. 24
Figure 5: Study design for the four-week treadmill training with D4KO mice. 34
Figure 6: Study design for the six-week treadmill interval training with NZO mice.....35
Figure 7: Physical capacity and blood lactate concentrations of WT and D4KO mice. 49
Figure 8: Glucose tolerance and insulin tolerance of WT and D4KO mice after chronic exercise. 51
Figure 9: Protein abundance of TBC1D4, GLUT1 and GLUT4 and expression of GLUT4 (*Slc2a4)* in *Soleus* muscle of WT and D4KO mice. 52
Figure 10: *Ex vivo* glucose uptake in *Soleus* muscle of WT and D4KO mice. 53
Figure 11: Hepatic and skeletal muscle glycogen content in WT and D4KO mice. 54
Figure 12: Protein abundance of GCK, PCK-1 and PCK-2 in liver of WT and D4KO mice. ...55
Figure 13: Hepatic triglyceride content of WT and D4KO mice. 56
Figure 14: Protein abundance of TBC1D4, GLUT1 and GLUT4 and gene expression of GLUT4 (*Slc2a4)* in WAT of WT and D4KO mice. 57
Figure 15: *Ex vivo* glucose uptake in isolated adipocytes from WAT of WT and D4KO mice. 58
Figure 16: Protein abundance of TBC1D4, GLUT1 and GLUT4 in BAT of WT and D4KO mice. 59
Figure 17: Expression of markers for mitochondrial biogenesis and browning in scWAT of WT and D4KO mice. 60
Figure 18: Protein abundance of UCP-1 in scWAT of WT and D4KO mice.....61
Figure 19: Physical capacity, blood lactate concentrations and glucose tolerance of B6 mice after chronic interval training.....63
Figure 20: Body composition and hepatic triglyceride content of B6 mice after chronic interval training. 64
Figure 21: Whole-body energy expenditure of B6 mice after chronic interval training. 65
Figure 22: Protein abundance of PGC-1α, AMPK and pAMPK in *Soleus* muscle of B6 mice after chronic interval training.....66
Figure 23: Physical capacity, blood lactate concentrations and glycaemia of NZO mice fed a SD after chronic interval training.....68
Figure 24: FBG of NZO mice fed a HFD after chronic interval training.....69

Figure 25: Physical capacity and blood lactate concentrations of ND and T2D mice after chronic interval training.....70
Figure 26: Whole-body energy expenditure of ND and T2D mice after chronic interval training. 72
Figure 27: Hepatic and skeletal muscle glycogen content of ND and T2D mice after chronic interval training. 73
Figure 28: Glucose tolerance and insulin tolerance of ND and T2D mice after chronic interval training. 74
Figure 29: Protein abundance of AMPK, pAMPK and GLUT4 in *Gastrocnemius* muscle of ND and T2D mice after chronic interval training.....75
Figure 30: *Ex vivo* glucose uptake in *EDL* muscle of ND and T2D mice after chronic interval training. 76
Figure 31: GLUT4 protein abundance and *ex vivo* glucose uptake in isolated adipocytes from WAT of ND and T2D mice after chronic interval training. 77
Figure 32: Protein abundance of GCK, PCK-1 and PCK-2 in liver of ND and T2D mice after chronic interval training.....78
Figure 33: Hepatic triglyceride content and protein abundance of FASN in liver of ND and T2D mice after chronic interval training. 79
Figure 34: Restored adipose tissue glycaemia accounts for the improved insulin sensitivity in trained D4KO mice. 89
Figure S1: Protein abundance of HK-II in skeletal muscle of WT and D4KO mice. 128
Figure S2: Whole-body CHO, FAO and voluntary activity of B6 mice after chronic interval training. 128
Figure S3: Body composition of NZO mice fed with four different HFDs. 129
Figure S4: Whole-body glycaemia of NZO mice fed with four different HFDs. 130
Figure S5: Voluntary activity and VO_2 consumption of ND and T2D NZO mice after chronic interval training. 130
Figure S6: Glucose tolerance of ND and T2D NZO mice normalized to basal values. 130
Figure S7: Plasma adiponectin concentrations of ND and T2D NZO mice after chronic interval training. 131
Figure S8: Hepatic β-oxidation- and citric acid (TCA)-cycle-linked maximal respiratory capacity of sedentary and trained NZO mice after chronic interval training. 131

6.6 List of Tables

Table 1: Mouse strains 28
Table 2: Composition of mouse diets....28
Table 3: SYBR Green primers 29
Table 4: Antibodies....29
Table 5: Reaction Kits 30
Table 6: Enzymes and molecular weight size markers 30
Table 7: Chemicals....31
Table 8: Buffers and solutions 33
Table 9: Composition of SDS gels....43
Table 10: cDNA synthesis protocol....45
Table 11: qPCR protocol 46
Table 12: Body composition and plasma parameters of WT and D4KO mice after chronic exercise....50
Table 13: Body composition and plasma parameters of ND and T2D NZO mice after chronic interval training. 72
Table 14: Comparison of the exercise-response in D4KO and diabetic NZO mice. 97
Table S1: Treadmill training protocol used for D4KO mice. 124
Table S2: Treadmill interval training protocol used for B6 mice. 125
Table S3: Treadmill interval training protocol used for NZO mice fed a 30 % HFD-RS. 126
Table S4: Whole-body energy expenditure of WT and D4KO mice measured by indirect calorimetry....127
Table S5: Body composition, plasma parameters and RER of NZO mice fed a SD after six weeks of chronic interval training....127

Acknowledgments

First of all, I want to thank Prof. Dr. Hadi Al-Hasani for the possibility to prepare my PhD thesis in his working group and for providing me with this interesting topic. He always gave great input and new suggestions for the project. I would also like to thank him for the opportunity to present my progress of research at national and international congresses on a regular basis.

I thank Prof. Dr. Michael Feldbrügge to supervise my PhD thesis as a second reviewer.

I am very thankful to Dr. Alexandra Chadt for her additional supervision of the present thesis. She always took the time to discuss the results and plan the next steps. I also thank her for the support during animal experiments, including general handling, preparation of tissues and isolation of skeletal muscles during *ex vivo* measurements. Furthermore, she always gave great suggestions on how to prepare and phrase scientific abstracts, which really helped me during the writing of this thesis.

Many thanks go to the animal care takers Peter Herdt, Denise Schauer and Jennifer Schwettmann for the breeding, maintenance and taking care of the experimental animals. I would also like to acknowledge Johannes Goebel from TSE systems, who provided technical support for the calorimetric treadmills.

I am very grateful to all technicians that helped me throughout the whole time of the thesis. I thank Angelika Horrighs, Anette Kurowski, Heidrun Podini and Ilka Römer for the genotyping of the transgenic animals. I particularly thank Angelika Horrighs for introducing me into many lab techniques, including Western Blot analysis and photometrical assays, as well as for the support during animal experiments such as *ex vivo* and indirect calorimetry measurements. For the experiments concerning RNA isolation and qPCR analysis and for conducting the *ex vivo* glucose uptake assays in adipocytes, I would like to thank Anette Kurowski and Heidrun Podini. In addition, I thank Birgit Knobloch for assisting me during treadmill experiments, GTTs and preparation of mouse tissues. I also thank Antonia Osmers, Dagmar Grittner and Annette Schober for general lab support.

Many thanks go to all the students for the support during the treadmill experiments. At first, I thank Sandra Karpinski, who established the initial protocols during her master thesis and introduced me into the operation of the treadmill system. She was a great help especially at

the beginning of my thesis, where she supported me during general mouse handling and basic experimental techniques. I am very thankful to Christian de Wendt, who assisted me during GTTs and preparation of mouse tissues. Many thanks also go to Dr. Martin Röhling, who helped me optimizing the exhaustion running protocol. I thank Taylor Schoen for conducting part of the B6 analysis in the context of her internship at our institute. Furthermore, I thank Nele Hamker, Annika Grieß and Laura Toska for additional help during treadmill experiments and Western Blot analyses, as well as for the opportunity to supervise their master theses.

I also would like to thank all my other present and former colleagues of our institute for the comfortable atmosphere as well as for additional discussion of results during general lab meetings. These include Dr. Ralf Flörke, Dr. Dhiraj Kabra, Dr. Samaneh Mafakheri, Dr. Sandra Lebek, Tanja Schallschmidt and Delsi Altenhofen. Moreover, I especially thank Tim Benninghoff, Christian Binsch, Christian de Wendt, David Barbosa, Matthias Dille, Dr. Torben Stermann, Dr. Simon Göddeke and Dr. Sven Görgens for creating a great working atmosphere and for spending time outside the lab at various bowling alleys.

I am very thankful to my family, who supported me during the entire course of studies. Also, thank you Marla, for being there and adding more joy to my life.

Finally, I want to express my deep gratitude to my wife Yonca. Although we first met each other in person in 2014, I have known you long before, so that in fact you accompanied me from the very beginning of my course of studies. You were always there for me (online or in person) and encouraged me to proceed with my Master and PhD thesis. Thank you for your endless sympathy and endurance, especially during times of frustration, you made it so much easier to stand everything. Thank you that I was able to start a new family with you, I love you.

Erklärung

Ich versichere an Eides Statt, dass die Dissertation von mir selbständig und ohne unzulässige fremde Hilfe unter Beachtung der „Grundsätze zur Sicherung guter wissenschaftlicher Praxis an der Heinrich-Heine-Universität Düsseldorf“ erstellt worden ist.

Ferner versichere ich, dass die Dissertation bisher keiner anderen Fakultät vorgelegt worden ist.

Düsseldorf, den 18.12.2018

Christian Springer